MINISTRY OF EDUCATION & TRAINING MINISTRY OF NATIONAL DEFENSE

MILITARY TECHNICAL ACADEMY

NGUYEN TIEN ĐONG

RESEARCH ON COMBINED SM AND STBC FOR MIMO CHANNELS

A Thesis for the Degree of Doctor of Philosophy

HA NOI - 2018

MINISTRY OF EDUCATION & TRAINING MINISTRY OF NATIONAL DEFENSE

MILITARY TECHNICAL ACADEMY

NGUYEN TIEN ĐONG

RESEARCH ON COMBINED SM AND STBC FOR MIMO CHANNELS

A Thesis for the Degree of Doctor of Philosophy

Speciality: Electronic Engineering
Serial number: 62 52 02 03

SUPERVISORS:
Dr. LE MINH TUAN
Assoc. Prof. TRAN XUAN NAM

HA NOI - 2018

ASSURANCE

I pledge that in this thesis the presented results are my work under the professor guidance. The data and presented results are completely honest and not yet published in any previous works. The references are fully cited in accordance with the regulations.

Ha Noi, August 12th, 2017

Author

Nguyen Tien Đong

ACKNOWLEDGEMENTS

In the reseaching process and thesis completion, I have received many valuable help and contributions. First, I would like to sincerely thank Dr. Le Minh Tuan and Assoc. Prof. Tran Xuan Nam who do not provide their advice and useful guidance but also stimulate me on the researching plan. Furthermore, I express my respectful gratitude to the teachers and technical staffs for helping and sharing their knowledge in the Department of Communication Engineering, Faculty of Radio-Electronics, Military Technical Academy where I have studied for four years.

Many thanks also to colleagues, Post-graduate Department-MTA, Telecommunications University, and Sharing Scientific Reference Group for their technical support.

Finally, I would like to express my honest gratitude to my family, my wife, and my son who always encourage and share the difficulties in life.

Contents

List of Abbreviates

Abbreviate	English mean
AWGN	Additive White Gaussian Noise
BEP	Bit Error Probability
BER	Bit Error Rate
bpcu	Bit per Channel Use
BOSTBC	Block-Orthogonal Space Time Code
CDG	Coding Gain Distance
CH	Channel Hopping
CSI	Channel State Information
DFE	Decision Feedback Equalization
DS-SM	Diagonal Space Time Block Coded Spatial Modulation
DSTTD	Double Space Time Transmit Diversity
D-STBC	Diagonal Space Time Block Code
DT-SM	Spatially Modulated Space Time Block Coding
EE	Energy Efficiency
flop	Floating Point Operation
GSM	Generalized Spatial Modulation
GSTSK	Generalized Space Time Shift Keying

HRSM	High Rate Spatial Modulation
HR-STBC-SM	High Rate Space Time Block Code Spatial Modulation
HSPA+	High Speed Downlink Packet Access Plus
IAS	Inter Antenna Synchronization
ICI	Inter Channel Interference
IEEE	Institute of Electrical and Electronics Engineers
ISQRD	Improved Sorted QR Decomposition
i.i.d.	Independent and identically distributed
LDC	Linear Dispersion Code
LTE	Long Term Evolution
MBLAST	Modified Bell Laboratories Layered Space-Time
MGF	Moment Generating Function
MIMO	Multiple Input Multiple Output
ML	Maximum-Likelihood
MMSE	Minimum Mean Square Error
MRC	Maximal-Ratio Combining
MSE	Mean Square Error
MSQRD	Modified Sorted QR Decomposition
OFDM	Orthogonal Frequency-Division Multiplexing
OSTBC	Orthogonal Space Time Block Coding
PDF	Probability Density Function
PEP	Pairwise Error Probability
PIC	Parallel Interference Cancellation

PSK	Phase Shift Keying
QAM	Quadrature Amplitude Modulation
QO-STBC	Quasi-Orthogonal STBC
RF	Radio Frequency
SC	Spatial Codeword
SD	Sphere Decoder
SDM	Spatial Division Multiplexing
SIC	Successive Interference Cancellation
SM	Spatial Modulation
SM-DC	Spatially Modulated Diagonal Space Time Code
SM-OSTBC	Spatially Modulated Orthogonal Space Time Block Code
SNR	Signal to Noise Ratio
SQRD	Sorted QR Decomposition
SSK	Space Shift Keying
STBC	Space Time Block Code
STBC-SM	Space Time Block Coded Spatial Modulation
STC	Space Time Code
STSK	Space Time Shift Keying
STTC	Space Time Trellis Code
V-BLAST	Vertical-Bell Laboratories Layered Space-Time
WiMAX	Worldwide Interoperability for Microwave Access
ZF	Zero Forcing

List of Figures

List of Tables

List of Symbols

Symbol	**Mean**.
a	A scalar number.
$\mathbf{a}$	A vector.
$\mathbf{A}$	A matrix.
a_{il}	i-th row l-th column element of the matrix $\mathbf{A}$.
$\mathbf{A}^H$	The Hermittian of the matrix $\mathbf{A}$.
$\mathbf{A}^T$	The transposition of the matrix $\mathbf{A}$.
γ	Average SNR at each receive antenna.
n_T	The number of transmit antennas.
n_R	The number of receive antennas.
n_A	The number of active antennas.
M	Modulation order.
$\mathbf{H}$	Channel matrix.
$\mathbf{N}$	Noise matrix.
$\mathbf{Y}$	Received signal matrix.
$\mathbf{I}$	Identity matrix.
$\mathbf{h}_i$	i-th column of the matrix $\mathbf{H}$.
$\Re(x)$	The real part of x.
$\Im(x)$	The imaginary part of x.
x^*	The complex conjugate of x.

Ω_S	Spatial constellation.
Ω_x	Signal constellation.
$\|.\|_F^2$	Frobenius norm of a matrix.
E_s	Average symbol energy of the modulated symbol.
$\|a\|$	The modulus of a.
slice(.)	Quantization step.
sign(.)	The sign of a real number.
trace(.)	Sum of the diagonal components of the matrix.
diag($\mathbf{x}$)	Create a diagonal matrix from a vector $\mathbf{x}$.
ρ	Calculation complexity.
$\delta_{\min}$	Coding gain distance.
θ_o	The optimal angle.
$\binom{n}{k}$	$\frac{n!}{(n-k)!k!}$.
$\lfloor x \rfloor$	Rounding down to the closest integer.
$\oslash$	The modulo operation.
$\otimes$	Kronecker product.
$\lfloor . \rceil$	Rounding to the closest integer.
$\log_2(.)$	The lograrithm base 2.
$\mathrm{E}\{.\}$	The expectation.

Introduction

Nowadays, along with the rapid development of the microelectronic technology, the demand of telecommunication users no longer makes a call, but changes to entertainment needs on mobile devices everywhere. In order to meet this demand, telecommunication designers and researchers must look for technical solutions to build wireless telecommunication networks which offer higher data transfer rates, better service qualities and larger network capacities. Over the years of research and development, Multiple-Input Multiple-Output (MIMO) wireless systems have emerged as the most promising technology to meet these requirements. In a MIMO system, multiple antennas at both transmitter and receiver are deployed to exploit multipath propagation. The main idea of the MIMO system is that the signals are transmitted over the spatial domain of the transmit antennas and the receive antennas and are combined in a method to produce the parallel multipath tranmission efficiency. Therefore, it can increase the transmission rate or the diversity order to improve the system performance, expressed by the Bit Error Rate (BER).

Exploited the multiplexing gain, Spatial Division Multiplexing (SDM) systems split a high-rate signal into multiple lower-rate streams and simultaneously transmit these streams through the transmit antennas in the same frequency channel. The number of parallel data streams is less than or equal to the number of transmit or receive antennas. The SDM main advantages

are channel capacity increase without requiring bandwidth expansion and no Channel State Information (CSI) at the transmitter. However, since parallel data streams are transmitted in the same frequency channel, it requires Inter-Antenna Synchronization (IAS) at the transmitter and creates Inter-Channel Interference (ICI) at the receiver. In addition, owing to the streamlining principle of the SDM system, the transmitter is only a signal divider, the system research focusses on the design of signal detection algorithms having good performance and low complexity at the receiver. Because of the simple structure, the linear detectors such as the Zero-Forcing (ZF) and Minimum Mean Square Error (MMSE) detectors could be first considered in the SDM system. However, these detectors' performances are quite low. Consequently, Succesive Interference Cancellation (SIC) [1], [9], [22], [71]-[73] or Parallel Interference Cancellation (PIC) [53], [75] detectors were devised to improve detection performance. The Vertical Bell Labs Layered Space Time (VBLAST) detector [71] is a typical one in the SDM scheme. Theoretically, this detector fulfills a combination of ZF or MMSE detection algorithms and the succesive interference cancellation approach to improve detection performance and reduce the computational complexity. At each iteration, the signal of each layer is separated and estimated in turn. Then, the newly estimated signal is used to suppress its effect on the remaining layers. Although the VBLAST detector has better performance than the linear ones, its performance is still far away compared with that of the Maximum Likelihood (ML) detection algorithm. Therefore, a sub-optimal SDM detector, having better performance, needs to be researched and developed. As a result, the Sphere Decoder (SD) algorithm was proposed in [51], [52] and was first applied by Viterbo $et.al$ in the

MIMO system. The SD detector obtains an equivalent detection efficiency as the ML one while its complexity has been proven to be far less than that of the ML [66].

Differently from the SDM technique, the Space Time Codes (STC) exploit the maximum diversity gain to improve the MIMO system reliability by sending transmitted signal replicas by time and space [60], [63]. In many proposed STCs, the Orthogonal Space Time Block Codes (OSTBC) [61] are the most noticeable because of simple design structure at the transmitter and low decoding complexity at the receiver. However, most STCs are limited in coding rates compared with the SDM technique [32] or satisfy the coding rate condition, in which these codes have high decoding complexity [4].

In [41], Mesleh *et. al* proposed a Spatial Modulation (SM) technique to take the MIMO advantages and overcome the existing MIMO challenges. This technique is developed to reduce the complexity, energy efficiency and cost of multiple-antenna systems without decreasing the system performance while it still exploits the multiplexing gain. In a MIMO-SM system, the transmitter activates one of the n_T transmit antennas at each symbol period and transmits a modulated signal of M-ary Quadrature Amplitude modulation (QAM) or Phase Shift Keying (PSK) [42]. The transmited information includes the modulated symbol and the index (or position) of the transmit antenna that is activated to transmit this symbol. Therefore, the ICI effect at the receiver and the IAS requirement at the transmiter, as faced by the SDM and other STC systems, are completely avoided in the MIMO-SM system. Furthermore, because of only one data stream, a low complexity ML detector is implemented at the MIMO-SM receiver [29]. A Space Shift Keying (SSK) scheme [30], a

special version of the SM, only conveys information bits by the antenna positions. Nevertheless, both the SM and the SSK schemes only have receive diversity and the spectral efficiencies of two schemes are limited because it depends on the logarithm function base 2 of n_T transmit antennas, i.e., $\log_2 n_T$. A Generalized SM (GSM) scheme, proposed by Wang *et. al* in [69], improves the SM spectral efficiency by simultaneously activating two or more transmit antennas. Meanwhile, by creating a set of Spatial Constellation (SC) vectors, Nguyen *et. al* proposed a High Rate Spatial Modulation (HRSM) scheme [46] whose spectral efficiency is linearly proportional to the number of transmit antennas. In addition, an optimal ML detection algorithm was proposed for the HRSM receiver. However, both of the GSM and the HRSM schemes are lack of transmit diversity.

Many techniques have been proposed to obtain diversity gain for the SM system [14], [16]. Recently, Basar *et. al* proposed a Space Time Block Coded Spatial Modulation (STBC-SM) technique [5] by combining the SM one with an Alamouti STBC [2]. The STBC-SM technique not only obtains the second-order transmit diversity and but also offers higher spectral efficiency than the SM one. Based on Basar's idea, the authors proposed a Spatially Modulated Orthogonal Space Time Block Coding (SM-OSTBC) scheme [35] for MIMO systems equipped with more than four transmit antennas. In the SM-OSTBC system, the amount of data information is conveyed not only by an Alamouti STBC but also by a set of SC matrices. Thus, the spatial spectral efficiency of the SM-OSTBC technique is higher than that of the STBC-SM one. Besides, different from optimizing the rotation angle in the STBC-SM scheme, the set of the SC matrices is simply designed in the SM-OSTBC one. Overcoming

the disadvantage of the SM-OSTBC scheme, Wang *et. al* proposed a Spatially Modulated Diagonal Space Time Code (SM-DC) scheme [70] that is flexibly used for MIMO systems where the number of transmit antennas is equal or less than four. The SM-DC technique attains the second-order transmit diversity. Furthermore, different from other MIMO-SM schemes, the SM-DC one is implemented the SD detection algorithm to reduce the computational complexity of the detection process.

From some above mentioned works, it can be seen that a new MIMO-SM system giving high spectral efficiency and the transmit diversity by a combination of the SM technique and the STC one is a promising research trend. In addition, another trend is to propose several sub-optimal detectors for MIMO-SM systems to decrease the computational complexity at the MIMO-SM receiver and also investigates tighter theoretical Bit Error Probability (BEP) bounds in the high Signal-to-Noise Ratio (SNR) region. For this reason, I have selected and performed the thesis "*Research on Combined SM and STBC for MIMO Channels*". The successful implementation of the thesis not only theoretically contributes to MIMO-SM systems but also builds basic background for the application of these systems in the next generation communication networks. Besides, the research and development of sub-optimal low-complexity detectors for the MIMO-SM systems also partially contributes to the design, implementation and application of these systems in real life.

2. The thesis research objectives

- Designing new MIMO-SM transmission techniques, obtaining the transmit diversity and having higher spectral efficiency than the existing

MIMO-SM ones by combining the STCs and the SM technique;

- Proposing optimal and sub-optimal low-complexity detection algorithms for the existing and proposed MIMO-SM systems.

3. The thesis research scope

- Theoretical studies of wireless communication channels such as channel characteristics, fading types and the solutions where the slow quasi-static Rayleigh flat fading is significantly considered, the existing point-to-point MIMO transmission systems;
- Investigating the detection algorithms in MIMO schemes such as ZF, MMSE, VBLAST, SQRD, and SD;
- Studying the SM technique and the STBC;

4. The thesis methodology

The thesis combines analytical methods and the Monte-Carlo simulation, specifically

- The analytical methods are used to establish the signal detection complexity at the MIMO-SM receiver and are derived the system bit error probability upper bound;
- The Monte-Carlo simulation is applied to evaluate and present the system performance figures where all systems are compared in a MIMO configuration at the same spectral efficiency over the quasi-static Rayleigh fading channel and the modulated symbols are mapped by the Gray code.

5. The thesis contribution

The major contributions of the thesis are summarized as follows

1. Based on sub-optimal detection algorithms of the SDM systems, several low-complexity modified detection algorithms are proposed for the HRSM scheme. In addition, a tighter theoretical BEP upper bound in the high SNR region for the HRSM one, ulitized the M-QAM technique, is derived;

2. A new SM scheme, called Spatially Modulated Space Time Block Coding (DT-SM), for MIMO systems having more than four transmit antennas is proposed by combining the SM technique and the Double Space Time Transmit Diversity (DSTTD). The DT-SM scheme attains the second-order transmit diversity and high spectral efficiency and has a low-complexity detection algorithm at its receiver;

3. A new SM scheme, called Diagonal Space Time Block Coded Spatial Modulation (DS-SM), is proposed by integrating the SM technique and the Diagonal Space Time Block Code (DSTBC). The DS-SM scheme obtains the fourth-order transmit diversity and has a reasonable computational complexity at the receiver.

6. Thesis structure

The thesis is organized in four chapters as follows

- Chapter 1: BACKGROUND OF THE SPATIAL MODULATION AND SPACE TIME CODES

  The chapter content summarizes the basic knowledge related to the spatial modulation technique, the space time codes as well as the research background of MIMO-SM systems.

- Chapter 2: LOW COMPLEXITY DETECTION ALGORITHMS AND

A NEW THEORETICAL UPPER BOUND FOR THE HIGH RATE SPATIAL MODULATION SCHEME

In this chapter, several detection algorithms for the high rate spatial modulation scheme are proposed. In addition, the computational complexities and the simulation results of these detectors are analyzed and compared. Finally, in order to exactly analyze the high rate spatial modulation scheme performance, a tighter new, theoretical BEP upper bound is derived for this scheme utilized the M-QAM technique.

- Chapter 3: A NEW MIMO-SM SCHEME ACHIEVING HIGH SPECTRAL EFICIENCY

  This chapter presents a new spatial modulation scheme, called Double Space Time Coded Spatial Modulation (DT-SM). The DT-SM one not only achieves good performance but also has high spectral efficiency. Besides, a general procedure of spatial constellation matrices for MIMO systems, having the number of transmit antennas greater than 5, is presented in this chapter. Later, a theoretical BEP upper bound for the DT-SM scheme under the correlated quasi-static Rayleigh fading channel is derived. In addition, in order to decrease the DT-SM computational complexity, a low-complexity modified Schnorr-Euchner sphere decoding algorithm is proposed. The DT-SM complexity is analyzed and compared with that of the existing MIMO-SM schemes. The simulation results show that the DT-SM scheme outperforms the existing MIMO and MIMO-SM ones and especially this scheme still performs roburstly when the spatial correlation effect occurs.

- Chapter 4: A NEW MIMO-SM SCHEME ACHIEVING HIGH ORDER TRANSMIT DIVERSITY

  The chapter content presents a Diagonal Space Time Block Coded Spatial Modulation (DS-SM) scheme obtaining the fourth order transmit diversity. In addition, a general procedure of spatial constellation matrices for MIMO systems, having the even number of transmit antennas greater than four, is proposed. The simulation results show that the DS-SM scheme achieves better performance than the existing MIMO-SM schemes when these schemes are equipped with the small number of receive antennas. The DS-SM performance is verified by the theoretical BEP upper bound. Furthermore, the complexity analysis shows that the DS-SM scheme has a reasonable computational complexity at its receiver. Finally, the DS-SM scheme is demonstrated to robustly operate when the spatial correlation effect occurs at the transmitter and receiver.

Chapter 1
BACKGROUND OF THE SPATIAL MODULATION AND SPACE TIME CODES

1.1. The spatial modulation technique

After more than a decade of research and development, the MIMO have recently been adopted in many wireless communication standards such as IEEE 802.11n, WiMAX, or Long Term Evolution (LTE). Multiple antennas in the MIMO systems are deployed to exploit multiplexing, diversity or antenna gains. Nevertheless, multiple antenna deployment in the MIMO systems has encountered the difficulties in cost and complexity [19], specifically

- The Inter-Channel Interference (ICI) at the MIMO receivers happens because the symbols in the MIMO systems are simultaneously transmitted from different transmit antennas at the same frequency channel;
- The Inter-Antenna Synchronization (IAS) at the MIMO transmitters as all transmit antennas are operated at the same time;
- Multiple Radio Frequency (RF) chains, corresponding to the number of transmit antennas, which are implemented to simultaneously transmit all signals. The multiple RF chain implementation leads to increase in the deployment cost and energy comsumption of the MIMO systems [26].

In addition, the MIMO systems are difficult to deploy for the radio downlink when the multiple antenna placement on a hand-held device is limited

due to the compact size of the device. These are the major barriers that must be overcome by telecommunication operators when deploying the MIMO systems in practice. Therefore, a new technique needs to be developed to exploit the MIMO system advantages as well as overcome the existing challenges. Mesleh *et. al* [41] proposed a Spatial Modulation (SM) technique to solve the MIMO system problems. The SM technique is developed with the goal of reducing the MIMO system cost and complexity while ensuring the system performance as well as achieving the high transmission rate. With a simple coding and modulation scheme, the SM technique allows not only to design a low-complexity transmiter and receiver but also to obtain high spectral efficiency as given

- Only one transmit antenna is activated to convey data at each symbol period. Therefore, the SM technique completely eliminates the ICI at its receiver and does not require synchronization among the number of transmit antennas. The SM transmitter design and deployment are very simply because of just one RF chain implementation [44]. Furthermore, the low-complexity ML detection algorithm can be implemented at the SM receiver [29];

- The indices of the transmit antennas are considered an extended information source through a one-to-one mapping between information bits and the transmit antenna positions. Thus, the SM technique attains the multiplexing gain compared with the conventional Single-Input Single-Output (SISO) one.

1.1.1. The spatial modulation principle

In the SM transmiter, each block of data bits is splitted into two different parts. The first part is used to activate one transmit antenna in the transmit antenna array (the spatial information). The remaining bits are mapped into the signal constellation of M-QAM or PSK technique to choose a modulated symbol (the signal information). Finally, the modulated symbol is transmitted from the active antenna. Therefore, the conveyed information including the spatial information (the antenna indices) and the signal information (the modulated symbol) is presented as a 3-D constellation diagram.

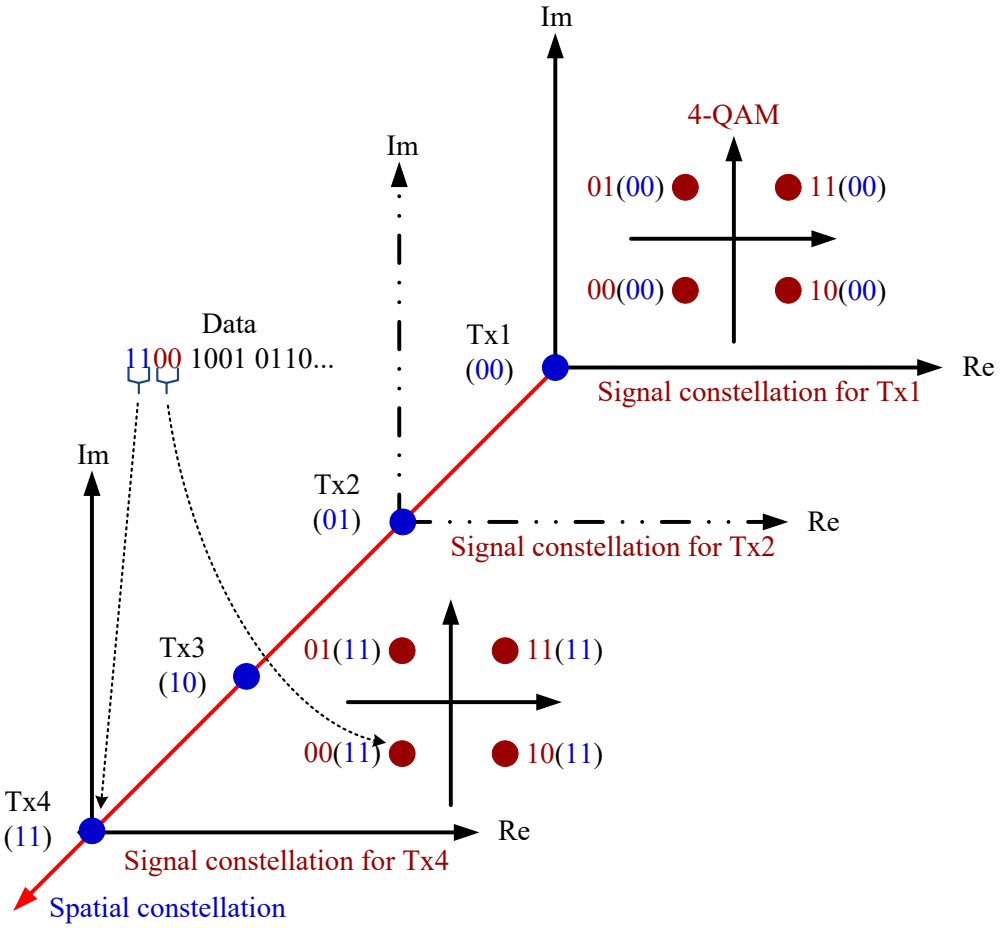

Figure 1.1: The 3-D constellation diagram with four transmit antennas, 4-QAM [18].

The Figure 1.1 presents a 3-D constellation diagram of the SM system

equipped with four transmit antennas and the 4-QAM technique. The transmitted signal includes the spatial information and the signal information. This signal from the activated antenna is transmitted in the medium. Since each transmit antenna has a different spatial position, the transmitted signal will be affectted by different wireless links from the transmitter to the receiver.

At the SM receiver, taking the advantage of the scattering richness of the MIMO channel, the transmitted signal is recovered by an optimal low-complexity ML detector [29]. According to the ML principle, the receiver must calculate the Euclidean distances between the received signal and a combination of the transmitted signals and then select the smallest distance. As a result, the transmitted signal is successfully recovered. In order to do this, the CSI is assumed to exactly estimate at the receiver. Therefore, the SM principle is built on the following factual basics

- Each wireless link from transmit antennas to receive antennas has a low correlation degree;
- The receiver knows pefect CSI to accurately estimate transmitted data.

In other words, the SM technique exploits the spatial chracteristics of the channel. That is uniqueness of each wireless link between the transmit antennas to the receive antennas.

1.1.2. The MIMO-SM system model

A MIMO-SM system equipped with n_T transmit antennas, n_R receive antennas, and a M-ary modulation technique is considered. At the transmitter, each block of $(\log_2 n_T + \log_2 M)$ information bits is separated into two different parts: $\log_2 n_T$ and $\log_2 M$ bits. The $\log_2 n_T$ bits are used to activate one

antenna in the transmit antenna array while the remaining $\log_2 M$ bits are mapped into a M-ary modulation technique to create a modulated symbol. Finally, this symbol is transmitted from the active antenna.

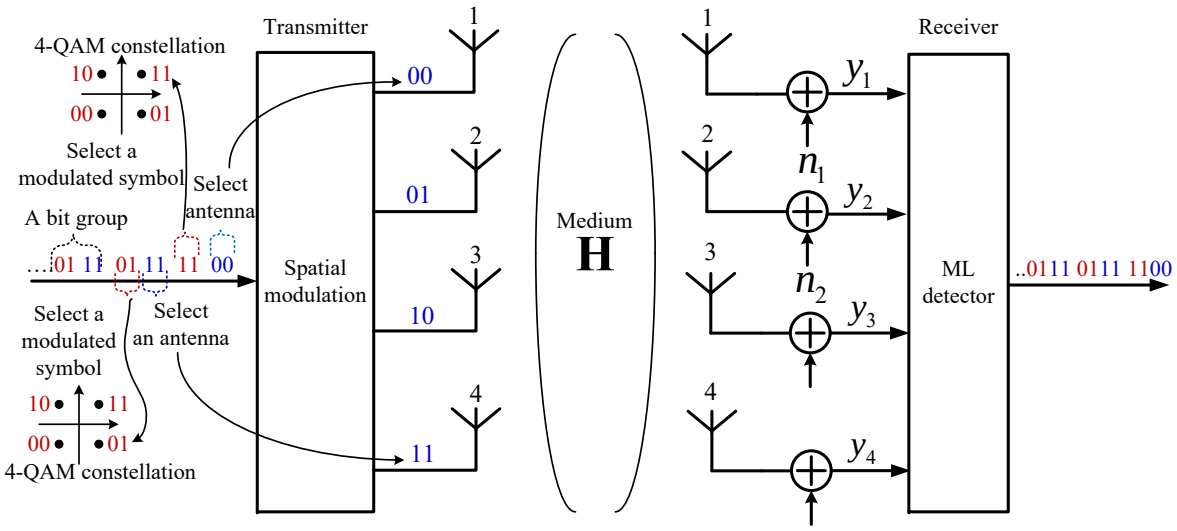

Figure 1.2: A MIMO-SM system, 4 transmit antennas, 4-QAM.

Figure 1.2 decribes the SM scheme operation where this model is equipped with four transmit antennas, four receive antennas, and a 4-QAM technique. In this model, each block of four data bits is processed by the transmitter. The first two bits are used to activate a transmit antenna while the last two bits are mapped into the 4-QAM technique to create a modulated symbol. For example, the first block of data is 0011 where two bits, 00, are used to activate the first antenna in four transmit antennas while two bits, 11, are mapped into the 4-QAM technique to generate the modulated symbol, i.e., $1 + j$. Finally, this symbol is transmitted from the first transmit antenna. At the receiver, four data bits, 0011, are exactly recovered by a ML detection algorithm.

The MIMO-SM system spectral efficiency is presented as given

$$C_{\text{SM}} = \log_2 n_T + \log_2 M \ \ (\text{bpcu})\,,$$

where bpcu, denoting bits per channel use, expresses the number of transmitted bits in once channel utilization. The bpcu parameter is used to compare the MIMO-SM system spectral efficiency while considering the discrete time MIMO channel model.

1.1.3. The MIMO-SM mathematical model

In general, a MIMO-SM system, equipped with n_T transmit antennas and n_R receive antennas, is considered. It is assumed that the MIMO channel is uncorrelated flat Rayleigh fading [5], [28], [42] where the Rayleigh fading channel only includes scattered waves and the quasi-static characteristic shows that the channel responses vary from message to message. MIMO-SM systems, working well on the Rayleigh fading channel, will have good performance on other channels. The channel coefficients are assumed to be independent and identically distributed (i.i.d.) Gaussian random variables with zero mean and unit variance, i.e., $\mathcal{CN}(0,1)$. Therefore, the MIMO system channel is presented by a complex matrix including n_R rows and n_T columns as follows

$$\mathbf{H} = \begin{bmatrix} h_{11} & h_{12} & \cdots & h_{1n_T} \\ h_{21} & h_{22} & \cdots & h_{2n_T} \\ \vdots & \vdots & \ddots & \vdots \\ h_{n_R1} & h_{n_R2} & \cdots & h_{n_Rn_T} \end{bmatrix}.$$

The received signal and the transmitted signal respectively are presented as given

$$\mathbf{y} = [\ y_1 \ \ y_2 \ \ \cdots \ \ y_{n_R}\ ]^T, \mathbf{x}_{i,q} = \mathbf{e}_i x_q = [\ 0 \ \ \cdots \ \ 0 \ \ x_q \ \ 0 \ \ \cdots \ \ 0\ ]^T,$$

where x_q is the q-th modulated symbol from the M-QAM/PSK technique and $\mathbf{e}_i$ is a $n_T \times 1$ vector taken from the spatial constellation Ω_S [18]. In the $\mathbf{e}_i$ vector, only the i-th element, corresponding to the position of the active antennas, has non-zero value. For example with four transmit antennas, if the third antenna is activated, the vector will be presented as $\mathbf{e}_3 = \begin{bmatrix} 0 & 0 & 1 & 0 \end{bmatrix}^T$. The transmit power constraint is $E_{\mathbf{x}}\left[|x_q|^2\right] = 1$.

Noise at the receiver is assumed to be Additive White Gausian Noise (AWGN). The entries of the noise vector are i.i.d. complex Gaussian random variables with zero mean and unit variance, i.e., $\mathcal{CN}(0,1)$

$$\mathbf{n} = \begin{bmatrix} n_1 & n_2 & \cdots & n_{n_R} \end{bmatrix}^T.$$

Under the assumption that the receiver knows pefect CSI [4], [28], [29], [36], [70]. Then, the relationship between the transmitted signal and the received signal is presented by a system equation as follows

$$\mathbf{y} = \sqrt{\gamma}\mathbf{H}\mathbf{x}_{i,q} + \mathbf{n} = \sqrt{\gamma}\mathbf{h}_i x_q + \mathbf{n}. \tag{1.1}$$

where x_q is transmitted from the i-th transmit antenna, $\mathbf{h}_i$ denotes i-th column of $\mathbf{H}$ and γ is an average SNR at each receive antenna.

1.1.4. An optimal ML detector

Jenganathan *et. al* [29] proposed an optimal detection algorithm for the MIMO-SM system based on the ML principle. Both the transmit antenna and the modulated symbol index are simultaneously detected as given

$$\begin{aligned}\left[\hat{i}_{ML}, \hat{q}_{ML}\right] &= \arg\max_{i,q} p_{\mathbf{Y}}\left(\mathbf{y}|\mathbf{x}_{i,q}, \mathbf{H}\right) \\ &= \operatorname*{argmin}_{i,q}\left\{\sqrt{\gamma}\left\|\mathbf{g}_{i,q}\right\|_F^2 - 2\Re\left(\mathbf{y}^H\mathbf{g}_{i,q}\right)\right\},\end{aligned} \tag{1.2}$$

where $p_{\mathbf{Y}}\left(\mathbf{y}|\mathbf{x}_{i,q},\mathbf{H}\right) = \pi^{-n_R}\exp\left(-\left\|\mathbf{y}-\sqrt{\gamma}\mathbf{H}\mathbf{x}_{i,q}\right\|_F^2\right)$ is the Probability Density Function (PDF) of $\mathbf{y}$ with the condition $\mathbf{x}_{i,q}$ and $\mathbf{H}$, and $\mathbf{g}_{i,q} = \mathbf{h}_i x_q$, $1 \le i \le n_T, 1 \le q \le M$. The computational complexity, calculated on the number of multiplications [29], is as follows

$$\rho_{\text{SMopt}} = 2n_R n_T + n_T M + M. \tag{1.3}$$

1.1.5. The SM advantages and disadvantages

Based on an analysis of the MIMO-SM operational principle and the comparision with the existing MIMO systems, some advantages and disadvantages of the SM technique are listed as follows

- **Advantages**
  - *High transmission throughput.* Because of the additional spatial constellation utilization for transmitting information, the spectral efficiency of the MIMO-SM transmission system is higher than that of the SISO one [42] and the STBC ones [74];
  - *Simple transmitter and receiver design.* Since only one transmit antenna is activated to transmit data in the MIMO-SM system, the MIMO-SM receiver completely avoids the ICI effect. As a result, a low complexity ML detector is implemented to recover the transmitted signal at its receiver [29]. In addition, since only one transmit antenna is operated at each symbol period, the MIMO-SM transmitter does not require IAS and just uses one RF chain. Therefore, the transmitter design becomes simple [44];
  - *Energy saving.* Unlike the MIMO transmission system, the MIMO-

SM one just utilizes one RF chain, so the amount of energy consumption reduces and is not dependent on the number of deployed antennas. As a result, the MIMO-SM system obtains Energy Efficiency (EE) [25];

- *The number of receive antennas is flexible.* The MIMO-SM transmission system still performs well when the number of transmit antennas is less than that of receive antennas, $n_R < n_T$ because the goal of multiple receive antenna deployment is to attain the receive diversity. In terms of the SM principle, the MIMO-SM receiver only needs to deploy one receive antenna. Therefore, the MIMO-SM system is suitable for the radio downlink with low-complexity compact simple handheld devices;
- *Used for multiple access systems.* Because of the different locations of the MIMO-SM transmitters and receivers, their impulse responses are almost independent together. Therefore, the signals of the pairs of users are considered to be orthogonal [54].

• **Disadvantages**

- *The spectral efficiency is limited by the number of transmit antennas.* The MIMO-SM spectral efficiency increases in the logarithm base 2 of the number of transmit antennas. Corresponding to high spectral efficiency, the MIMO-SM system must be deployed the large number of transmit antennas. This is difficult to implement in practice;
- *Only the receive diversity.* Although the MIMO-SM systems and the special case, the SSK one [30], outperform the existing MIMO ones

[41], both systems can not actually achieve the transmit diversity gain [23]. Therefore, these systems have to rely on multiple receive antenna deployment to counteract fading channel effects;

– *Suitable channel condition.* The MIMO-SM system performance significantly depends on the wireless communication environment, i.e., the rich scattering channel [43]. If the impulse responses of pairs of users are not different in the MIMO-SM channel, the receiver easily misidentifies the position of the active transmit antennas. As a result, the MIMO-SM performance significantly deteriorates [19];

– *Complicated channel estimation.* As the MIMO-SM system only uses one RF chain, channel estimation algorithms must to be performed in turn. As a result, the required length of training sequences significantly increase and this decreases the system transmission efficiency.

Based on mentioned advantage and disadvantage analysis, it can be seen that the SM technique is oustanding, potential and suitable for the low complexity MIMO systems.

1.2. The space time codes

1.2.1. Introduction

The space time code (STC) [61]-[63] is an effective way to improve the reliability of the multiple-antenna wireless communication systems by exploiting the spatial and time diversity. Particularly, redundant copies of transmitted signals are transmitted from different antennas at different times and hoping that received copies will undergo different effects of fading channels. Therefore, the STC application allows multiple-antenna wireless communication

systems to achieve the diversity gain of transmit diversity.

Currently, the STC technique can be classified in two main categories

- **Space Time Trellis Codes (STTC) [63]:** This is the first coding technique suggested by Tarokh *et. al.* The main advantages of these codes are that these codes attain not only diversity gain but also coding gain. However, the STTCs are difficult to be applied in practice because of the Viterbi decoding algorithm implementation. As a result, the complexity of these codes are propotional to the square of the number of states [37], [38];

- **Space Time Block Codes (STBC) [2], [62]:** In the STBCs, the transmit data is constructed in a matrix block form whose elements are created from replicas of a set of modulated symbols where the rows denote the number of transmit antennas and the columns present the time slots of the data block. Although the STBCs can not achieve the coding gain, these codes have a low decoding complexity at their receiver. As a result, the STBCs has potential applications and practical implementation in the wireless communication systems.

1.2.2. Space time block codes

Figure 1.3 decribes a MIMO system ulitized the STBC technique. In this model, information bits s_i are mapped into the M-ary modulation technique to create N_s modulated symbols, $x_i, i = 1, 2, ..., N_s$. Then, these symbols are arranged to make a signal matrix block including n_T rows and T

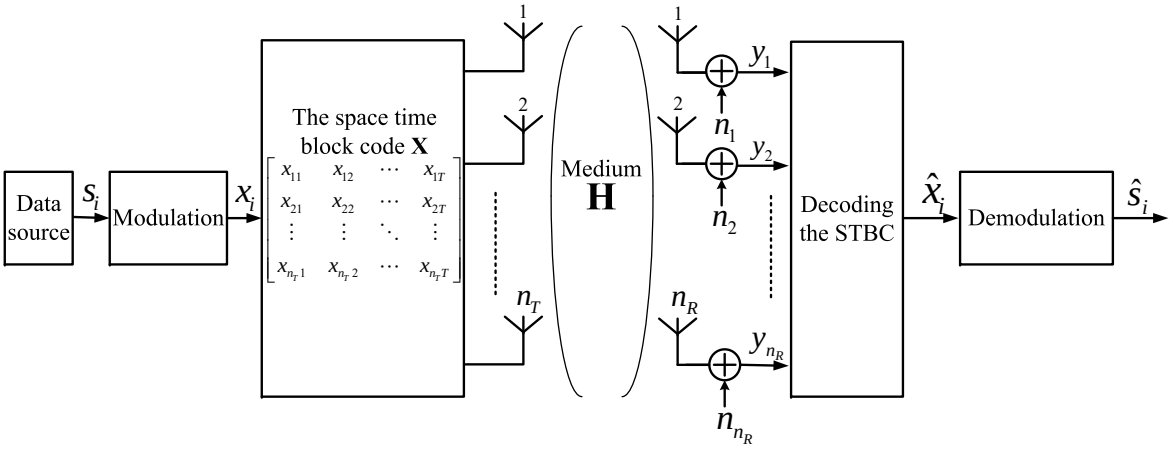

Figure 1.3: A general diagram of the STBC system.

columns as given

$$\mathbf{X} = \begin{bmatrix} x_{11} & x_{12} & \cdots & x_{1T} \\ x_{21} & x_{22} & \cdots & x_{2T} \\ \vdots & \vdots & \ddots & \vdots \\ x_{n_T 1} & x_{n_T 2} & \cdots & x_{n_T T} \end{bmatrix},$$

where $x_{v,t}$ is the value or the complex congugate of the incoming symbol sequence x_i, $i = 1, 2, ..., N_s$. $x_{v,t}$ is transmitted from the v-th transmit anttenna and the t-th time slot.

In addition, linear STBCs are also presented as follows [32]

$$\mathbf{X} = \sum_{i=1}^{N_s} \left(\widehat{x}_i \mathbf{A}_i + j \breve{x}_i \mathbf{B}_i \right),$$

where $\widehat{x}_i = \Re\left(x_i\right)$ is the real part of x_i and $\breve{x}_i = \Im\left(x_i\right)$ is the imagine part of x_i. $\mathbf{A}_i$ and $\mathbf{B}_i$ are available dispersion matrices. Because N_s symbols are transmitted in T symbol periods, the STBC code rate is as follows [68]

$$R = \frac{N_s}{T}.$$

An example with the STBC proposed by Alamouti [2] has a structure as given

$$\mathbf{X} = \begin{bmatrix} x_{11} & x_{12} \\ x_{21} & x_{22} \end{bmatrix} = \begin{bmatrix} x_1 & -x_2^* \\ x_2 & x_1^* \end{bmatrix}.$$

Therefore, the dispersion matrices are as follows

$$\mathbf{A}_1 = \begin{bmatrix} 1 & 0 \\ 0 & 1 \end{bmatrix}; \quad \mathbf{A}_2 = \begin{bmatrix} 0 & -1 \\ 1 & 0 \end{bmatrix};$$

$$\mathbf{B}_1 = \begin{bmatrix} 1 & 0 \\ 0 & -1 \end{bmatrix}; \mathbf{B}_2 = \begin{bmatrix} 0 & 1 \\ 1 & 0 \end{bmatrix}.$$

Besides, Tarokh *et. al* [61] also proposed two criteria in the STBC design to achieve full diveristy and coding gain. From two different coding matrices $\mathbf{X_1}$ and $\mathbf{X_2}$, the difference matrix is defined as given

$$\mathbf{A}\left(\mathbf{X}_1, \mathbf{X}_2\right) = \mathbf{X}_1 - \mathbf{X}_2. \tag{1.4}$$

The determinant of the difference matrix is calculated as follows

$$\mathbf{B}\left(\mathbf{X}_1, \mathbf{X}_2\right) = \mathbf{A}^H \mathbf{A}. \tag{1.5}$$

- **Rank criterion:** In order to achieve full diversity $n_T n_R$ for the STBC $\mathbf{X}$, with two arbitrary matrices $\mathbf{X}_i$ and $\mathbf{X}_q$, $i \neq q$, the difference matrix $\mathbf{A}\left(\mathbf{X}_i, \mathbf{X}_q\right)$ has to be full rank;
- **Determinant criterion:** To increase coding gain for a full diversity code, the minimum determinant $\mathbf{B}\left(\mathbf{X}_i, \mathbf{X}_q\right)$ has to be maximized.

In order to obtain full diversity, the STBC is constructed as an orthogonal structure, called Orthogonal STBC (OSTBC), as given [68]

$$\mathbf{X}\mathbf{X}^H = C \sum_{i=1}^{N_s} |x_i|^2 \mathbf{I},$$

where C is a constant and $\mathbf{I}$ is an $n_T \times n_T$ identity matrix. The Alamouti STBC is the unique complex O-STBC achieving full diversity and full rate [61]. With STBCs for MIMO systems having more than three transmit antennas, several proposed O-STBCs have the code rate $R = 1/2$ [61], [68] or $R = 3/4$ [20], [32] as given

$$\mathbf{X}_4^{1/2} = \begin{bmatrix} x_1 & -x_2 & -x_3 & -x_4 & x_1^* & -x_2^* & -x_3^* & -x_4^* \\ x_2 & x_1 & x_4 & -x_3 & x_2^* & x_1^* & x_4^* & -x_3^* \\ x_3 & -x_4 & x_1 & x_2 & x_3^* & -x_4^* & x_1^* & x_2^* \\ x_4 & x_3 & -x_2 & x_1 & x_4^* & x_3^* & -x_2^* & x_1^* \end{bmatrix},$$

$$\mathbf{X}_4^{3/4} = \begin{bmatrix} x_1 & 0 & x_2 & -x_3 \\ 0 & x_1 & x_3^* & x_2^* \\ -x_2^* & -x_3 & x_1^* & 0 \\ x_3^* & -x_2 & 0 & x_1^* \end{bmatrix}.$$

where $\mathbf{X}_4^{1/2}$ và $\mathbf{X}_4^{3/4}$ respectively denotes that the O-STBC is transmitted from four antennas and has the code rate $1/2$ and $3/4$.

Another solution to attain a code rate $R = 1$ is Quasi-Orthogonal STBC (QO-STBC) [28] where the first and second row, the first and the third row, the second and the fourth row, the third and the fourth row of the matrix $\mathbf{X}$ are orthogonal as follows

$$\mathbf{X}_4^1 = \begin{bmatrix} x_1 & x_2 & x_3 & x_4 \\ -x_2^* & x_1^* & -x_4^* & x_3^* \\ -x_3^* & -x_4^* & x_1^* & x_2^* \\ x_4 & -x_3 & -x_2 & x_1 \end{bmatrix}.$$

At the receiver equipped with n_R receive antennas, the transmitted signals are estimated by the ML detection algorithm. For the O-STBC, the ML algorithm is equivalent to the Maximum Ratio Combining (MRC) technique [32], [68]. Under an assumption that the receiver knows perfect CSI, the transmitted signals are decided based on calculating the minimum distance. Because of coding block design, the detection process at the receiver is linear and is done quickly and accurately [32], [68].

1.3. Research backgound

The spatial modulation (SM) technique was first proposed by Chau *et. al* [12] at the Vehicular Technology Conference in 2001. In [12], the Space Shift Keying system was proposed to exploit the received signals' difference from different antennas to distinguish the transmitted message. However, many antennas are simultaneously switched, this scheme requires synchronization between transmit antennas and utilizes many RF chains. After that, another study brought the SM technique in the Orthogonal Frequency Division Multiplexing (OFDM) system [21]. Using the same principle as the scheme [21], Song *et. al* proposed the Channel Hopping (CH) modulation [55]. However, unlike [21], the CH modulation technique is applied for the arbitrary number of transmit antennas and the position of the active transmit antenna at each symbol period will be known.

The SM technique was proposed for the MIMO systems by Mesleh *et. al* [41], [42] and then it has attracted the researchers' attention. This technique is developed to reduce the complexity and cost of multiple antenna systems without deteriorating the system performance while exploiting the multi-

plexing gain. A special version of the SM technique, called Space Shift Keying (SSK) [30], was proposed by Jeganathan *et. al*. In this model, the SSK transmiter transmits a certain amount of energy from a selected antenna being suitable for information data without transmitting modulated symbols from M-QAM or PSK technique. Both the SM and SSK schemes have been demonstrated to outperform the existing MIMO ones [23], [42]. However, both schemes rely on multiple receive antenna deployment to overcome effects of fading channels. In addition, the SM/SSK spectral efficiency is limited when deployed for wireless systems, equipped with a small or medium number of transmit antennas. As a result, the Generalized SM (GSM) scheme [69] was proposed. By simultaneously activating two or more transmit antennas, the GSM scheme obtains higher spectral efficiency than the SM one. Similarly, Nguyen *el. al* [46] proposed the high rate spatial modulation (HRSM) scheme. The HRSM scheme has a maximum spectral efficiency being linearly proportional with the number of transmit antennas. However, like the SM/SSK scheme, both the GSM and HRSM ones are lack of transmit diversity.

In order to overcome the disadvantage of the SM/SSK scheme, several MIMO-SM transmission systems have recently been proposed. In [14], [15], Di Renzo *et. al* proposed a system that is implemented temporal orthogonal format filters. As a result, the proposed system obtains the second-order transmit diversity without decreasing the transmission rate although this system only utilizes one RF chain. These authors has also extended their proposal by combining the SM technique and the OSTBC in a MIMO architecture that flexibly harmonizes between throughput and the obtained diversity order [16], [17]. More importantly, in this MIMO system, the transmitted signals can be

recovered with a low complexity because of the optimal single-stream detector application.

A new transmission technique, called Space Time Block Coded Spatial Modulation (STBC-SM), was proposed by combining the SM technique and the Alamouti STBC [5]. In the STBC-SM scheme, both the Alamouti matrix and combinations of the transmit antennas carry information. As a result, this scheme obtains the second order transmit diversity. The STBC-SM spectral efficiency, linearly increasing the logarithm of the conbinations of antenna positions, is higher than that of the Alamouti STBC. Besides, because of the Alamouti STBC orthogonality, the transmitted signals are recovered by a low-complexity ML detector at the STBC-SM receiver [5]. Nevertheless, the rotation angles of the STBC-SM matrices must be optimized. As a result, the design of the STBC-SM matrices are significantly complicated, especially when the number of transmit antennas and the modulation order increase.

In [58], Suguira *et. al* extended the SM concept to both spatial and temporal domains to create a new architecture, called Space Time Shift Keying (STSK). The STSK scheme operates by activating one of the Q dispersion matrices to transmit a STSK signal block instead of using the transmit antenna indices to encode information bits as in the SM and SSK ones. In addition, the STSK scheme can flexibly reconciles the diversity order and the spectral efficiency through the optimization of the number and size of dispersion matrices and the number of transmit and receive antennas. At the STSK receiver, because there is no the ICI effect, the transmitted signals are detected by a single-antenna ML detection algorithm. Later, Suguira *et. al* generalized and developed the STSK technique to the General STSK

(G-STSK) [59]. Similar to the STSK scheme, the G-STSK one can flexibly reconcile the diversity order and the spatial multiplexing. Different from the STSK scheme, the G-STSK one selects P of the Q dispersion matrices combining with P modulated symbols to create a G-STSK coding matrix. As demonstrated in [59], the G-STSK architecture encompasses the existing MIMO ones such as SM/SSK, Linear Dispersion Code (LDC), STBC, and V-BLAST. However, there are two main weaknesses of the G-STSK scheme as given

1. There is no general design method for the dispersion matrices of the G-STSK scheme, but only the computerized search method can be used. As a result, the G-STSK matrices' design is significantly complex, especially when the number of transmit antennas or the spectral efficiency increases;

2. The optimal detector in the G-STSK scheme has a high complexity because it is a multiple-stream detector.

The ideas of Basar [5] and Suguira [59] motivated the Vietnamese research group, proposing new MIMO-SM schemes. In [34], this team proposed the high rate STBC-SM (HR-STBC-SM) scheme. In this paper, the spatial constellation (SC) concept was introduced and then the HR-STBC-SM coding matrices are generated by multiplying the Alamouti STBC and the SC matrices. By using the SC matrices, the design of the HR-STBC-SM matrices becomes the design of the SC matrices so that the HR-STBC-SM achieves the second order transmit diversity. Later, based on the SC concept, this group also proposed the Spatially Modulated Orthogonal Space-Time Block Coding (SM-OSTBC) scheme [40] for the MIMO systems, equipped with four

transmit antennas. The SM-OSTBC scheme obtains the third order transmit diversity and has two main benefits such as good performance and low complexity. More importantly, this group developped and proposed a SM-OSTBC technique for the number of transmit antennas greater than 3 [35]. The SM-OSTBC scheme [35] was demonstrated to have higher spatial spectral efficiency than the Basar [5] and Suguira [59] scheme in the same antenna configuration. At the same spectral efficiency and the same antenna configuration, the SM-OSTBC scheme outperforms most existing MIMO ones such as Alamouti [2], V-BLAST [71], QO-STBC [33]. The SM-OSTBC attractiveness compared with the G-STSK scheme is simple coding matrices' design and has a low detection complexity at its receiver because of the single-stream optimal detection algorithm application. However, the SM-OSTBC scheme is suitable for the MIMO systems, equipped with the number of transmit antennas greater than or equal to 4. In order to overcome this drawback, Wang *et. al* proposed the Spatially Modulated Diagonal Space Time Code (SM-DC) scheme [70] that is flexibly used for the MIMO systems, equipped with the number of transmit antennas equal to or less than 4. Based on the SC matrices [35] and the Diagonal Space Time Block Code (D-STBC), the SM-DC scheme obtains the same diversity order as the SM-OSTBC one. In [48], Park *et. al* combined the Double Space Time Transmit Diveristy (DSTTD) scheme and the SM one to create the Double Space Time Transmit Diversity with Spatial Modulation (DSTTD-SM) one. The DSTTD-SM spectral efficiency is twice higher than that of the STBC-SM. However, in this model, the rotation angles must be optimized to eliminate the ICI. In addition, this scheme is only utilized for the MIMO systems, equipped with four transmit antennas,

and only constructs four combinations of transmit antennas to convey two information bits in the spatial domain.

1.4. Conclusion

Basic knowledge directly related to research subjects including the spatial modulation technique, the space time codes, and the MIMO-SM sytem research background is presented in detail in the first chapter. This knowledge will be used as a theoretical background supportting the research issues in the later chapter.

Chapter 2

LOW COMPLEXITY DETECTION ALGORITHMS AND A NEW THEORETICAL UPPER BOUND FOR THE HIGH RATE SPATIAL MODULATION SCHEME

The first section of this chapter provides a brief introduction to the High Rate Spatial Modulation (HRSM) scheme and the optimal ML detector that is used to recover the transmitted signal at the receiver. After that, several sub-optimal low-complexity detectors for the HRSM scheme are presented. Furthermore, the last section decribes a tighter new theoretical BEP upper bound for the HRSM scheme, using the M-QAM technique, in the high SNR region. These results have been published in the works 1, 2 and 5.

2.1. The high rate spatial modulation (HRSM) scheme

2.1.1. The HRSM system model

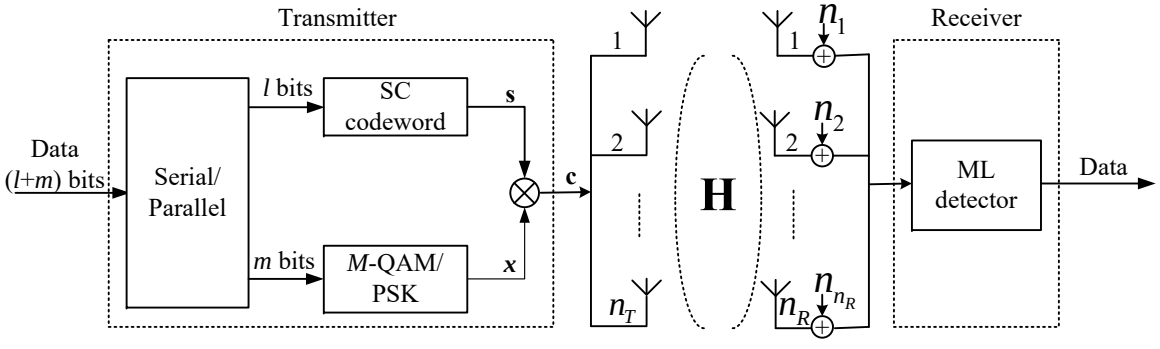

Figure 2.1: A general HRSM scheme [46].

A HRSM system equipped with n_T transmit and n_R receive antennas under a quasi-static Rayleigh fading channel is described in the Figure 2.1. During a

symbol period, each block of $(l+m)$ bits are fed into the HRSM transmitter. In this block, the l bits are mapped into a spatial modulation (SC) codeword out of K SC codewords Ω_S, $(l = \log_2 K)$ while the remaining m bits are modulated by a conventional M-QAM/PSK technique to create a modulated symbol x, $(m = \log_2 M)$. As proposed in [46], the $n_T \times 1$ SC codeword is designed as given

- The first entry of the codeword $\mathbf{s}$ is fixed by 1;
- The $n_T - 1$ remaining entries are randomly selected from the set $\{\pm 1, \pm j\}$, $j^2 = -1$.

  As a result, we have $K = 4^{n_T - 1}$ SC codewords in Ω_S.

For example, a HRSM system with $n_T = 3$ transmit antennas will correspondingly have $K = 4^{n_T-1} = 4^2 = 16$ SC codewords as follows

$$\begin{aligned}
\mathbf{s}_1 &= [\ 1 \ \ 1 \ \ 1\ ]^T; & \mathbf{s}_9 &= [\ 1 \ \ j \ \ 1\ ]^T;\\
\mathbf{s}_2 &= [\ 1 \ \ 1 \ \ -1\ ]^T; & \mathbf{s}_{10} &= [\ 1 \ \ j \ \ -1\ ]^T;\\
\mathbf{s}_3 &= [\ 1 \ \ -1 \ \ 1\ ]^T; & \mathbf{s}_{11} &= [\ 1 \ \ -j \ \ 1\ ]^T;\\
\mathbf{s}_4 &= [\ 1 \ \ -1 \ \ -1\ ]^T; & \mathbf{s}_{12} &= [\ 1 \ \ -j \ \ -1\ ]^T;\\
\mathbf{s}_5 &= [\ 1 \ \ 1 \ \ j\ ]^T; & \mathbf{s}_{13} &= [\ 1 \ \ j \ \ j\ ]^T;\\
\mathbf{s}_6 &= [\ 1 \ \ 1 \ \ -j\ ]^T; & \mathbf{s}_{14} &= [\ 1 \ \ j \ \ -j\ ]^T;\\
\mathbf{s}_7 &= [\ 1 \ \ -1 \ \ j\ ]^T; & \mathbf{s}_{15} &= [\ 1 \ \ -j \ \ j\ ]^T;\\
\mathbf{s}_8 &= [\ 1 \ \ -1 \ \ -j\ ]^T; & \mathbf{s}_{16} &= [\ 1 \ \ -j \ \ -j\ ]^T.
\end{aligned}$$

A $n_T \times 1$ transmit HRSM codeword $\mathbf{c}$ is simply created by multiplying the SC codeword $\mathbf{s}$ and the modulated symbol x, i.e., $\mathbf{c} = \mathbf{s}x$.

At the receiver, the $n_R \times 1$ received signal vector $\mathbf{y}$ is given by

$$\mathbf{y} = \sqrt{\frac{\gamma}{n_T E_s}}\mathbf{H}\mathbf{c} + \mathbf{n} = \sqrt{\frac{\gamma}{n_T E_s}}\mathbf{H}\mathbf{s}x + \mathbf{n}, \tag{2.1}$$

where $\mathbf{H}$ and $\mathbf{n}$ respectively denotes a $n_R \times n_T$ channel matrix and a $n_R \times 1$ noise vector. The entries of $\mathbf{H}$ and $\mathbf{n}$ are assumed to be i.i.d. complex Gaussian random variables with zero mean and unit variance $\mathcal{CN}(0,1)$. E_s is the average symbol energy of x. γ is the average SNR at each receive antenna.

The HRSM spectral efficiency is calculated as given

$$C_{\text{HRSM}} = 2\left(n_T - 1\right) + \log_2 M \ \ (\text{bpcu})\,. \tag{2.2}$$

2.1.2. An optimal ML detection algorithm

Table 2.1: A ML detection algorithm

Step	**Performance**
(1)	Input: $\mathbf{H}, \mathbf{y}$.
(2)	Compute the equivalent channel matrix $\tilde{\mathbf{h}}_k = \sqrt{\frac{\gamma}{n_T E_s}}\mathbf{H}\mathbf{s}_k, \forall k = 1, ..., K$.
(3)	For each matrix $\tilde{\mathbf{h}}_k$ and for each symbol $x_m \in \Omega_x$, compute the Euclidean distances from (2.6) $d_k^m = d_k\left(x_m\right), \forall m = 1, ..., M$.
(4)	Find $d_k^{\min}$ among M values of d_k^m and $\hat{x}_k$ corresponding to $d_k^{\min}$.
(5)	Find index $\hat{k}$ corresponding to the minimum distance $d_{\min}$ among K values of $d_k^{\min}$.
(6)	The estimated SC codeword and modulated symbol are given by $\hat{\mathbf{s}} = \hat{\mathbf{s}}_k, \hat{x} = \hat{x}_k$.
(7)	Output: $\hat{\mathbf{s}}, \hat{x}$.

Under an assumption that the receiver knows perfect CSI [46]. by exhaustively searching in the entire spatial constellation Ω_S and the signal constellation Ω_x, the selected signal pair $(\hat{\mathbf{s}}, \hat{x})$ must satisfy the ML detection algorithm as given [46]

$$(\hat{\mathbf{s}}, \hat{x}) = \underset{\mathbf{s}\in\Omega_s, x\in\Omega_x}{\arg\min} \left\| \mathbf{y} - \sqrt{\frac{\gamma}{n_T E_s}}\mathbf{H}\mathbf{s}x \right\|_F^2, \tag{2.3}$$

where $\|.\|_F$ is the Frobenius norm. Ω_S denotes the spatial constellation and Ω_x is the M-QAM/PSK signal constellation. Corresponding to each codeword $\mathbf{s}_k, \forall k = 1, .., K$, the equivalent channel matrix is presented as $\tilde{\mathbf{h}}_k = \sqrt{\frac{\gamma}{n_T E_s}}\mathbf{H}\mathbf{s}_k$. Therefore, the system equation (2.1) becomes as given

$$\mathbf{y} = \tilde{\mathbf{h}}_k x + \mathbf{n}. \tag{2.4}$$

The ML rule from the equation (2.3) can remove extra elements in the corresponding codeword condition $\mathbf{s}_k$ as follows [46]

$$\hat{x}_k = \underset{x \in \Omega_x}{\arg\min} \left\| \mathbf{y} - \tilde{\mathbf{h}}_k x \right\|_F^2 = d_k(x) + C, \tag{2.5}$$

where C is a constant, $d_k(x)$ is the Euclidean distance corresponding to symbol $\hat{x}_k$ and SC codeword $\mathbf{s}_k$. $d_k(x)$ is calculated as given

$$d_k(x) = \left\| \tilde{\mathbf{h}}_k \right\|_F^2 |x|^2 - 2\Re\left(\mathbf{y}^H \tilde{\mathbf{h}}_k x \right), \tag{2.6}$$

where $\Re(a)$ and $|a|$ respectively denotes the real and the modulus of a complex number a. The condition in the equation (2.5) is rewritten as given

$$\hat{x}_k = \underset{x \in \Omega_x}{\arg\min}\, d_k(x). \tag{2.7}$$

The ML detection algorithm for the conditional signal pair $(\hat{\mathbf{s}}, \hat{x})$ is summarized in the Table 2.1.

2.2. Low complexity detectors for the HRSM system

2.2.1. The modified MMSE-BLAST and MMSE-SQRD detector

First, the HRSM codeword $\mathbf{c}$ can be explicitly expressed as given

$$\mathbf{c} = \begin{bmatrix} c_1 & c_2 & \cdots & c_{n_T} \end{bmatrix}^T = \begin{bmatrix} x & s_2 x & \cdots & s_{n_T} x \end{bmatrix}^T, \tag{2.8}$$

where $[.]^T$ denotes matrix transpose. Since $s_i \in \{\pm 1, \pm j\}, i = 2, 3, ..., n_T$ and $x \in \Omega_x$ belongs to a M-QAM/PSK constellation, $c_k, k = 2, 3, ..., n_T$ also

belongs to the M-QAM/PSK constellation when considering symmetric or square signal constellations $M = 2^{2n}, \forall n \in \mathbb{Z}^+$ such as 4-QAM, 16-QAM. As a result, this means that conventional SIC detectors can be applied to detect the transmitted signals at the HRSM receiver. From the equation (2.8), it can be seen that after recovering the transmitted HRSM vector $\hat{\mathbf{c}}$, the modulated symbol and the transmitted SC codeword are estimated as $\hat{x} = \hat{c}_1, \hat{\mathbf{s}} = \frac{\hat{\mathbf{c}}}{\hat{x}}$.

2.2.1.1. The modified MMSE-VBLAST detector

In a MIMO system, the VBLAST detector [71] has been demostrated to be effective in signal detection close to the ML one while it has lower complexity than the ML algorithm. Therefore, this detector implementation in the HRSM system can reduces the computational complexity in detection process compared with the ML algorithm while ensuring the HRSM system performance.

Considering the HRSM system as an SDM one, the MMSE filter matrix at the receiver can be computed as follows

$$\mathbf{G}_{\text{MMSE}} = \tilde{\mathbf{H}}^H \left(\tilde{\mathbf{H}} \tilde{\mathbf{H}}^H + \frac{1}{E_s} \mathbf{I}_{n_R} \right)^{-1}, \tag{2.9}$$

where $\tilde{\mathbf{H}} = \sqrt{\frac{\gamma}{n_T E_s}} \mathbf{H}$ and $\mathbf{I}_{n_R}$ is an identity matrix. The equation (2.9) is demonstrated in Appendix **A**.

In the detection process, the strongest signal, in terms of the smallest Minimum Square Error (MSE) one that is presented in the third step of the algorithm (Table 2.2) is first detected and then is quantized to the closest value in the signal constellation. After that, the scarcely estimated signal is used to cancel its effect from the received signal vector $\mathbf{y}$. The detection procedure repeats in the same manner untill all signal are detected.

Table 2.2: The MBLAST detection algorithm

Step	Performance
(1)	Input: $\tilde{\mathbf{H}}, \mathbf{y}, E_s$.
(2)	Compute $\mathbf{P} = \left(\tilde{\mathbf{H}}^H \tilde{\mathbf{H}} + \frac{1}{E_s}\mathbf{I}_{n_T}\right)^{-1}$.
(3)	Find the strongest signal index based on $k = \arg\min_i \mathbf{P}_{i,i}$ where $p_{i,i}$ is i diagonal entry of $\mathbf{P}$ and rearrange the entries of $\mathbf{c}$ so that the smallest diagonal entry is the first one.
(4)	Compute $\mathbf{G}_{\text{MMSE}}$ and estimate the LMS $\tilde{c}_k = \mathbf{g}_{\text{MMSE},k}\mathbf{y}$ where $\mathbf{g}_{\text{MMSE},k}$ is the k-th row of $\mathbf{G}_{\text{MMSE}}$.
(5)	$\hat{c}_k = \text{slice}(\tilde{c}_k)$.
(6)	Cancel the effect of $\hat{c}_k$ from $\mathbf{y}$ and reorganize $\tilde{\mathbf{H}}$ by delecting its k-th column.
(7)	Repeat Step 2 to 6 untill all entries of $\hat{\mathbf{c}}$ are detected.
(8)	Rearrange $\hat{\mathbf{c}}$ in the original order.
(9)	Recovering the signal pair $\hat{x} = \hat{c}_1, \hat{\mathbf{s}} = \frac{\hat{\mathbf{c}}}{\hat{x}}$.
(10)	Output: $\hat{\mathbf{s}}, \hat{x}$.

2.2.1.2. The modified MMSE-SQRD detector

As shown in Table 2.2, it can be seen that the MBLAST detector needs to repeatedly do matrix inversion. Therefore, its computational complexity is significantly high, particularly when the number of transmit antennas increases. As a result, the MMSE-SQRD detector [9] is implemented to reduce the detection complexity at the HRSM receiver.

An $(n_T + n_R) \times n_T$ extended channel matrix and an extended received vector $\mathbf{z}$ are defined as given

$$\mathbf{D} = \begin{bmatrix} \tilde{\mathbf{H}} \\ \frac{1}{\sqrt{E_s}}\mathbf{I}_{n_T} \end{bmatrix}, \mathbf{z} = \begin{bmatrix} \mathbf{y} \\ \mathbf{0} \end{bmatrix}.$$

Applying the MMSE-SQRD algorithm [9] to decompose the $\mathbf{D}$, we have

$$\mathbf{D} = \mathbf{QR}, \tag{2.10}$$

where $\mathbf{Q}$ is a $(n_T + n_R) \times n_T$ matrix with orthogonal columns, i.e., $\mathbf{Q}^H\mathbf{Q} = \mathbf{I}_{n_T}$. $\mathbf{R}$ is an $n_T \times n_T$ upper triangular matrix. In addition, the permutation vector $\mathbf{p}$ is used to store the original positional values of the entries of the transmitted signal when implementing the SQRD algorithm. Multiplying $\mathbf{z}$ with $\mathbf{Q}^H$, we have

$$\begin{aligned}\mathbf{v} &= \mathbf{Q}^H\mathbf{z} \\ &= \mathbf{Q}^H\mathbf{Q}\mathbf{R}\mathbf{c} + \mathbf{Q}^H\tilde{\mathbf{n}} \\ &= \mathbf{R}\mathbf{c} + \mathbf{w}, \end{aligned} \tag{2.11}$$

where $\mathbf{w} = \mathbf{Q}^H\tilde{\mathbf{n}}$ and $\tilde{\mathbf{n}}$ is an extended noise vector corresponding to $\mathbf{D}$ and $\mathbf{z}$.

Due to the struture of the $\mathbf{R}$ matrix, the last element of $\mathbf{v}$ is not affected by other elements. Particularly, v_{n_T} only depends on c_{n_T}, so this element is first detected. After that, $\hat{c}_{n_T}$ is estimated by slicing $v_{n_T}/r_{n_T,n_T}$. It is assumed that $\hat{c}_{n_T}$ is exactly recovered and then its effect will be cancelled out from v_{n_T-1}. The v_{n_T-1} only depends on c_{n_T-1}. Hence, $\hat{c}_{n_T-1}$ can be immediately estimated by slicing $v_{n_T-1}/r_{n_T-1,n_T-1}$. Similarly, $\hat{c}_{n_T}$ and $\hat{c}_{n_T-1}$ will be cancelled out from v_{n_T-1} to detect $\hat{c}_{n_T-2}$. The procudure continues until $\hat{c}_1$ is obtained. Later, the transmitted vector $\hat{\mathbf{c}}$ is recovered by arranging the estimated vector in the original order from the permutation vector $\mathbf{p}$. Finally, data bits are completely recovered. The modified MMSE-SQRD (MSQRD) detection algorithm can be summarized in Table 2.3.

2.2.2. The improved SQRD detection algorithm

From the above analysis, it can be seen that the MSQRD detector obtains a low computational complexity, but its performance is poor. Therefore, a new detection algorithm based on the MSQRD one is proposed to improve

Table 2.3: The MSQRD detection algorithm

Step	**Performance**
(1)	Input: $\mathbf{z}, \mathbf{D}$.
(2)	Decompose $\mathbf{D}$ using MMSE-SQRD algorithm to get $\mathbf{Q}, \mathbf{R}$ and the permutation vector $\mathbf{p}$.
(3)	Compute $\mathbf{v} = \mathbf{Q}^H \mathbf{z}$.
(4)	Detection and cancellation: For $k = n_T : -1 : 1$ If $k == n_T$ $\hat{c}_k = \text{slice}\left(\frac{v_k}{r_{k,k}}\right)$ Else For $l = k+1 : n_T$ $v_k = v_k - r_{k,l}\hat{c}_l$ End $\hat{c}_k = \text{slice}\left(\frac{v_k}{r_{k,k}}\right)$ End End.
(5)	Rearrange $\hat{\mathbf{c}}$ in the original order from the permutation vector $\mathbf{p}$.
(6)	Recover the signal pair $\hat{x} = \hat{c}_1, \hat{\mathbf{s}} = \frac{\hat{\mathbf{c}}}{\hat{x}}$.
(7)	Output: $\hat{\mathbf{s}}, \hat{x}$.

the detection performance in the HRSM system. From the equation (2.8), it can be seen that the first entry of the transmitted signal $\mathbf{c}$ is the modulated symbol x, $\mathbf{c}_1 = x$ and $n_T - 1$ remaining entries of the vector $\mathbf{c}$ is a multiplication of x and $s_i \in \{\pm 1, \pm j\}, i = 2, 3, ..., n_T$. Therefore, in the ISQRD detector, the first column of the $\mathbf{H}$ channel matrix corresponding to the first entry of the $\mathbf{c}$ vector is removed and then the Euclidean distance for the remaing entries of the $\mathbf{c}$ vector in the signal constellation Ω_x is calculated to find the modulated symbol, having the smallest distance.

The equation (2.1) is re-expressed as given

$$\mathbf{t}_x = \bar{\mathbf{H}}\bar{\mathbf{c}} + \mathbf{n}, \tag{2.12}$$

Table 2.4: The ISQRD detection algorithm

Step	**Performance**
(1)	Input: $\mathbf{y}, \tilde{\mathbf{H}}$.
(2)	Decompose $\tilde{\mathbf{H}}$ using MMSE-SQRD algorithm to get $\mathbf{Q}, \mathbf{R}$ and the permutation vector $\mathbf{p}$.
(3)	Detection and cancellation: For $m = 1 : M$ Compute $\mathbf{t}_m = \mathbf{y} - \tilde{\mathbf{h}}_1 x_m$ và $\mathbf{v} = \mathbf{Q}^H \begin{bmatrix} \mathbf{t}_m \\ 0 \end{bmatrix}$ For $k = n_T - 1 : -1 : 1$ If $k == n_T - 1$ $\hat{\bar{c}}_{m,k} = \text{slice}\left(\frac{v_k}{r_{k,k}}\right)$ Else For $l = k + 1 : n_T - 1$ $v_k = v_k - r_{k,l}\hat{\bar{c}}_{m,l}$ End $\hat{\bar{c}}_{m,k} = \text{slice}\left(\frac{v_k}{r_{k,k}}\right)$ End End Compute $d_m = \left\|\mathbf{t}_m - \bar{\mathbf{H}}\hat{\bar{\mathbf{c}}}_{m,p}\right\|^2$ End.
(4)	Find $\hat{m}$: $\hat{m} = \arg\min_m d_m$.
(5)	Recover the signal pair $\hat{x} = x_{\hat{m}}$, $\hat{\mathbf{s}} = \frac{1}{\hat{x}}\begin{bmatrix} \hat{x} & \hat{\bar{\mathbf{c}}}_{\hat{m},p} \end{bmatrix}^T$.
(6)	Output: $\hat{\mathbf{s}}, \hat{x}$.

where $\mathbf{t}_x = \mathbf{y} - \tilde{\mathbf{h}}_1 x$, $\bar{\mathbf{H}} = [\ \tilde{\mathbf{h}}_2 \ \ \tilde{\mathbf{h}}_3 \ \ \cdots \ \ \tilde{\mathbf{h}}_{n_T}\ ]$, $\tilde{\mathbf{h}}_k$ is the k-th column of $\tilde{\mathbf{H}}$. $\bar{\mathbf{c}}$ includes the $n_T - 1$ remaining entries of the $\mathbf{c}$ vector (remove the first entry). For an arbitrary $x_m, \forall m = 1, ..., M$, in the signal constellation, we have a corresponding system similar to that in the equation (2.1). Therefore, we apply the MMSE-SQRD algorithm [9] for the equation (2.12) to recover $\hat{\bar{\mathbf{c}}}_m$ and then calculate the corresponding Euclidean distance $d_m = \left\|\mathbf{t}_m - \bar{\mathbf{H}}\hat{\bar{\mathbf{c}}}_{m,p}\right\|^2$ where $\hat{\bar{\mathbf{c}}}_{m,p}$ is the vector, re-arranged from $\hat{\bar{\mathbf{c}}}_m$ by using the permutation vector $\mathbf{p}$ and $\mathbf{t}_m = \mathbf{y} - \tilde{\mathbf{h}}_1 x_m$. The index m of the transmitted symbol x is determined by

using $\hat{m} = \arg\min_{m} d_m$. Finally, the modulated symbol and the transmitted SC codeword is respectively recovered as $\hat{x} = x_{\hat{m}}$ and $\hat{\mathbf{s}} = \frac{1}{\hat{x}}[\ \hat{x}\ \ \hat{\tilde{\mathbf{c}}}_{\hat{m},p}\ ]$. The improved SQRD (ISQRD) can be summarized in Table 2.4.

2.2.3. Detector complexity analysis

When calculating the complexity of each detector, it is assumed that each real algebraic operation such as a real addition/subtraction, a real division or a real multiplication is considered as a floating point operation (flop). Therefore, a complex addition/subtration is equal two real operations, i.e., 2 flops. A complex multiplication includes 4 real multiplications and two real additions, i.e., 6 flops. A complex division is considered as 11 flops. The flop calculation regulations is presented in Appendix **B**. The optimal ML detector complexity is calculated as given

$$\rho_{\mathrm{ML}} = MK\left(16n_R + 6\right) + \left(8n_R n_T - 2n_R\right)K. \tag{2.13}$$

Based on the complexity analysis from [22], the MBLAST complexity is calculated as follows

$$\rho_{\mathrm{MBLAST}} = 15n_T^4 + 2n_T^3 n_R + n_T^2 n_R^2 + n_T\left(16n_R - 2\right). \tag{2.14}$$

In turn, the MSQRD and ISQRD complexities are calculated as given

$$\rho_{\mathrm{MSQRD}} = 8n_T^3 + n_T^2\left(8n_R - 3\right) - n_T\left(10n_R + 13\right) + 8, \tag{2.15}$$

$$\begin{aligned}\rho_{\mathrm{ISQRD}} &= 8(n_T - 1)^3 + \left(8n_R - 11 + 12M\right)\left(n_T - 1\right)^2 \\ &+ \left(M\left(16n_R - 12\right) - 14n_R + 4\right)\left(n_T - 1\right) + M\left(10n_R + 7\right) + 5.\end{aligned} \tag{2.16}$$

The complexity equation of the MBLAST, ML, MSQRD, ISQRD detectors are presented in Appendix **B**.

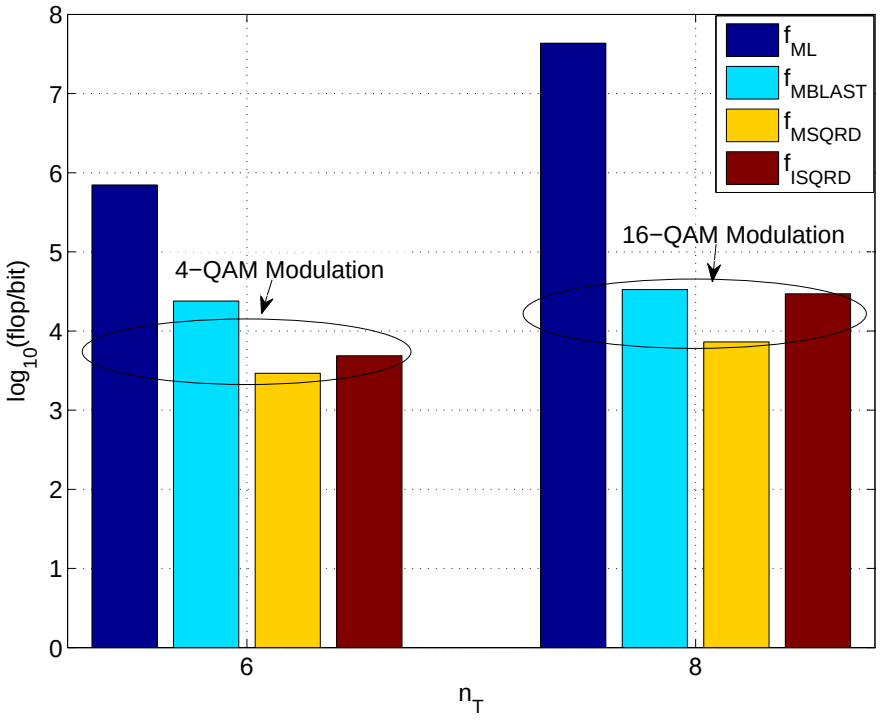

Figure 2.2: Complexities of ML, MBLAST, MSQRD, and ISQRD detectors in different MIMO configurations; 4-QAM and 16-QAM technique.

The Figure 2.2 compares the complexities of the ML, MBLAST, MSQRD, and ISQRD detectors at the same spectral efficiency in two different circumstances as given

1. The (6,6) MIMO system, i.e., the number of transmit and receive antennas, $n_T = n_R = 6$ using the 4-QAM technique;

2. The (8,8) MIMO system with the number of transmit and receive antennas, $n_T = n_R = 8$ using the 16-QAM technique.

From Figure 2.2, it can be seen that although the ML detection algorithm is optimized, its complexity is the highest. Meanwhile, the MSQRD detector achieves the lowest complexity. In the (6,6) MIMO system, the ISQRD detector has lower complexity than that of MBLAST one. However, when the number of transmit antennas increases, the ISQRD complexity is ap-

proximately equivalent to the MBLAST one. It can be explained that the ISQRD complexity depends on the M modulation order which is increased from 4-QAM in the (6,6) MIMO system to 16-QAM in the (8,8) MIMO one.

2.2.4. Simulation results

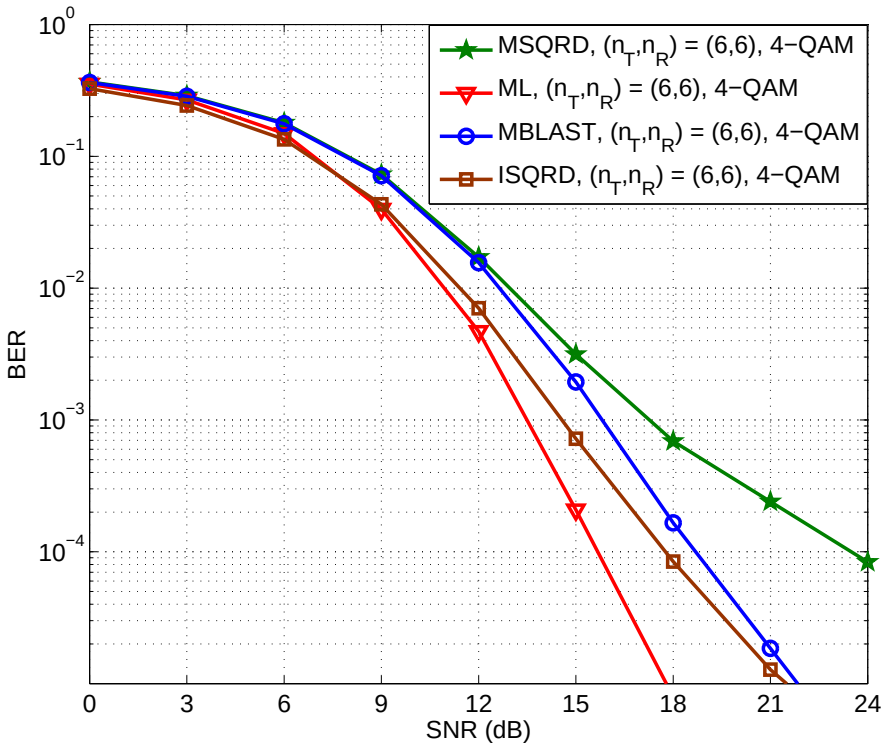

Figure 2.3: BERs of a HRSM scheme with $n_T = n_R = 6$ using ML, MBLAST, MSQRD, and ISQRD detectors; 4-QAM technique.

Figure 2.3 and Figure 2.4 respectively compares bit error rates (BER) of the ML, MBLAST, MSQRD, and ISQRD detectors in the (6,6) MIMO system using 4-QAM technique and the (8,8) MIMO system using 16-QAM technique. From analytical and simulation results in Figure 2.2, Figure 2.3, and Figure 2.4, one can see that although the ML detector has the best performance, its complexity is also the highest. As a result, it is difficult to implement this detector in practice. On the other hand, in spite of the fact that the MSQRD detector offers the lowest detection complexity, it suffers

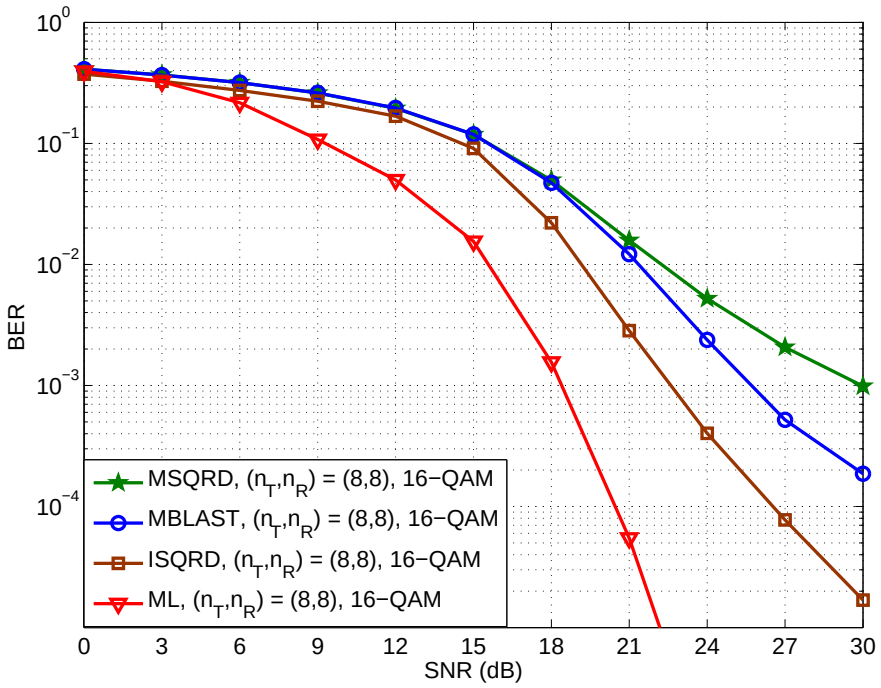

Figure 2.4: BERs of a HRSM scheme with $n_T = n_R = 8$ using ML, MBLAST, MSQRD, and ISQRD detectors; 16-QAM technique.

from significant performance degradation. Particularly, at the BER $= 10^{-4}$ in Figure 2.3, the MSQRD detector loses about 8,5 dB, 5,5 dB, 4,8 dB SNR gains compared with the ML, ISQRD and MBLAST ones, respectively. The SNR gain gaps between the MSQRD detector and other detectors increase when the BER is smaller. At BER $= 10^{-5}$, the MBLAST and the ISQRD detectors have lower SNR gains about 4,5 dB and 4 dB than the ML one. However, two detectors' complexities significantly decrease. Particularly, at the HRSM (6,6) system in Figure 2.2, the MBLAST and ISQRD detectors respectively decreases 75 and 149 times about complexity compared to the ML one.

When the number of transmit antennas increases to 8, i.e., the HRSM (8,8) system using 16-QAM technique, the complexity gaps between the MBLAST, ISQRD detectors and the ML one increase. Particularly, these detectors' com-

plexities respectively decreases about 1509 and 1523 times compared with that of the ML one. However, the cost of decreasing complexity is that two detectors' performances is respectively loser 7,5 dB and 4,5 dB about SNR gains than that of the ML one at $\mathrm{BER} = 10^{-3}$ in Figure 2.4. Figure 2.2 and Figure 2.4 show that the MBLAST and the ISQRD complexities are nearly the same. However, the ISQRD detector remarkably achieves higher performance than that of the MBLAST one, especially at the high SNR region. In addition, the MBLAST detector tends to make the diversity order of the HRSM system reduce more seriously than the ISQRD one as the SNR increases. Based on performance and complexity analyses, telecommunication researchers and designers can select an appropriate detector compromising complexity and performance when they implement HRSM systems in practice.

2.2.5. The HRSM performance under spatial correlation effect

Theoretically, it is assumed that the space at the transmitter and the receiver is large enough to deploy the transmit and receive antennas. Therefore, there is no correlation among these antennas. However, because the transmitter and the receiver do not have a sufficiently large space to deploy the transmit and receive antennas, it will creates a local dispersion effect. As a result, the MIMO systems' performances are affected by the spatial correlation effect among the transmit or the receive antennas.

To evaluate the spatial correlation effect, the channel matrix is supplemented the correlation element in the below model as follows

$$\mathbf{H}_{\mathrm{corr}} = \mathbf{R}_R^{\frac{1}{2}} \mathbf{H} \left(\mathbf{R}_T^{\frac{1}{2}} \right)^T \tag{2.17}$$

where $(n_R \times n_R)\,\mathbf{R}_R$ and $(n_T \times n_T)\,\mathbf{R}_T$ is respectively the spatial correlation matrix at the receiver and transmitter.

In this section, we use a realistic correlated model that is the exponential correlation one [39] to clearly illustrate the spatial correlation effect. In this model, the components of $\mathbf{R}_R$ and $\mathbf{R}_T$ are determined as given

$$r_{iq} = \begin{cases} r^{q-i}, & i \leq q \\ r^{*}_{qi}, & i > q \end{cases}, |r| \leq 1, \tag{2.18}$$

where r the correlation coefficient between two adjacent receive or transmit antennas, $r \geq 0$ and $r = 0$ when there is no spatial correlation effect. When occuring the spatial correlation effect among transmit or receive antennas, the detectors' performances in the HRSM system decrease because the incorrect detection probability of the SC codewords increases.

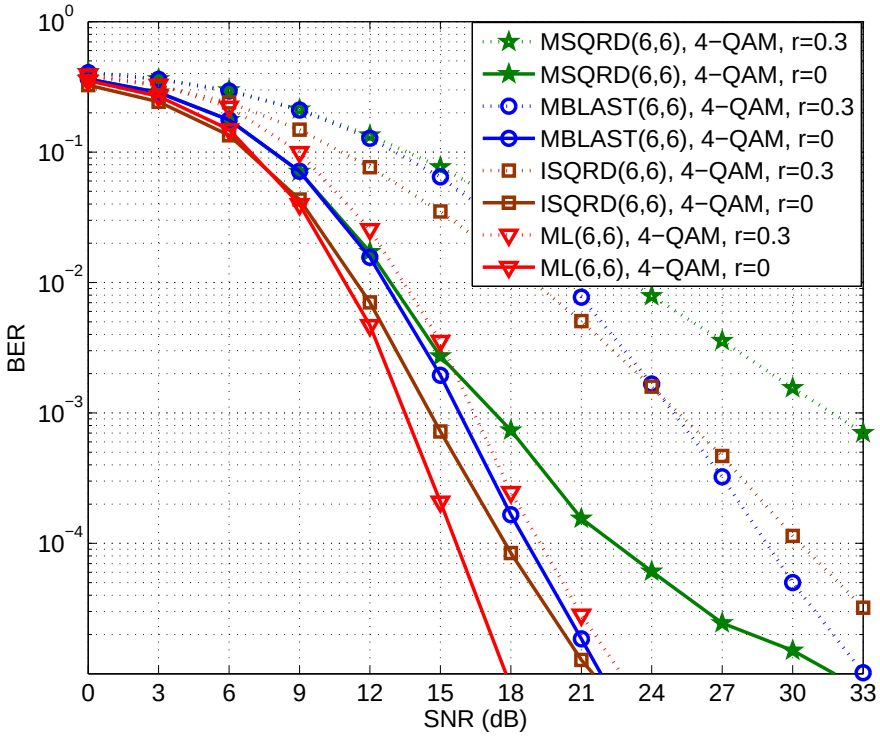

Figure 2.5: BER comparison of the ML, MBLAST, MSQRD, and ISQRD detectors for the (6,6) HRSM system, 4-QAM, correlation coefficients r=0 and 0.3.

Figure 2.5 compares the detectors' performances in the HRSM (6,6) system using the 4-QAM technique under two channel conditions such as the low correlated MIMO channel where the correlation coefficient r=0.3 and the uncorrelated MIMO channel, r=0. The simulation results in Figure 2.5 show that these detectors still achieve good performances under the low correlated MIMO channel condition. At BER $= 10^{-3}$, the MSQRD performance is less about 6 dB SNR gain than that of the MBLAST and the ISQRD and approximately 15 dB SNR gain than that of the ML one. At SNR $> 24,2$ dB, the MBLAST performance is better than that of the ISQRD. It can be explained that because of the MBLAST detection structure, the MBLAST detector always selects the best signal to first detect. Meanwhile, the ISQRD detector does not consider the first column of the channel matrix, so there will be cases where the best signal can not be selected for detection process.

2.2.6. The HRSM system under imperfect channel

To evaluate the HRSM performance in simulation results, it is always assumed to know perfect CSI at the receiver. However, in practice the HRSM receiver is implemented channel estimation algorithms to estimate the channel matrix. Therefore, the estimated channel matrix always has a certain error that will affect to the HRSM performance. As a result, in order to evaluate imperfect CSI (I-CSI) effect to the system performance, a measurement parameter, β, expressing error estimation value, is proposed in [56] to evaluate the channel estimation effect on the performances of wireless communication systems, $0 \leq \beta \leq 1$. Pefect CSI (p-CSI) when $\beta = 1$, i.e., $1 - \beta = 0$. At

that time, the channel matrix of the HRSM system is presented as given

$$\breve{\mathbf{H}} = \beta\mathbf{H} + (1-\beta)\,\mathbf{E}, \tag{2.19}$$

where $\mathbf{E}$ is a $n_R \times n_T$ matrix. The entries of the $\mathbf{E}$ matrix are i.i.d. complex Gaussian random variables with zero mean and unit variance, i.e., $\mathcal{CN}(0,1)$.

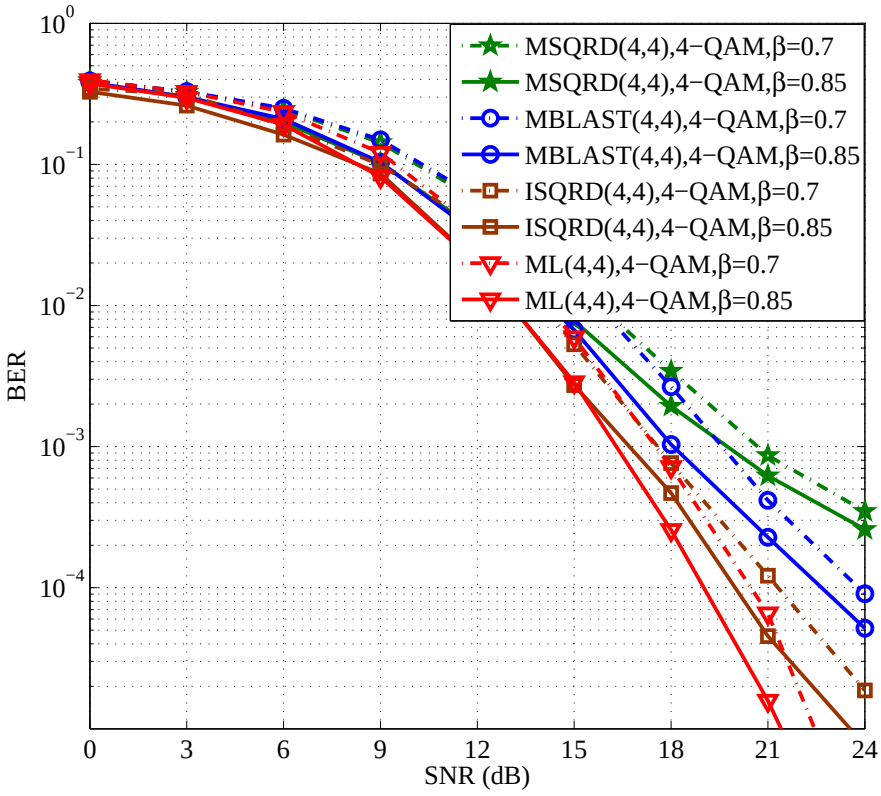

Figure 2.6: Comparison the performance of the ML, MBLAST, MSQRD, and ISQRD detectors in the HRSM system (4,4), 4-QAM technique under imperfect CSIs such as β=0.85 and 0.7.

Figure 2.6 compares the performance of the MSQRD, MBLAST, ISQRD, and ML detectors for the HRSM system, having 4 transmit and 4 receive antennas using 4-QAM technique, in two I-CSI scenarios β =0.85 and β =0.7, i.e., the channel estimation errors is respectively 15% and 30%. The simulation results show that with low estimation error, these detectors still have good performances. When the estimation error increases, these detector per-

formances deteriorate approximately 1 dB about SNR gain. Therefore, we can infer the HRSM performance when the channel estimation error increases, i.e., the coefficient β decreases.

2.3. A new BEP upper bound of the HRSM system

In this section, the above ML detection algorithm is re-expressed as in [35]. In addition, before begining to demonstrate the tigher new BEP upper bound, the proposed BEP upper bound for the HRSM system [46] is also briefly discussed.

For a given $\mathbf{s}_k, k = 1, 2, ..., K,$, the modulated symbol $\hat{x}_k$ is recovered as given

$$\hat{x}_k = \underset{x \in \Omega_x}{\arg\min} \left\| \mathbf{y} - \tilde{\mathbf{h}}_k x \right\|^2. \tag{2.20}$$

Several parameters are defined as follows

$$\bar{x}_k = \frac{\Re\left(\mathbf{y}^H \tilde{\mathbf{h}}_k\right)}{\left\|\tilde{\mathbf{h}}_k\right\|^2} - j\frac{\Im\left(\mathbf{y}^H \tilde{\mathbf{h}}_k\right)}{\left\|\tilde{\mathbf{h}}_k\right\|^2}, \tag{2.21}$$

$$R_k = \|\mathbf{y}\|^2 - \left\|\tilde{\mathbf{h}}_k\right\|^2 \|\bar{x}_k\|^2, \tag{2.22}$$

$$d_k(\mathbf{y}, x) = \|x - \bar{x}_k\|^2. \tag{2.23}$$

At that time, the target function in the equation (2.20) is rewritten as given

$$\left\| \mathbf{y} - \tilde{\mathbf{h}}_k x \right\|^2 = \left\|\tilde{\mathbf{h}}_k\right\|^2 d_k(\mathbf{y}, x) + R_k. \tag{2.24}$$

Because R_k does not depend on x, the equation (2.20) can be reduced as given

$$\hat{x}_k = \underset{x \in \Omega_x}{\arg\min}\, d_k(\mathbf{y}, x). \tag{2.25}$$

With each $\hat{x}_k$ detected above, we define the L_k parameter as follows

$$L_k = \left\|\tilde{\mathbf{h}}_k\right\|^2 \left(d_k(\mathbf{y}, \hat{x}_k) - |\bar{x}_k|^2\right). \tag{2.26}$$

Therefore, the index of $\mathbf{s}_k$ can be recovered according to

$$\hat{k} = \underset{k=1,2,\ldots,K}{\arg\min} L_k. \tag{2.27}$$

Finally, the SC codeword and the modulated symbol are estimated by the k index as follows

$$\hat{\mathbf{s}} = \mathbf{s}_{\hat{k}}, \hat{x} = \hat{x}_{\hat{k}}. \tag{2.28}$$

From $\hat{\mathbf{s}}$ and $\hat{x}$ estimated above, $(l+m)$ data bits are recovered.

2.3.1. The union bound of the HRSM system

According to [34], [46], the union bound (i.e., upper bound) of the HRSM scheme is given by

$$P_e \leq \frac{1}{(l+m)\,N} \sum_{i=1}^{N} \sum_{q=1}^{N} P\left(\mathbf{c}_i \rightarrow \mathbf{c}_q\right) w_{i,q}, \tag{2.29}$$

where $P\left(\mathbf{c}_i \rightarrow \mathbf{c}_q\right)$ is the pairwise error probability (PEP) of deciding $\mathbf{c}_q$ while $\mathbf{c}_i$ is transmitted. The PEP $P\left(\mathbf{c}_i \rightarrow \mathbf{c}_q\right)$ is evaluated by averaging $P\left(\mathbf{c}_i \rightarrow \mathbf{c}_q|\mathbf{H}\right)$ over the channel matrix $\mathbf{H}$ as presented in [34], [45]. $N = KM = 2^{l+m}$ is the total number of the HRSM codewords and $w_{i,q}$ is the number of erroneous bits between $\mathbf{c}_i$ and $\mathbf{c}_q$.

2.3.2. A new BEP upper bound of the HRSM system

In this section, a novel theorem and the corresponding demonstration are presented so as to derive the new upper bound for the HRSM scheme using QAM modulation. Firstly, we define the concept of "nearest symbol" as follows: Let $x, x' \in \Omega_x$, $x' \neq x$ where Ω_x is a QAM constellation. Then x and x' are said to be "nearest symbol" if and only if the Euclidean distance between x and x' is minimum.

Theorem: Given a transmitted HRSM codeword matrix $\mathbf{c}_i = \mathbf{s}_k x_n$, $i = 1, 2, ..., N$; $k = 1, 2, ..., K$; and $n = 1, 2, ..., M$, Let us define V_n is the set of nearest symbols of x_n and $\bar{V}_n = \Omega_x - V_n$ is the set of remaining symbols that are not nearest symbols of x_n. In addition, we define the set of SC codewords from the nearest symbols as given

$$\Omega_i = \Omega_{\mathbf{c}} - \left\{ \mathbf{c} \in \Omega_{\mathbf{c}} | \mathbf{c} = \mathbf{s}_k x_v, x_v \in \bar{V}_n \right\}, \tag{2.30}$$

where $\Omega_{\mathbf{c}}$ is the set of the total N HRSM codewords $\mathbf{c}$. The new upper bound for the BEP of the HRSM scheme is given as follows

$$P_e \leq \frac{1}{(l+m)\, N} \sum_{i=1}^{N} \sum_{\mathbf{c}_q \in \Omega_i} P\left(\mathbf{c}_i \to \mathbf{c}_q\right) w_{i,q}. \tag{2.31}$$

Proof: Assumed that $\mathbf{y}$ is the received signal vector and then the receiver decides the codeword $\mathbf{c}_q = \mathbf{s}_k x_v \in \Omega_{\mathbf{c}} - \Omega_i$ while the codeword $\mathbf{c}_i = \mathbf{s}_k x_n$ is transmitted, where $x_v \in \bar{V}_n$ and $x_v \neq x_n$. By the above definition of $\mathbf{c}_i$ and $\mathbf{c}_q$, we can clearly see that as both $\mathbf{c}_i$ and $\mathbf{c}_q$ have the same $\mathbf{s}_k$, the detector estimates x as x_v instead of x_n.

Let us define $V_n = \{x_{n1}, x_{n2}, ..., x_{nQ}\}$ where Q only can be equal to 2, 3 or 4 when considering the construction of the QAM constellation symbols. In order to prove the equation (2.31), we need to prove that the PEP $P\left(\mathbf{c}_i \to \mathbf{c}_q\right)$ is repeatedly calculated and can be eliminated in the estimation process of the average error probability P_e. An example illustrating the calculation overlap in the average PEP estimation process of the union bound is presented as in Appendix **C**.

Following the definition in the equation (2.23), we can see that $d_k\left(\mathbf{y}, x_v\right)$ is the minimum value among $\left\{d_k\left(\mathbf{y}, x\right) | x \in \Omega_x\right\}$ because x_v is the solution of equation (2.25). With two nearest symbols x_v and x_n, the distance between

two SC codewords $\mathbf{c}_q = \mathbf{s}_k x_v$ and $\mathbf{c}_i = \mathbf{s}_k x_n$ is always the closest because of

$$\begin{aligned}\left(\mathbf{c}_i - \mathbf{c}_q\right)^H \left(\mathbf{c}_i - \mathbf{c}_q\right) &= \left(\mathbf{s}_k \Delta_x\right)^H \left(\mathbf{s}_k \Delta_x\right) \\ &= \left\|\mathbf{s}_k\right\|^2 \left|\Delta_x\right|^2,\end{aligned}$$

where $\left\|\mathbf{s}_k\right\|^2 = C, \forall \mathbf{s}_k \in \Omega_S$, with C is a fixed constant as all entries of $\mathbf{s}_k$, $\mathbf{s}_k \in \{\pm 1, \pm j\}$, $\Delta_x = x_v - x_n$. The Euclidean distance among two SC codewords depends on the distance among two nearest symbols $\left|\Delta_x\right|^2$. To eliminate $P\left(\mathbf{c}_i \to \mathbf{c}_q\right)$ from the upper bound (2.29), we have to prove that there exists at least a index $n_q \in \{n_1, n_2, ..., n_Q\}$ such that [8]

$$\left\{\mathbf{y} | d_k\left(\mathbf{y}, x_v\right) = \min_{x \in \Omega_x} d_k\left(\mathbf{y}, x\right)\right\} \subset \left\{\mathbf{y} | d_k\left(\mathbf{y}, x_{n_q}\right) \leq d_k\left(\mathbf{y}, x_n\right)\right\}. \quad (2.32)$$

This is equivalent to show that

$$d_k\left(\mathbf{y}, x_{n_q}\right) \leq d_k\left(\mathbf{y}, x_n\right). \quad (2.33)$$

For each $n_q \in \{n_1, n_2, ..., n_Q\}$, let us define

$$V_{n,n_q} = \left\{\mathbf{y} | d_k\left(\mathbf{y}, x_{n_q}\right) \leq d_k\left(\mathbf{y}, x_n\right)\right\}, \quad (2.34)$$

$$E_n = E - \left\{\mathbf{y} | d_k\left(\mathbf{y}, x_n\right) = \min_{x \in \Omega_x} d_k\left(\mathbf{y}, x\right)\right\}. \quad (2.35)$$

where the set E contains every point on the QAM modulation plane. Here, to prove the equation (2.33), we need to show that

$$\bigcup_{n_q = n_1, n_2, ..., n_Q} V_{n,n_q} = E_n. \quad (2.36)$$

We consider the plane E as a Voronoi diagram generated by M-QAM modulation symbols. For the case of $Q = 2$, i.e., x_n has two nearest symbols x_{n_1} and x_{n_2} as shown in Figure 2.7. we can easy see that the Voronoi region generated by x_n corresponds to $E - E_n$ as the blue region and the remaining

white region corresponds to E_n. The red vertical line divides the plane E into 2 half-plane, one of them that contains x_{n_1}, corresponds to V_{n,n_1}. Similarly, we also define the region of V_{n,n_2}. By observing 2.7, we can easily verify the accuracy of the equation (2.36). Similarly to the case of $Q = 2$, we also successfully prove the equation (2.36) is true in case of $Q = 3$ or $Q = 4$. Hence, the prove is proved completely.

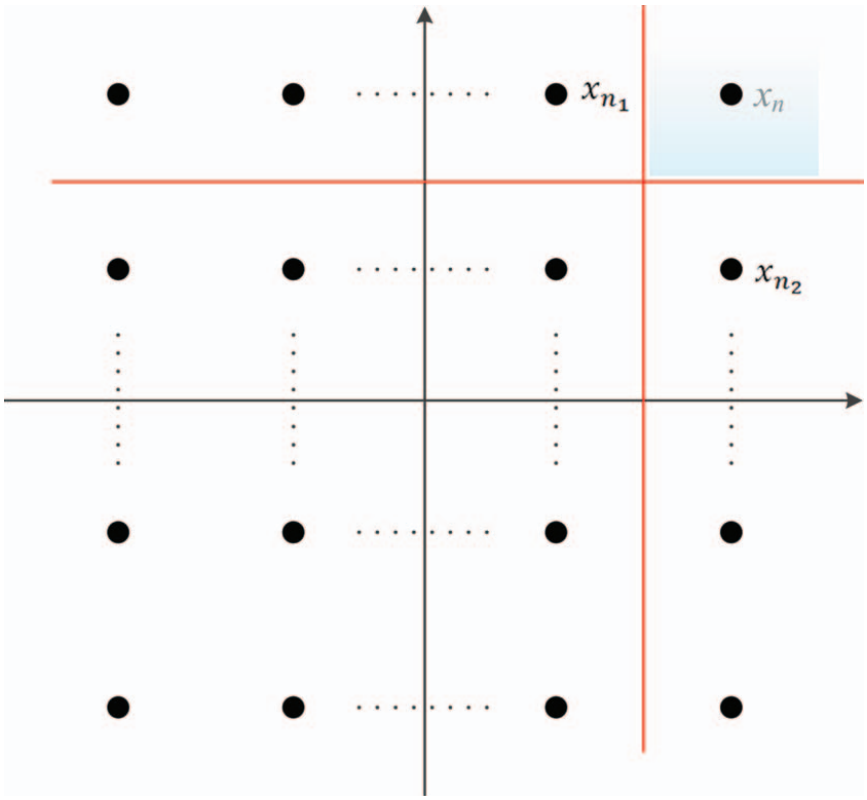

Figure 2.7: The construction of QAM constellation with two nearest symbols x_{n_1} and x_{n_2} of x_n.

Finally, we will formulate the number of excluded PEPs. Among the total of $M = 2^m$ QAM constellation symbols, where $m \geq 2$ is an even number, there are 4 symbols which has 2 nearest symbols, $4\left(\sqrt{M}-2\right)$ symbols which have 3 nearest symbols and $\left(\sqrt{M}-2\right)^2$ symbols which have 4 nearest symbols. For instance, with 16-QAM modulation (i.e., M=16), the number of symbols

having 2, 3, or 4 nearest symbols respectively is 4, 8, and 4. Each symbol having 2, 3, or 4 nearest symbols, the number of excluded non-zero PEPs is $M-3$, $M-4$, and $M-5$, respectively. Thus, the total number of excluded non-zero PEPs is calculated as follows

$$\begin{aligned} & K\left(4\left(M-3\right)+4\left(\sqrt{M}-2\right)\left(M-4\right)+\left(\sqrt{M}-2\right)^{2}\left(M-5\right)\right) \\ & =K\left(M^{2}-5M+4\sqrt{M}\right). \end{aligned} \tag{2.37}$$

while, the number of non-zero PEPs of the union bound in the equation (2.29) is $N\left(N-1\right)=KM\left(KM-1\right)$. The equation (2.37) shows that the number of excluded non-zero PEPs increase when the modulation order M increases. In such cases, we expect that the new upper bound is much tighter than the union bound.

2.3.3. Result analysis

In this section, we compare the new bound with the union bound and simulation results of a number of HRSM configurations. For convenience, we denote a MIMO system with n_T transmit and n_R receive antennas as the (n_T, n_R) system.

In Fig 2.8, the new upper bound, the union bound and simulation results for the BER of the (2,2) HRSM system using 64-QAM are shown. As indicated in Fig 2.8, we can see that the union bound and the new bound are very close to the simulation curve in sufficiently high SNR region, SNR $\geq$ 30 dB, however, in low SNR region they are still loose. We observe that the new bound is closer to the simulation curve. Particularly, at BER $= 10^{-3}$, the new bound is tighter than the union bound by an SNR gain of approximately 0.5 dB.

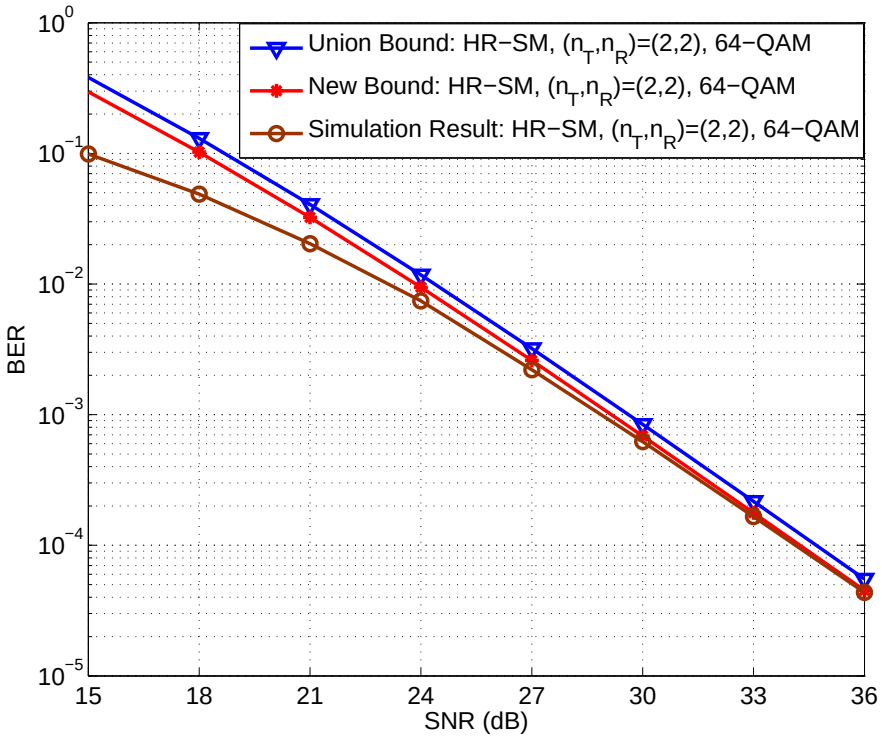

Figure 2.8: The new upper bound, the union bound and simulation curve for the BER of the (2,2) HRSM system using 64-QAM.

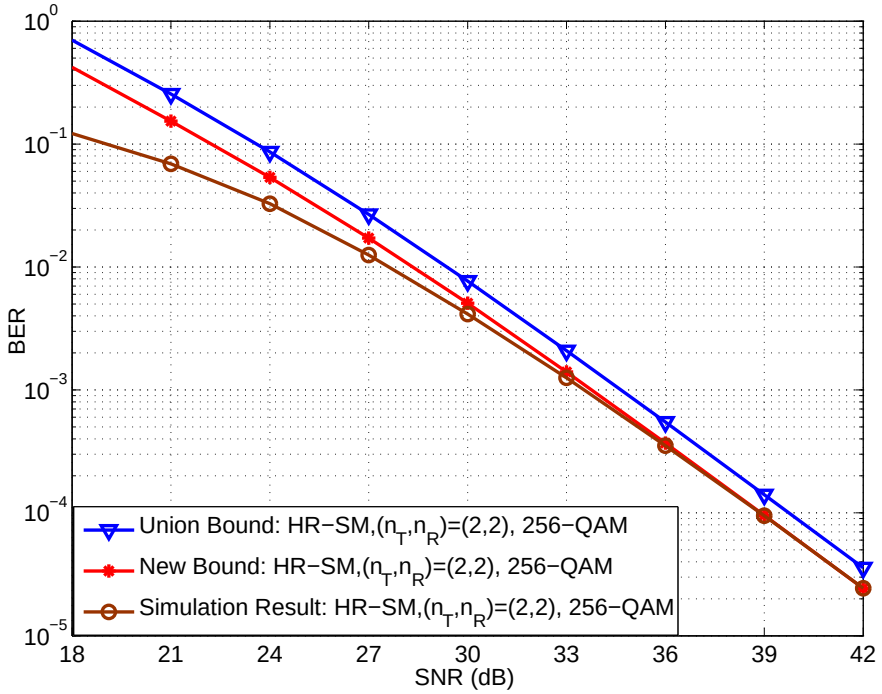

Figure 2.9: The new upper bound, the union bound and simulation curve for the BER of the (2,2) HRSM system using 256-QAM.

Fig. 2.9 compares the new upper bound with the union bound and simulation results for the BER of (2,2) HRSM system using 256-QAM technique. we again see from Fig. 2.9 that the new upper bound is remarkably closer to the simulation curve than the union bound. Obviously, by using the higher modulation order, the new bound in Fig. 2.9 is much better than that in Fig. 2.8. Particularly, at BER $= 10^{-4}$, the new bound is tighter than the union bound by approximately 1 dB in SNR.

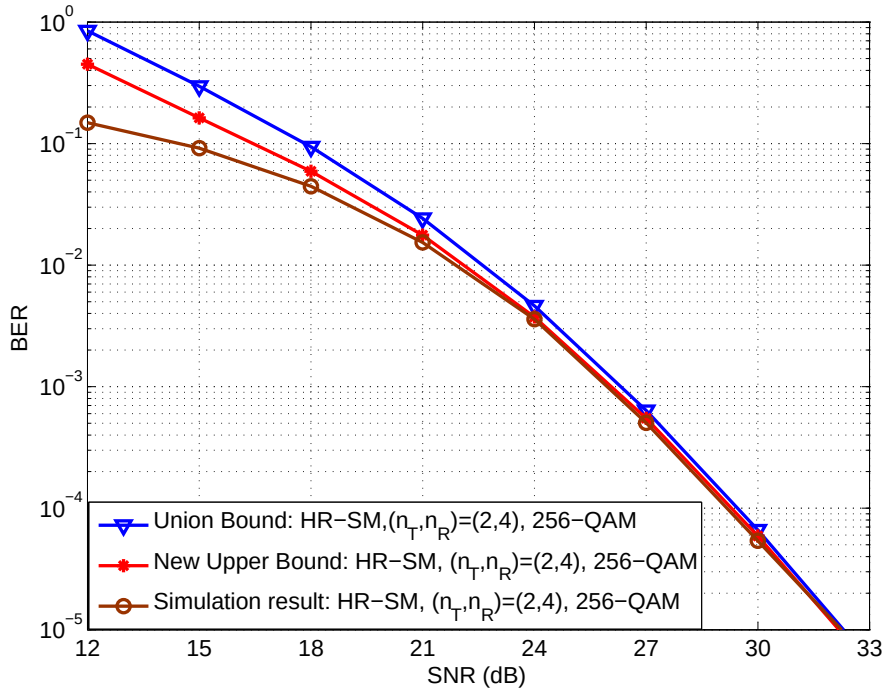

Figure 2.10: The new upper bound, the union bound and simulation curve for the BER of the (2,4) HRSM system using 256-QAM.

Similarly, the comparison for the (2,4) HRSM system using 256-QAM technique is shown as in Fig. 2.10. The new upper bound is very close to the simulation curve, especially when the SNR is greater than 20 dB. We also can look at BER $= 10^{-1}$, the new bound is tighter than the union bound abour 1.5 dB in SNR.

From these above figures, we can see that the tighter new bound is verified

by simulation results. In addition, the higher the modulation order is used, the tighter the new upper bound is.

2.4. Conclusion

The related studies about the HRSM system are generated and presented. In this model, although the ML detection algorithm has the best performance, this algorithm is difficult to implement in practice because of the high detection complexity. As a result, to overcome this issue, low complexity sub-optimal detection algorithms, attaining good performances, are proposed for the HRSM system. In addition, a tighter new PEP upper bound for this system is also proposed to exactly verify the HRSM performance at high SNR region. Particularly, the new scientific results in this chapter are presented as follows

- Based on the conventional detectors for the MIMO systems, three detectors such as MBLAST, MSQRD and ISQRD, having low complexity and significantly good performance, is proposed for the HRSM systems. These detectors have potential applications when the HRSM systems are deployed in practice;
- Based on the Verdu theorem [65], a tighter new PEP upper bound for the HRSM system using M-QAM technique is proposed. Through this new upper bound, we can estimate the HRSM performance more accuracy, especially at the high SNR region.

Chapter 3
A NEW MIMO-SM SCHEME ACHIEVING HIGH SPECTRAL EFICIENCY

In this section, a Spatially Modulated Space Time Block Coding scheme, called DT-SM is proposed by combining the conventional Double Space Time Transmit Diversity (DSTTD) [27] with Spatial Modulation. From a set of 16 SC codewords for the DT-SM system equipped with 4 transmit antennas, a generalized procedure to design SC codewords for this system equipped with the arbitrary number of transmit antennas greater than 4 is proposed. Therefore, the DT-SM spectral efficiency significantly increases compared with the existing MIMO-SM systems, particularly $C_{\mathrm{DT-SM}} = \frac{1}{2}\log_2(16n_C) + 2\log_2 M$ (bpcu) where $\bar{n}_T = n_T - 4$ và $n_C = 2^{\left\lfloor \log_2 \binom{n_T}{\bar{n}_T} \right\rfloor}$. In addition, a PEP union bound of the DT-SM system under the correlated quasi-static Rayleigh fading channel is derived. In order to achieve the ML performance at reduced detection complexity, a modified SD algorithm based on the conventional Schnorr-Euchner SD algorithm is developped. Finally, simulation results show that the DT-SM scheme outperforms the existing MIMO and MIMO-SM schemes even in the case of correlation channel. This study is published in the fourth work.

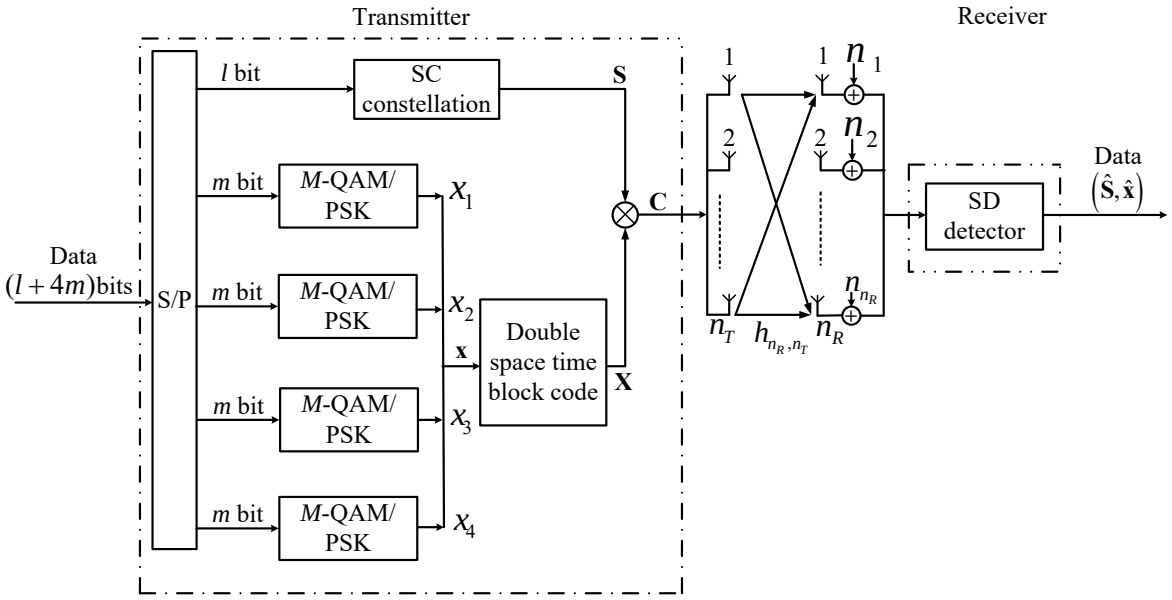

Figure 3.1: A DT-SM system diagram.

3.1. The DT-SM system model

Fig. 3.1 presents a DT-SM scheme equipped with n_T transmit and n_R receive antennas. At each symbol period, 4 out of n_T transmit antennas are activated to emit signals into the air. In this model, information bits are conveyed by two parts such as

- An $n_T \times 4$ SC codeword $\mathbf{S}$;
- An $4 \times T$ DSTTD codeword $\mathbf{X}$ where $T = 2$ symbol periods.

We assume that data are fed into the DT-SM transmitter in blocks including $(l + 4m)$ bits as given

- The first part, l bits, are mapped into a SC codeword $\mathbf{S}$ which is selected from the set of K SC codewords $(K = 2^l)$ in the spatial constellation Ω_S;
- The last part, $4m$ bits, are modulated by M-QAM/PSK modulators to get a 4×1 signal vector $\mathbf{x} = [\ x_1 \quad x_2 \quad x_3 \quad x_4\ ]^T$. This vector is then

encoded to generate a 4×2 DSTTD code matrix $\mathbf{X}$ as follows

$$\mathbf{X} = \begin{bmatrix} x_1 & x_2 & x_3 & x_4 \\ -x_2^* & x_1^* & -x_4^* & x_3^* \end{bmatrix}^T . \tag{3.1}$$

After that, the DT-SM codeword $\mathbf{C}$ is generated by multiplying the SC codeword $\mathbf{S}$ by the DSTTD matrix $\mathbf{X}$, i.e., $\mathbf{C} = \mathbf{SX}$. Finally, this codeword is transmitted over n_T transmit antennas in 2 symbol periods.

Under the assumption that the channel is quasi-static flat fading, the $n_R \times 2$ received signal matrix $\mathbf{Y}$ is given by

$$\mathbf{Y} = \sqrt{\frac{\gamma}{4E_s}}\mathbf{HC} + \mathbf{N} = \sqrt{\frac{\gamma}{4E_s}}\mathbf{HSX} + \mathbf{N} \tag{3.2}$$

where $\mathbf{H}$ and $\mathbf{N}$ respectivelty denotes the $n_R \times n_T$ channel matrix and the $n_R \times 2$ noise matrix. The entries of both $\mathbf{H}$ and $\mathbf{N}$ are assumed to be i.i.d. Gaussian random variables with zero mean and unit variance, i.e., $\mathcal{CN}(0, 1)$. γ is the average SNR at each receive antenna. E_s is the average energy of a M-QAM/PSK modulated symbol. Furthermore, the SC codeword $\mathbf{S}$ is normalized such that the ensemble average of the trace of $\mathbf{S}^H\mathbf{S}$ is equal to 4, i.e., $\mathrm{E}\left(\mathrm{trace}\left(\mathbf{S}^H\mathbf{S}\right)\right) = 4$.

3.2. SC codeword design for 4 transmit antennas

In this section, a set of 4 basic SC codewords are first designed. Then, the number of SC codewords are extended to 16 by multiplying the basic SC codewords by appropriate post-coding matrices where these post-coding matrices' application is the most optimal way without deteriorating the coding gain of the DT-SM system.

3.2.1. Basic SC codeword design

For the DT-SM system with $n_T = 4$ transmit antennas, the set of 4 basic SC codewords is proposed as follows

$$\begin{aligned}
\mathbf{S}_1 &= \begin{bmatrix} 1 & 0 & 0 & 0 \\ 0 & 1 & 0 & 0 \\ 0 & 0 & e^{j\theta} & 0 \\ 0 & 0 & 0 & e^{-j\theta} \end{bmatrix}; \\
\mathbf{S}_2 &= \begin{bmatrix} 0 & 0 & e^{j\theta} & 0 \\ 0 & 0 & 0 & e^{-j\theta} \\ 1 & 0 & 0 & 0 \\ 0 & 1 & 0 & 0 \end{bmatrix}; \\
\mathbf{S}_3 &= \begin{bmatrix} 0 & 0 & e^{j2\theta} & 0 \\ 0 & e^{-j\theta} & 0 & 0 \\ e^{j\theta} & 0 & 0 & 0 \\ 0 & 0 & 0 & e^{-j2\theta} \end{bmatrix}; \\
\mathbf{S}_4 &= \begin{bmatrix} e^{j\theta} & 0 & 0 & 0 \\ 0 & 0 & 0 & e^{-j2\theta} \\ 0 & 0 & e^{j2\theta} & 0 \\ 0 & e^{-j\theta} & 0 & 0 \end{bmatrix}.
\end{aligned} \tag{3.3}$$

where θ is a rotation angle to optimize. In order for the proposed DT-SM scheme to achieve second order transmit diversity, the rotation angle θ is optimized using the rank and determinant criteria in [61]. Particularly, the rotation angle θ is exhaustively searched on computer in $[0, \pi/2]$ interval to find the optimal value of θ, θ_o, that maximizes the minimum coding gain

distance (CDG), $\delta_{\min}(\theta)$, for all pairs of distinct DT-SM codewords $\mathbf{C} \neq \hat{\mathbf{C}}$ is given by

$$\delta_{\min}(\theta) = \min_{\mathbf{C}\neq\hat{\mathbf{C}}} \det\left[\left(\mathbf{C}-\hat{\mathbf{C}}\right)^{H}\left(\mathbf{C}-\hat{\mathbf{C}}\right)\right], \tag{3.4}$$

$$\theta_o = \arg\max_{\theta\in[0,\pi/2]} \delta_{\min}(\theta). \tag{3.5}$$

Because of the symmetry of the DSTTD matrix $\mathbf{X}$ and the SC codeword $\mathbf{S}$, the searching process for the optimal angle θ_o can be reduced as given

$$\delta_{\min,1}(\theta) = \min_{\forall x_k,\hat{x}_n} f_{\mathrm{I}}(\theta), \tag{3.6}$$

$$\delta_{\min,2}(\theta) = \min_{\forall x_k,\hat{x}_n} f_{\mathrm{II}}(\theta), \tag{3.7}$$

$$\delta_{\min}(\theta) = \min(\delta_{\min,1}(\theta), \delta_{\min,2}(\theta)), \tag{3.8}$$

$$\theta_o = \arg\max_{\theta} \delta_{\min}(\theta). \tag{3.9}$$

where $f_{\mathrm{I}}(\theta)$ and $f_{\mathrm{II}}(\theta)$ are the CDG functions clearly presented in Appendix **D**.

Comparing the search based on the equations (3.4)-(3.5) with those in (3.6)-(3.9), we can see clearly that the complexity of the searching process has been greatly reduced. This complexity reduction allows to use computer search to find the optimum rotation angle θ_o. Table 3.1 summarizes the optimum rotation angle θ_o and the corresponding minimum CDGs obtained for different types of modulation.

Table 3.1: Optimal θ_o and the corresponding minimum CDGs for the DT-SM scheme with basic SC codewords

Modulation	BPSK	4QAM	8QAM	16QAM	32QAM
θ_o(rad)	1.01	1.068	1.068	1.17	1.3
$d_{\min}$	13.56	3.9	3.9	1.17	0.55

3.2.2. Design of extended SC codewords

In order to have more SC codewords, we first define a basic 4×4 post-coding matrix as follows

$$\mathbf{E} = \begin{bmatrix} 0 & e^{j\alpha} & 0 & 0 \\ 0 & 0 & e^{j\alpha} & 0 \\ 0 & 0 & 0 & e^{j\alpha} \\ 1 & 0 & 0 & 0 \end{bmatrix} \tag{3.10}$$

where α is another rotation angle to be optimized.

Multiplying the basic codewords in the equation (3.3) by appropriate versions of this post-coding matrix $\mathbf{E}$ provides us 12 additional SC codewords as given

$$\mathbf{S}_{5:8} = \mathbf{S}_{1:4}\mathbf{E} \tag{3.11}$$

$$\mathbf{S}_{9:12} = \mathbf{S}_{1:4}\mathbf{E}^2 \tag{3.12}$$

$$\mathbf{S}_{13:16} = \mathbf{S}_{1:4}\mathbf{E}^3. \tag{3.13}$$

As a result, generally we will have 16 SC codewords for the DT-SM system equipped with 4 transmit antennas. Therefore, being beside the information bits conveyed by the DSTTD matrix, the DT-SM system will additionally carry 4 information bits in 2 symbol periods.

Similarly, in order for the DT-SM scheme to achieve full diversity with maximum coding gain, the rotation angle α is also optimized for $\mathbf{E}$ using the rank and determinant criteria similar to those defined in the equation (3.4)-(3.5). Table 3.2 shows the optimum rotation angle θ_o, α_o and the corresponding minimum CDGs for different types of modulation with 16 SC codeword [1].

[1]The larger constellation size M is, the more searching time is required for the optimal θ_o and α_o. Our simulation

Table 3.2: Optimum θ_o, α_o, and the corresponding minimum CGDs for the DT-SM scheme with 16 SC codewords

Modulation	BPSK	4QAM	8QAM	16QAM
θ_o(rad)	1.01	1.068	1.068	1.17
α_o(rad)	1.4	1.43	0.9	1.29
$\delta_{\min}$	1.05	0.73	0.19	0.035

3.3. SC codeword design for an arbitrary transmit antennas

In this section, we utilize 16 SC codewords constructed above to generate suitable SC codewords for a DT-SM system equipped with the number of transmit antennas greater than 4. Particularly, a DT-SM system with 6 transmit antennas is presented to illustrate the generalized SC codeword design procedure. Simply, we only consider an example of a SC codeword and then this generalizes it to the entire spatial constellation Ω_S. From the first SC codeword $\mathbf{S}_1$ in the equation (3.3), we can build 15 SC codewords $\mathbf{S}^1_{1:15}$, for $n_T = 6$ by combining two 1×4 zero vectors $0 = [\ 0 \quad 0 \quad 0 \quad 0\ ]$ with 4 rows of $\mathbf{S}_1$, namely, $[\ \mathbf{s}_{1,1} \quad \mathbf{s}_{1,2} \quad \mathbf{s}_{1,3} \quad \mathbf{s}_{1,4}\ ]^T$, as follows

$$\mathbf{S}^1_1 = \begin{bmatrix} \mathbf{s}_{1,1} \\ \mathbf{s}_{1,2} \\ \mathbf{s}_{1,3} \\ \mathbf{s}_{1,4} \\ \mathbf{0} \\ \mathbf{0} \end{bmatrix}, \quad \mathbf{S}^1_2 = \begin{bmatrix} \mathbf{s}_{1,1} \\ \mathbf{s}_{1,2} \\ \mathbf{s}_{1,3} \\ \mathbf{0} \\ \mathbf{s}_{1,4} \\ \mathbf{0} \end{bmatrix}, \quad \mathbf{S}^1_3 = \begin{bmatrix} \mathbf{s}_{1,1} \\ \mathbf{s}_{1,2} \\ \mathbf{s}_{1,3} \\ \mathbf{0} \\ \mathbf{0} \\ \mathbf{s}_{1,4} \end{bmatrix},$$

results show that the proposed DT-SM scheme can achieve high BER performance if it utilizes ($\theta_o = 1.3, \alpha_o = 0.43$) for 32-QAM and ($\theta_o = 1.37, \alpha_o = 0.785$) for the remaining M-QAM constellations.

$$\mathbf{S}_4^1 = \begin{bmatrix} \mathbf{s}_{1,1} \\ \mathbf{s}_{1,2} \\ \mathbf{0} \\ \mathbf{s}_{1,3} \\ \mathbf{s}_{1,4} \\ \mathbf{0} \end{bmatrix}, \quad \mathbf{S}_5^1 = \begin{bmatrix} \mathbf{s}_{1,1} \\ \mathbf{s}_{1,2} \\ \mathbf{0} \\ \mathbf{s}_{1,3} \\ \mathbf{0} \\ \mathbf{s}_{1,4} \end{bmatrix}, \quad \mathbf{S}_6^1 = \begin{bmatrix} \mathbf{s}_{1,1} \\ \mathbf{s}_{1,2} \\ \mathbf{0} \\ \mathbf{0} \\ \mathbf{s}_{1,3} \\ \mathbf{s}_{1,4} \end{bmatrix},$$

$$\mathbf{S}_7^1 = \begin{bmatrix} \mathbf{s}_{1,1} \\ \mathbf{0} \\ \mathbf{s}_{1,2} \\ \mathbf{s}_{1,3} \\ \mathbf{s}_{1,4} \\ \mathbf{0} \end{bmatrix}, \quad \mathbf{S}_8^1 = \begin{bmatrix} \mathbf{s}_{1,1} \\ \mathbf{0} \\ \mathbf{s}_{1,2} \\ \mathbf{s}_{1,3} \\ \mathbf{0} \\ \mathbf{s}_{1,4} \end{bmatrix}, \quad \mathbf{S}_9^1 = \begin{bmatrix} \mathbf{s}_{1,1} \\ \mathbf{0} \\ \mathbf{s}_{1,2} \\ \mathbf{0} \\ \mathbf{s}_{1,3} \\ \mathbf{s}_{1,4} \end{bmatrix},$$

$$\mathbf{S}_{10}^1 = \begin{bmatrix} \mathbf{s}_{1,1} \\ \mathbf{0} \\ \mathbf{0} \\ \mathbf{s}_{1,2} \\ \mathbf{s}_{1,3} \\ \mathbf{s}_{1,4} \end{bmatrix}, \; \mathbf{S}_{11}^1 = \begin{bmatrix} \mathbf{0} \\ \mathbf{s}_{1,1} \\ \mathbf{s}_{1,2} \\ \mathbf{s}_{1,3} \\ \mathbf{s}_{1,4} \\ \mathbf{0} \end{bmatrix}, \; \mathbf{S}_{12}^1 = \begin{bmatrix} \mathbf{0} \\ \mathbf{s}_{1,1} \\ \mathbf{s}_{1,2} \\ \mathbf{s}_{1,3} \\ \mathbf{0} \\ \mathbf{s}_{1,4} \end{bmatrix},$$

$$\mathbf{S}_{13}^1 = \begin{bmatrix} \mathbf{0} \\ \mathbf{s}_{1,1} \\ \mathbf{s}_{1,2} \\ \mathbf{0} \\ \mathbf{s}_{1,3} \\ \mathbf{s}_{1,4} \end{bmatrix}, \; \mathbf{S}_{14}^1 = \begin{bmatrix} \mathbf{0} \\ \mathbf{s}_{1,1} \\ \mathbf{0} \\ \mathbf{s}_{1,2} \\ \mathbf{s}_{1,3} \\ \mathbf{s}_{1,4} \end{bmatrix}, \; \mathbf{S}_{15}^1 = \begin{bmatrix} \mathbf{0} \\ \mathbf{0} \\ \mathbf{s}_{1,1} \\ \mathbf{s}_{1,2} \\ \mathbf{s}_{1,3} \\ \mathbf{s}_{1,4} \end{bmatrix}.$$

Let us define $\bar{n}_T = n_T - 4$. Then, it is straightforward to verify that for each $\mathbf{S}_k, \forall k = 1, 2, \cdots, 16$, constructed in Section 3.2.2, we can generate $N = \binom{n_T}{\bar{n}_T}$ distinct SC codewords. This means that totally we can obtain $K = 16n_C$ SC codewords where $n_C = 2^{\left\lfloor \log_2 \binom{n_T}{\bar{n}_T} \right\rfloor}$ for a DT-SM system with $n_T \geq 5$ transmit antennas. Then, the DT-SM spectral efficiency is calculated as given

$$\begin{aligned} C_{\text{DT-SM}} &= \frac{1}{2}\log_2(16n_C) + 2m \\ &= \frac{1}{2}\left\lfloor \log_2 \binom{n_T}{\bar{n}_T} \right\rfloor + 2(m+1)\,(\text{bpcu}) \end{aligned} \tag{3.14}$$

However, this above SC codeword design method exists a problem that needs to be solved. Particularly, in a MIMO channel with high correlation among neighbouring antenna elements, the two SC codewords that have only two different rows, e.g., $\mathbf{S}_1^1$ and $\mathbf{S}_2^1$, or $\mathbf{S}_2^1$ and $\mathbf{S}_3^1$ may be viewed as one SC codeword at the receiver. In other words, there is a high probability that the receiver can not distinguish them, leading to high bit error rate. In order to overcome this problem, we propose to weight each combination with a complex factor $w_l = e^{j\frac{l \oslash \Upsilon}{\Upsilon}}$, where $\oslash$ is the modulo operator of l and Υ, $l = 1, 2, \cdots$, corresponding to the SC codeword indices determined in the generalized SC codeword design procedure, and Υ is some positive integer to be optimized. For example, $l = 1, \Upsilon = 6$, we have $w_1 = e^{j\frac{1 \oslash 6}{6}} = e^{j\frac{1}{6}}$.

In general, for a given $n_T \geq 5$ transmit antennas and an M-QAM modulation type, the design procedure for SC codewords is summerized as follows

1. Select suitable optimum rotation angles θ_o and α_o according to Table 3.2; generate 16 basic SC codewords based on (3.3), and (3.11)-(3.13); Define $\bar{n}_T = n_T - 4$ as the number of inactive transmit antennas at

a symbol period.

2. Compute the number of antenna combinations $N = \binom{n_T}{\bar{n}_T}$, and set $l = 1$.

3. Generate the l-th combination of $\bar{n}_T$ zero vectors, $\mathbf{0}$, with the 4 rows of a 4×4 matrix $\mathbf{Z}$, i.e., generate the combination vector $\mathbf{g}_l$ that indicates the indices of active and inactive antennas (making sure that $\mathbf{g}_l \neq \mathbf{g}_n$ for $n = 1, 2, \cdots, l-1$); and set $q = 1$.

4. Set $\mathbf{Z} = \mathbf{S}_q$; generate a new SC codeword using the combination vector $\mathbf{g}_l$; and multiply the newly generated SC codeword by the weight factor w_l.

5. Let $q = q + 1$; if $q \leq 16$, then go to Step 4.

6. Let $l = l + 1$; if $l \leq N$, then go to Step 3.

7. Select the first $K = 2^{\lfloor \log_2(16N) \rfloor}$ generated codewords as the desired SC codewords for the DT-SM system.

Table 3.3: Comparison of number of SC codewords and spectral efficiency of the DT-SM system and SM-OSTBC system $C(n_T, n_R, 4)$ using M-QAM.

n_T	5	6	7	8
n_C	4	8	32	64
$K_{\text{DT-SM}}$	64	128	512	1024
$C_{\text{DT-SM}}$ (bpcu)	$3 + 2m$	$3.5 + 2m$	$4.5 + 2m$	$5 + 2m$
$K_{\text{SM-OSTBC}}$	16	32	32	64
$C_{\text{SM-OSTBC}}$ (bpcu)	$2 + m$	$2.5 + m$	$2.5 + m$	$3 + m$

Table 3.3 compares the number of SC codewords and spectral efficiency of a DT-SM system with those of an SM-OSTBC system [35], [70] for n_T transmit antennas and 4 active antennas. Ome can see from Table 3.3 that the proposed DT-SM scheme noticeably increases the number of SC codewords, thereby enabling us to achieve higher spectral efficiencies in the spatial modulation

domain. For example, when $n_T = 8$, the DT-SM scheme offers 1024 SC codewords (corresponding to a spectral efficiency of 5bpcu) as compared to 64 SC codewords (3bpcu) of the SM-OSTBC system.

3.4. The DT-SM performance evaluation

In this section, we analyze error performance of the proposed DT-SM schemes by evaluating their PEP and providing an upper bound for the bit error probability (BEP) under the assumption that the channel is correlated quasi-static Rayleigh fading.

Assuming $b = (l + 4m)$ information bits are transmitted using one among the total of $N = KM^4$ DT-SM codeword matrices $\mathbf{C}_1, \mathbf{C}_2, ..., \mathbf{C}_N$, i.e, $b = \log_2 N$. An upper bound on the average BEP of the proposed DT-SM scheme is given by the following union bound [3]

$$P_b \leq \frac{1}{N} \sum_{i=1}^{N} \sum_{q=1}^{N} \frac{P\left(\mathbf{C}_i \rightarrow \mathbf{C}_q\right) w_{i,q}}{b}, \tag{3.15}$$

where $P\left(\mathbf{C}_i \rightarrow \mathbf{C}_q\right)$ is the PEP of deciding the DT-SM codeword $\mathbf{C}_q$ given that the codeword $\mathbf{C}_i$ is transmitted. $w_{i,q}$ is the Hamming distance between the two codewords $\mathbf{C}_i$ and $\mathbf{C}_q$.

For a correlated quasi-static Rayleigh fading channel, the correlated channel matrix can be modeled as in the equation (2.17) of Section 2.2.5, Chapter 2. Therefore, we can write as given

$$\mathrm{vec}\left(\mathbf{H}_{\mathrm{corr}}\right) = \mathbf{R}^{\frac{1}{2}} \mathrm{vec}\left(\mathbf{H}\right).$$

Then, the PEP, conditioned on the channel $\mathbf{H}_{\mathrm{corr}}$ is determined [3] as given

$$P\left(\mathbf{C}_i \rightarrow \mathbf{C}_q | \mathbf{H}_{\mathrm{corr}}\right) = Q\left(\sqrt{\frac{1}{2}\left(\frac{\gamma}{4E_s}\right) d^2\left(\mathbf{C}_i, \mathbf{C}_q\right)}\right), \tag{3.16}$$

where $Q(y) = \frac{1}{\sqrt{2\pi}} \int_{y}^{\infty} e^{-\frac{x^2}{2}} dx$ is the Gaussian tail probability, and $d^2(\mathbf{C}_i, \mathbf{C}_q)$ is the modified Euclidean distance between $\mathbf{C}_i$ and $\mathbf{C}_q$ given by

$$d^2(\mathbf{C}_i, \mathbf{C}_q) = \|\mathbf{H}_{\text{corr}}(\mathbf{C}_i - \mathbf{C}_q)\|^2. \tag{3.17}$$

The PEP $P(\mathbf{C}_i \to \mathbf{C}_q)$ can be obtained by averaging the conditional PEP in the equation (3.16) over all realizations of $\mathbf{H}_{\text{corr}}$ as in [3] as given

$$P(\mathbf{C}_i \to \mathbf{C}_q) = \frac{1}{\pi} \int_0^{\frac{\pi}{2}} \Phi\left(-\frac{\gamma}{16E_s \sin^2\theta}\right) d\theta, \tag{3.18}$$

where $\Phi(s)$ is the moment generating function (MFG) of the random variable $d^2(\mathbf{C}_i, \mathbf{C}_q)$, and $P(\mathbf{C}_i \to \mathbf{C}_q)$ is evaluated at $s = -\frac{\gamma}{16E_s \sin^2\theta}$.

Defining $\mathbf{\Delta}_{i,q} = (\mathbf{C}_i - \mathbf{C}_q)(\mathbf{C}_i - \mathbf{C}_q)^H$, the modified Euclidean distance $d^2(\mathbf{C}_i, \mathbf{C}_q)$ can be evaluated as follows [24]

$$\begin{aligned} d^2(\mathbf{C}_i, \mathbf{C}_q) &= \text{trace}\left(\mathbf{H}_{\text{corr}} \mathbf{\Delta}_{i,q} \mathbf{H}_{\text{corr}}^H\right) \\ &= \text{vec}\left(\mathbf{H}_{\text{corr}}^H\right)^H \left(\mathbf{I}_{n_R} \otimes \mathbf{\Delta}_{i,q}\right) \text{vec}\left(\mathbf{H}_{\text{corr}}^H\right) \\ &= \text{vec}\left(\mathbf{H}^H\right)^H \mathbf{R}^{\frac{H}{2}} \left(\mathbf{I}_{n_R} \otimes \mathbf{\Delta}_{i,q}\right) \mathbf{R}^{\frac{1}{2}} \text{vec}\left(\mathbf{H}^H\right), \end{aligned} \tag{3.19}$$

where $\mathbf{R} = \mathbf{R}_R \otimes \mathbf{R}_T$ is the covariance matrix of $\text{vec}(\mathbf{H}_{\text{corr}}^H)$.

From the equation (3.19), we can see that $\text{vec}(\mathbf{H}^H)^H$ lis a zero-mean Gaussian vector with covariance matrix $\mathbf{R}_H = \mathbf{I}_{n_T n_R}$ and that $\mathbf{R}^{\frac{H}{2}} \left(\mathbf{I}_{n_R} \otimes \mathbf{\Delta}_{i,q}\right) \mathbf{R}^{\frac{1}{2}}$ is a ma Hermitian matrix, the MGF of $d^2(\mathbf{C}_i, \mathbf{C}_q)$ is shown to be [24]

$$\begin{aligned} \Phi(s) &= \det\left(\mathbf{I}_{n_T n_R} - s\mathbf{R}^{\frac{H}{2}} \left(\mathbf{I}_{n_R} \otimes \mathbf{\Delta}_{i,q}\right) \mathbf{R}^{\frac{1}{2}}\right)^{-1} \\ &= \det\left(\mathbf{I}_{n_T n_R} - s\mathbf{R}_R \otimes \left(\mathbf{\Delta}_{i,q} \mathbf{R}_T\right)\right)^{-1}. \end{aligned} \tag{3.20}$$

We decompose $\mathbf{R}_R$ and $\mathbf{\Delta}_{i,q}\mathbf{R}_T$ as given

$$\begin{aligned} \mathbf{R}_R &= \mathbf{V}\mathbf{\Psi}\mathbf{V}^H, \\ \mathbf{\Delta}_{i,q}\mathbf{R}_T &= \mathbf{U}\mathbf{\Theta}\mathbf{U}^H, \end{aligned} \tag{3.21}$$

where $\mathbf{V}$ and $\mathbf{U}$ are respectively the $n_R \times n_R$ and $n_T \times n_T$ unitary matrices, $\mathbf{\Psi}$ is an $n_R \times n_R$ diagonal matrix containing n_R eigenvalues of $\mathbf{R}_R$, and $\mathbf{\Theta}$ is an $n_T \times n_T$ diagonal matrix containing n_T eigenvalues of $\mathbf{\Delta}_{ij}\mathbf{R}_T$. We can write [10] as follows

$$\begin{aligned}\mathbf{R}_R \otimes (\mathbf{\Delta}_{i,q}\mathbf{R}_T) &= \left(\mathbf{V}\mathbf{\Psi}\mathbf{V}^H\right) \otimes \left(\mathbf{U}\mathbf{\Theta}\mathbf{U}^H\right) \\ &= \left(\mathbf{V} \otimes \mathbf{U}\right)\left(\mathbf{\Psi} \otimes \mathbf{\Theta}\right)\left(\mathbf{V}^H \otimes \mathbf{U}^H\right). \end{aligned} \tag{3.22}$$

Because $\mathbf{V}$ and $\mathbf{U}$ are unitary matrices, it follows that $(\mathbf{V} \otimes \mathbf{U})$ is also an unitary one. Particularly, $\mathbf{V}\mathbf{V}^H = \mathbf{I} = \mathbf{U}\mathbf{U}^H$, we have

$$\begin{aligned}\left(\mathbf{V} \otimes \mathbf{U}\right)\left(\mathbf{V} \otimes \mathbf{U}\right)^H &= \left(\mathbf{V} \otimes \mathbf{U}\right)\left(\mathbf{V}^H \otimes \mathbf{U}^H\right) \\ &= \left(\mathbf{V}\mathbf{V}^H\right) \otimes \left(\mathbf{U}\mathbf{U}^H\right) \\ &= \mathbf{I}.\end{aligned}$$

This implies that: 1) The equation (3.22) is the eigenvalue decomposition of the matrix $\mathbf{R}_R \otimes (\mathbf{\Delta}_{i,q}\mathbf{R}_T)$; 2) $(\mathbf{\Psi} \otimes \mathbf{\Theta})$ contains all $n_R n_T$ the eigenvalue of $\mathbf{R}_R \otimes (\mathbf{\Delta}_{i,q}\mathbf{R}_T)$, $\kappa_{i,q,l}, l = 1, 2, \cdots, n_R n_T$.

Using the result in (3.22), the MGF in (3.20) can be re-expressed as

$$\Phi(s) = \prod_{l=1}^{n_R n_T} \left(1 - s\kappa_{i,q,l}\right)^{-1}. \tag{3.23}$$

However, note that since the rank of $(\mathbf{\Delta}_{i,q}\mathbf{R}_T)$ is always equal to two, $\mathbf{\Theta}$ and $\mathbf{R}_R \otimes (\mathbf{\Delta}_{i,q}\mathbf{R}_T)$ respectively have at most 2 and $2n_R$ non-zero eigenvalues. Consequently, the PEP in the equation (3.18) can be re-written as given

$$P\left(\mathbf{C}_i \to \mathbf{C}_q\right) = \frac{1}{\pi}\int_0^{\frac{\pi}{2}} \prod_{l=1}^{2n_R} \left(1 + \frac{\gamma\kappa_{i,q,l}}{16E_s \sin^2\theta}\right)^{-1} d\theta. \tag{3.24}$$

Substituting (3.24) into (3.15) and taking into account the fact that $w_{i,q} =$

$w_{q,i}$, $w_{i,i} = 0$, and $P(\mathbf{C}_i \to \mathbf{C}_q) = P(\mathbf{C}_q \to \mathbf{C}_i)$, we finally get

$$P_b \leq \frac{2}{bN} \sum_{i=1}^{N-1} \sum_{q=i}^{N} \frac{w_{i,q}}{\pi} \int_0^{\frac{\pi}{2}} \prod_{l=1}^{2n_R} \left(1 + \frac{\gamma \kappa_{i,q,l}}{16 E_s \sin^2 \theta}\right)^{-1} d\theta. \tag{3.25}$$

Considering the equations (3.21)-(3.24) we can see that under spatially correlated MIMO channels, the BER performance of the DT-SM depends not only on the receive correlation matrix $\mathbf{R}_R$ but also on product of the transmit correlation matrix $\mathbf{R}_T$ and $\mathbf{\Delta}_{ij}$. It can also be inferred from the equation (3.21) that may alter the characteristics, i.e., reduce the rank and/or the coding gain, of the proposed DT-SM codewords because $\mathbf{\Theta}$ depends on both $\mathbf{R}_T$ and $\mathbf{\Delta}_{ij}$. Consequently, a good design of the SC codewords could reduce the impact of the transmit antenna correlation. This insight allows us to come up with a simple way of weighting the SC codewords so as to ease the effect of transmit antenna correlation. The approach has been presented in the Section 3.3. The effectiveness of the proposed approach will be proved via simulation and analytical results in Section 3.7.

3.5. Signal detection for the DT-SM system

For a given matrix $\mathbf{S}_k, k = 1, \ldots, K$, we can construct an $n_R \times 4$ equivalent matrix $\tilde{\mathbf{H}}_k$ as $\tilde{\mathbf{H}}_k = \sqrt{\frac{\gamma}{4E_s}} \mathbf{H} \mathbf{S}_k$. Therefore, the system equation in (3.2) can be re-written as

$$\mathbf{Y} = \tilde{\mathbf{H}}_k \mathbf{X} + \mathbf{N}. \tag{3.26}$$

The structure of the DSTTD codeword $\mathbf{X}$ allows us to re-express (3.26) as

$$\mathbf{u} = \mathbf{H}_{e,k} \mathbf{x} + \mathbf{n}, \tag{3.27}$$

where

$$\mathbf{x} = [\ x_1 \quad x_2 \quad x_3 \quad x_4\ ]^T,$$
$$\mathbf{H}_{e,k} = \begin{bmatrix} \tilde{\mathbf{h}}_1 & \tilde{\mathbf{h}}_2 & \tilde{\mathbf{h}}_3 & \tilde{\mathbf{h}}_4 \\ \tilde{\mathbf{h}}_2^* & -\tilde{\mathbf{h}}_1^* & \tilde{\mathbf{h}}_4^* & -\tilde{\mathbf{h}}_3^* \end{bmatrix},$$

with $\tilde{\mathbf{h}}_\mathbf{q}, q = 1, 2, .., 4$, being the q-th column of $\tilde{\mathbf{H}}_k$; $\mathbf{u} = [\ \mathbf{y}_1 \quad \mathbf{y}_2^*\ ]^T$; $\mathbf{n} = [\ \mathbf{n}_1 \quad \mathbf{n}_2^*\ ]^T$; $\mathbf{y}_q$ and $\mathbf{n}_q, q = 1, 2$, are respectively the qth column of $\mathbf{Y}$ and $\mathbf{N}$.

Further converting the complex-valued system equation (3.27) into the equivalent real-valued one, we finally obtain

$$\mathbf{v} = \mathbf{M}_k\mathbf{s} + \mathbf{w}, \tag{3.28}$$

where

$$\mathbf{M}_k = \begin{bmatrix} \Re\left(\mathbf{H}_{e,k}\right) & -\Im\left(\mathbf{H}_{e,k}\right) \\ \Im\left(\mathbf{H}_{e,k}\right) & \Re\left(\mathbf{H}_{e,k}\right) \end{bmatrix}, \tag{3.29}$$

$\mathbf{s} = [\ \Re(\mathbf{x}) \quad \Im(\mathbf{x})\ ]^T$, $\mathbf{v} = [\ \Re(\mathbf{u}) \quad \Im(\mathbf{u})\ ]^T$, và $\mathbf{w} = [\ \Re(\mathbf{n}) \quad \Im(\mathbf{n})\ ]^T$.

The DT-SM system equation in (3.28) is now similar to that of the conventional MIMO SMX system. As a result, the sphere decoders in [7], [11], [13] can be applied to detect the modulated symbol $\mathbf{x}$ for the given SC codeword $\mathbf{S}_k$. In this paper, based on Schnorr-Euchner sphere decoder in [13], we propose a low-complexity SD decoder for signal recovery at the DT-SM receiver.

Performing QR decomposition on $\mathbf{M}_k$, we have

$$\mathbf{M}_k = \mathbf{Q}_k\mathbf{R}_k, \tag{3.30}$$

where $\mathbf{Q}_k$ is a $4n_R \times 8$ orthogonal matrix, i.e., $\mathbf{Q}_k^H\mathbf{Q}_k = \mathbf{I}_8$. $\mathbf{R}_k$ is an 8×8 upper triangular matrix.

Pre-multiplying both sides of (3.28) by $\mathbf{Q}_k^H$, we obtain

$$\mathbf{t}_k = \mathbf{R}_k\mathbf{s} + \bar{\mathbf{w}}_k, \tag{3.31}$$

where $\mathbf{t}_k$ và $\bar{\mathbf{w}}_k$ are respectively the 8×1 received signal vector and the 8×1 noise vector after pre-filtering $\mathbf{v}_k$ by $\mathbf{Q}_k$.

Applying the detection equation in [35], we have

$$\|\mathbf{t}_k - \mathbf{R}_k\mathbf{s}\|^2 = \|\mathbf{v} - \mathbf{M}_k\mathbf{s}\|^2 - \mathbf{v}^H\mathbf{v} + \mathbf{t}_k^H\mathbf{t}_k. \tag{3.32}$$

Thus, the ML decoding rule for $\mathbf{s}$ conditioned on $\mathbf{S}_k$ can be written as

$$\begin{aligned}(\hat{\mathbf{s}})_k &= \arg\min_{\mathbf{s}\in\Omega_N} \|\mathbf{v} - \mathbf{M}_k\mathbf{s}\|^2 \\ &= \arg\min_{\mathbf{s}\in\Omega_N} \|\mathbf{t}_k - \mathbf{R}_k\mathbf{s}\|^2 + \mathbf{v}^H\mathbf{v} - \mathbf{t}_k^H\mathbf{t}_k,\end{aligned} \tag{3.33}$$

where Ω_N is the set of integers corresponding to the M-QAM constellation.

Using all possible $(\hat{\mathbf{s}})_k$, for $k = 1, 2, \cdots, K$, it is possible to determine the index $\hat{k}$ associated with the transmitted SC codeword $\mathbf{S}_k$ using the following cost function

$$\hat{k} = \arg\min_{k=1,2,\cdots,K} \|\mathbf{t}_k - \mathbf{R}_k(\hat{\mathbf{s}})_k\|^2 + \mathbf{v}^H\mathbf{v} - \mathbf{t}_k^H\mathbf{t}_k. \tag{3.34}$$

After that, the signal vector $\hat{\mathbf{s}}$ corresponding to the transmitted signal vector $\mathbf{x}$ can be recovered as $\hat{\mathbf{s}} = (\hat{\mathbf{s}})_{\hat{k}}$.

The proposed SD can be summarized in Table 3.4.

3.6. Complexity analysis

In this section, we analyze the detection complexity of the DT-SM receiver using the proposed SD and compare it with several related MIMO receivers adopting the conventional SE-SD sphere decoder in [13]. The flop regulations are similar as in Section 2.2, Chapter 2.

Table 3.4: The modified SE-SD detection algorithm

Step	Performance
(1)	Set $k = 1$, $D_{\min} = C_0$, $\hat{k} = 0$, and $\hat{\mathbf{s}} = \emptyset$.
(2)	Compute $\tilde{\mathbf{H}}_k = \sqrt{\frac{\gamma}{4E_S}}\mathbf{H}\mathbf{S}_k$, generate $\mathbf{M}_k$, compute QR decomposition of $\mathbf{M}_k$ ($\mathbf{M}_k = \mathbf{Q}\mathbf{R}$) and $\mathbf{t} = \mathbf{Q}^H\mathbf{v}$.
(3)	Compute the sphere radius $R = D_{\min} - \mathbf{v}^H\mathbf{v} + \mathbf{t}^H\mathbf{t}$, and set $D_{\text{temp}} = \infty$.
(4)	If $R \leq 0$, go to Step 11, else set $i = 8, T_8 = 0, \xi_8 = 0$.
(5)	(DFE^2 trên s_i) Set $s_i = \lfloor (t_i - \xi_i)/r_{i,i} \rceil$, and $\Delta = \text{sign}(t_i - \xi_i - r_{i,i}s_i)$.
(6)	(Main step) If $R < T_i + (t_i - \xi_i - r_{i,i}s_i)^2$, then go to Step 7. Else if $s_i \notin \Omega_N$ go to Step 9. Else if $i > 1$, then let $\xi_{i-1} = \sum_{j=i}^{8} r_{i-1,j}s_j$, $T_{i-1} = T_i + (t_i - \xi_i - r_{i,i}s_i)^2$, $i = i - 1$, go to Step 5. Else go to Step 8.
(7)	If $i = 8$, go to Step 10, else set $i = i + 1$ and go to Step 9.
(8)	Set $R = T_1 + (t_1 - \xi_1 - r_{1,1}s_1)^2$, $D_{\text{temp}} = R$, save $\breve{\mathbf{s}} = \mathbf{s}$, and set $i = i + 1$.
(9)	Let $s_i = s_i + \Delta_i$, $\Delta_i = -\Delta_i - \text{sign}(\Delta_i)$, and go to Step 6.
(10)	Let $D_{\text{temp}} = D_{\text{temp}} + (\mathbf{v}^H\mathbf{v} - \mathbf{t}^H\mathbf{t})$. If $D_{\text{temp}} < D_{\min}$, then save $\hat{\mathbf{s}} = \breve{\mathbf{s}}$ and $\hat{k} = k$, set $D_{\min} = D_{\text{temp}}$.
(11)	Set $k = k + 1$, if $k \leq K$, goto Step 2.
(12)	If $\hat{\mathbf{s}} = \emptyset$ (i.e., no solution found), then increase C_0 then go to Step 1, else terminate.

The complexity of the pre-processing stage ρ_{Pre}, including those of computing $\tilde{\mathbf{H}}_k$ in (3.26), decomposition of $\mathbf{M}_k$ in (3.28), and signal vector $\mathbf{t}_k$, $k = 1, 2, ..., K$, in (3.31) is calculated as given

$$\rho_{\text{Pre}} = \left[\frac{2}{T}(32n_Rn_T + 536n_R - 36) + (64n_R - 8)\right]K. \tag{3.35}$$

Therefore, the complexity calculation equation of the proposed SD is presented in the number of flops per bit as given

$$\rho = \frac{\rho_{\text{Pre}} + \rho_s}{l + 4m}, \tag{3.36}$$

where the average complexity ρ_s per DT-SM codeword is obtained by counting the number of flops required to obtain the recovered signals in the searching stage (i.e., the flops required to carry out Step 3 to Step 11 of the proposed SD). The complexity of the proposed SD algorithm is detailed in Appendix **E**.

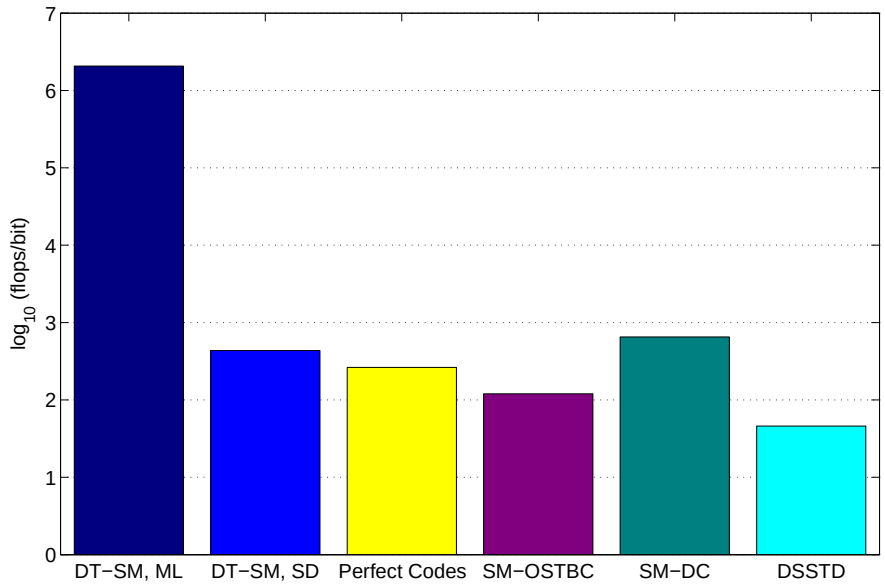

Figure 3.2: Detection complexities of DT-SM, Perfect Codes, SM-OSTBC $C(4,4,4)$, SM-DC, and DSTTD with $n_T = 4, n_R = 4$ at SNR = 9 dB and 8 bpcu; $T = 80$ symbol periods.

Fig. 3.2 compares the detection complexity of the DT-SM with that of related MIMO schemes including SM-OSTBC [35], DSTTD [27], [31], Perfect Codes [47], SM-DC [70] using a $(4, 4)$ MIMO configuration. The complexity of the SM-OSTBC has already been given in [35]. Suitable modulation schemes are employed so that the spectral efficiencies of all schemes are equal to 8 bpcu. All compared systems use the SD algorithm at their receivers. It can be observed from Fig. 3.2 that the proposed SD enables the DT-SM scheme to substantially reduce detection complexity compared with the ML decoder. With the aid of the proposed SD, detection complexity of the DT-SM scheme

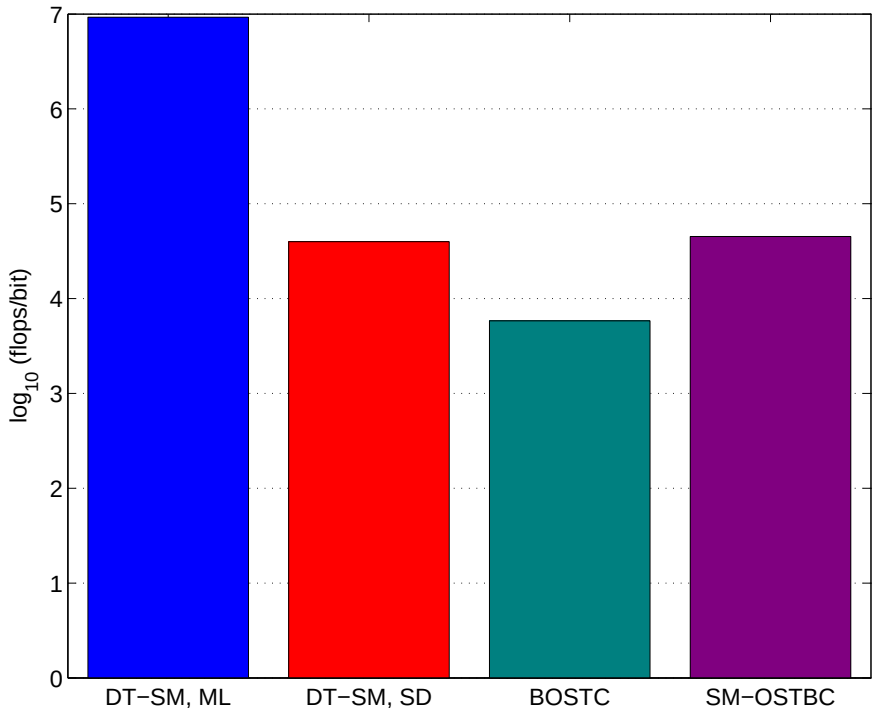

Figure 3.3: Detection complexities of DT-SM, SM-OSTBC $C(8, 8, 8)$ at SNR = 9 dB and 9 bpcu, and BOSTC at SNR = 9 dB and 8 bpcu; with $n_T = 8, n_R = 8$; $T = 80$ symbol periods.

is even lower than that of the SM-DC. Although, the DT-SM scheme has slightly higher complexity than the Perfect Codes, the SM-OSTBC and the DSTTD, it can provide better performance through the BER parameter, as shown later.

In Fig. 3.3 we again see that a remarkable reduction in detection complexity of the DT-SM can be obtained via the use of the proposed SD compared to the adoption of the ML decoder. For the same spectral efficiency and antenna configuration, the DT-SM offers lower detection complexity than the SM-OSTBC $C(8, 8, 8)$. In this case, the DT-SM utilizes 4-QAM modulation and 1024 SC codewords, while the SM-OSTBC adopts 8-QAM modulation and 4096 SC codewords to provide 9 bpcu. Consequently, the SM-OSTBC requires higher computational load to process not only higher modulation order but

also more equivalent system equations. Note that in Fig. 3.3 although the DT-SM exhibits a little higher detection complexity than the BOSTC, it actually provides higher spectral efficiency.

3.7. Simulation results

The BER performance of the proposed DT-SM scheme is compared with those of the state-of-the-art MIMO schemes such as SM-OSTBC [35], DSTTD [27], SM-DC [70], Srinath-STBC [57], Perfect Codes [47], BOSTBC [64], and HRSM [46]. For fair comparison, all schemes are equipped with the same number of transmit antennas n_T, receive antennas n_R, and simultaneously activated antennas n_A, denoted as (n_T, n_R, n_A). In order to achieve the same spectral efficiency, appropriate modulation techniques are deployed at each system. We further assume that the receiver perfectly knows the channel state information and that all MIMO schemes use sphere decoders at their receivers.

3.7.1. Performance comparison

Fig. 3.4 compares the BER performance of the DT-SM with those of the SM-OSTBC $C(4, 4, 4)$, the rate-2 Srinath-STBC, the rate-2 Perfect Codes, the SM-DC, and the DSTTD at 6 bpcu for $(4, 4, 4)$ MIMO configuration. It can be seen from the figure that the DT-SM outperforms all related schemes for sufficiently high SNR$\in [6, 16]$ dB. Specifically, at BER $= 10^{-3}$, the proposed scheme offers about 1.1 dB gain over the Srinath-STBC and the SM-DC, and around 1.5 dB over the SM-OSTBC, the DSTTD and the Perfect Codes. The gaps between the BER curve of the DT-SM and those of the Srinath-STBC and the Perfect Codes becomes smaller at BER $= 10^{-5}$. This is due to the fact that both the Srinath-STBC and the Perfect Codes achieve

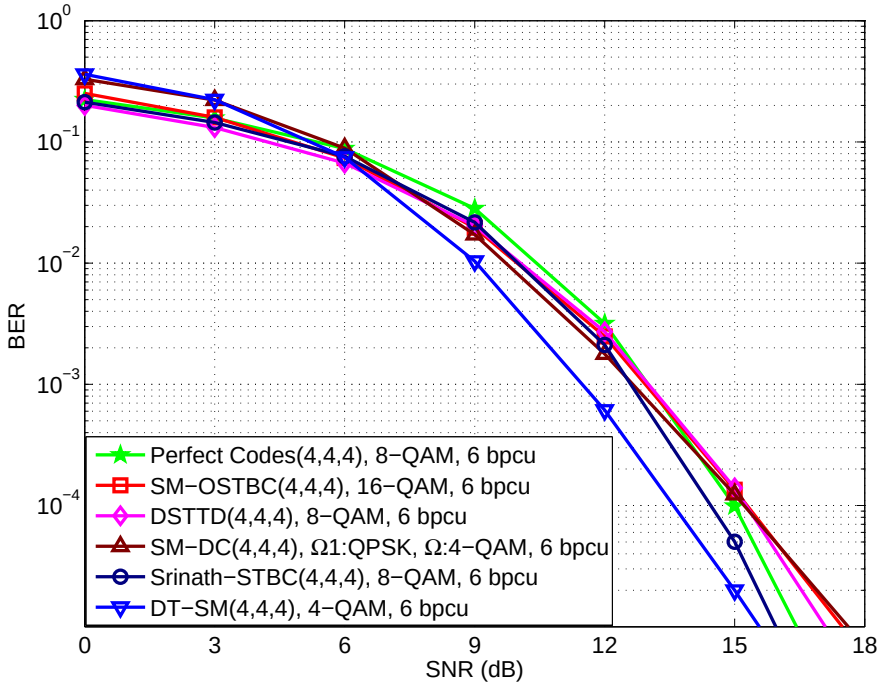

Figure 3.4: BER performances of the DT-SM, SM-OSTBC $C(4,4,4)$, SM-DC, DSTTD, Srinath-STBC, and Perfect Codes at spectral efficiency of 6 bpcu.

higher transmit diversity order than the proposed DT-SM.

In Fig. 3.5, we again see that the proposed DT-SM scheme still outperforms most of related MIMO ones, including the SM-OSTBC, SM-DC, DSTTD, and Perfect Codes, as the spectral efficiency increases to 8 bpcu. At BER $= 10^{-3}$, the SNR gains are approximately equal to 3.4 dB, 2 dB, 0.9 dB, and 0.7 dB, respectively. Note that these performance improvements are achieved at the cost of higher decoding complexity, as discussed in Section 3.6. As SNR reaches to about 12.5 dB, the performance of the DT-SM scheme surpasses that of the HR-SM counterpart. Among related schemes, Srinath-STBC is the only one that can offer higher BER performance than the DT-SM. However, the performance gap in the SNR axis is only 0.5 dB at BER $= 10^{-5}$.

Fig. 3.6 illustrates the BER curves of the DT-SM, STBC-SM, SM-OSTBC

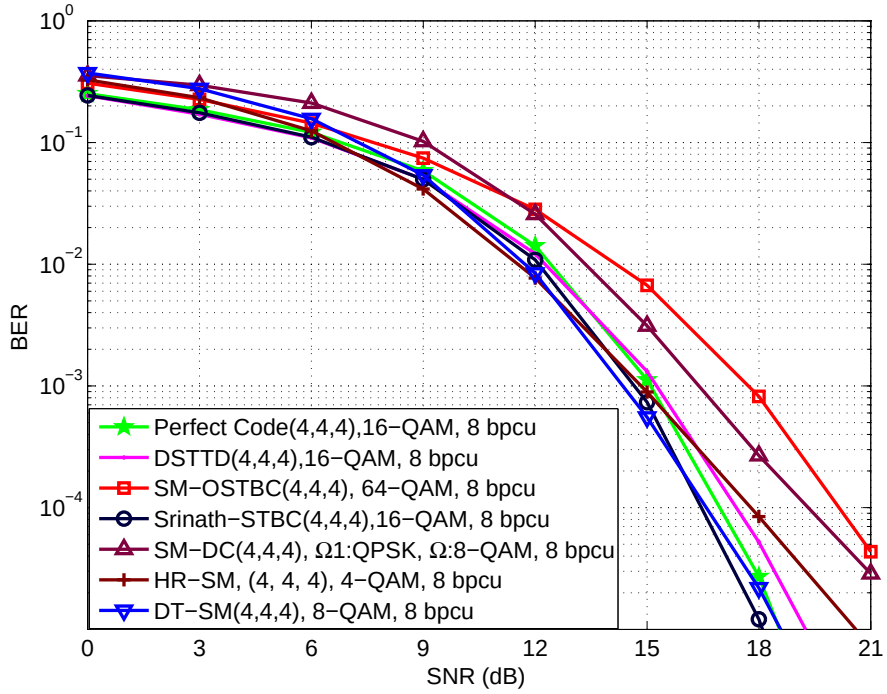

Figure 3.5: BER performances of the DT-SM, SM-OSTBC $C(4,4,4)$, SM-DC, DSTTD, Srinath-STBC, and Perfect Codes at spectral efficiency of 8 bpcu.

$C(8,8,8)$, SM-OSTBC $C(8,8,4)$, and BOSTC schemes in $(n_T, n_R) = (8,8)$ antennna configuration and BER curve of the DSTTD scheme in $(n_T, n_R) = (4,8)$ antenna configuration. Here, the number of active antennas is 2 for the STBC-SM, 4 for the DSTTD, DT-SM and SM-OSTBC $C(8,8,4)$, and 8 for the remaining systems. The spectral efficiency is equal to 9 bpcu for the DT-SM, $C(8,8,8)$ and $C(8,8,4)$ and equal to 8 bpcu for the DSTTD and BOSTC. We also include the upper bound for the BER of the DT-SM in the figure. As we can see from Fig. 3.6, the upper bound guarantees that our simulation results are reliable. In addition, the proposed DT-SM scheme significantly outperforms all existing schemes except the BOSTC. The reasons for this are as follows. To provide the same spectral efficiency of 9 bpcu, both the STBC-SM and $C(8,8,4)$ have to adopt high-order QAM constel-

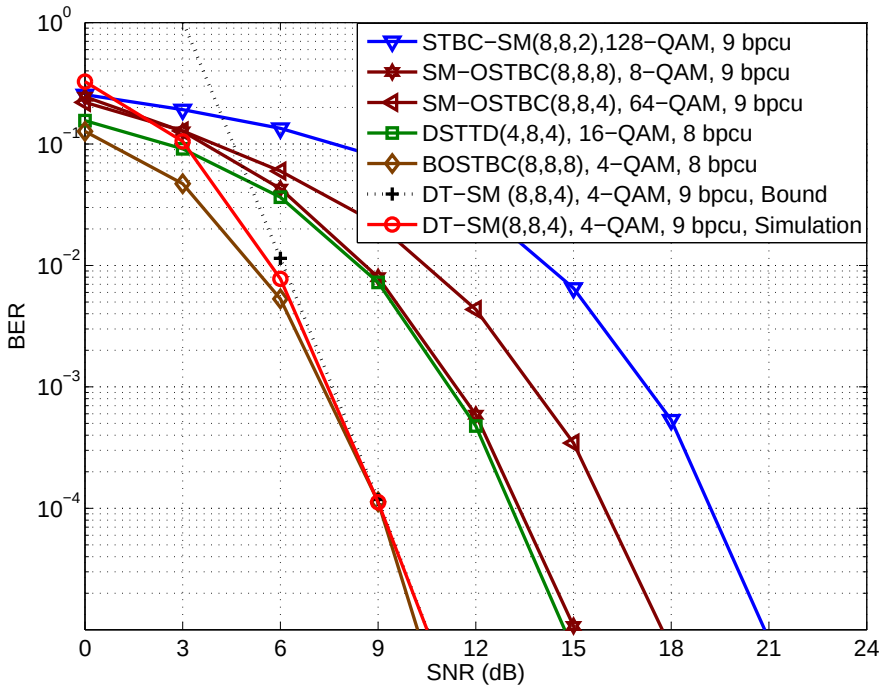

Figure 3.6: BER performances of the DT-SM, STBC-SM, SM-OSTBC $C(8,8,8)$, SM-OSTBC $C(8,8,4)$ and BOSTC with $n_T = 8$, DSTTD với $n_T = 4$ at spectral efficiency of 8 bpcu and 9 bpcu. all schemes adopt $n_R = 8$ receive antennas.

lations (i.e., 64-QAM and 128-QAM). Therefore, the BERs of both systems are dominated by the BERs of QAM modulations. Although the $C(8,8,8)$ can reduce the modulation order to 8 (i.e., 8-QAM). This modulation still results in much worse BER performance than 4-QAM modulation. Moreover, the BER performance of $C(8,8,8)$ is now dominated by the SC modulation because it has to utilize a total of 4096 SC codewords to bear 12 information bits. Consequently, its BER performance gets even worse. In contrast, the combination of SM modulation (with as total of 1204 SC codewords) and the rate-2 DSTTD coding scheme allows the DT-SM to adopt 4-QAM modulation. Therefore, it is able to obtain very high BER performance. Specifically, at BER $= 10^{-5}$, the proposed scheme offers around 3.8 dB, 4.3 dB and 7 dB

gain over the DSTTD, $C(8,8,8)$, and $C(8,8,4)$, respectively. Note, however, that the proposed scheme uses 4 transmit antenna elements more than the DSTTD but 4 RF-chains fewer than the $C(8,8,8)$. Compared to the BOSTC, the proposed DT-SM is more advantageous in 2 aspects

1. providing an improvement of 1 bpcu in spectral efficiency;
2. reducing 4 required RF chains, yet at the cost of increased decoding complexity as shown in Fig. 3.3 and slightly higher BER.

3.7.2. DT-SM performance under spatial correlation

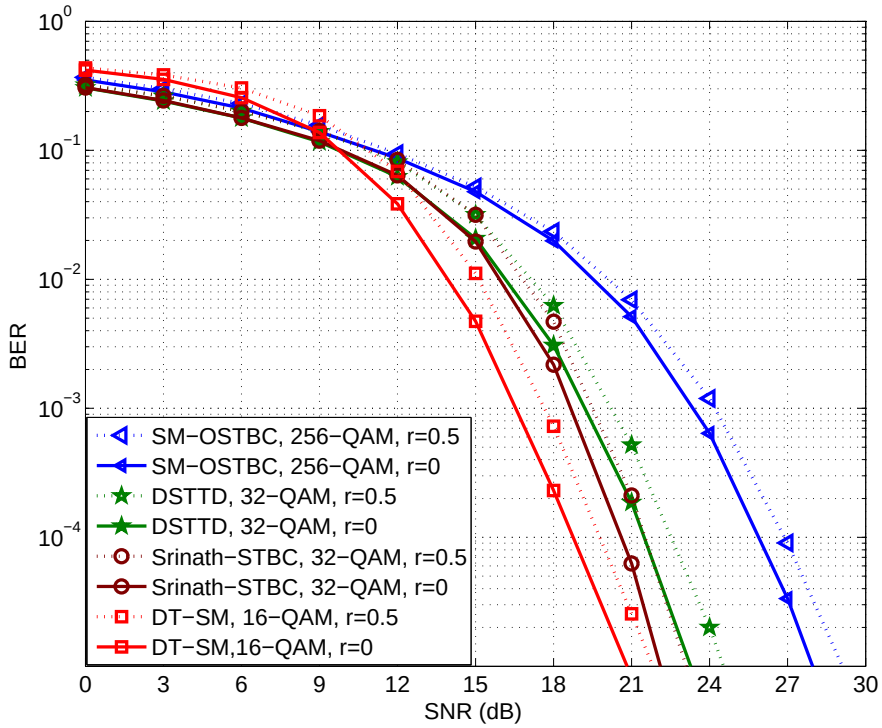

Figure 3.7: BER performances of the DT-SM, SM-OSTBC $C(4,4,4)$, DSTTD, and Srinath-STBC schemes in an $(n_T = 4, n_R = 4)$ exponentially correlated MIMO channel at the spectral efficiency of 10 bpcu.

The correlation MIMO channel model is considered in Section 2.2.5, Chapter 2. In Fig. 3.7, BER performances of the DT-SM, SM-OSTBC $C(4,4,4)$,

DSTTD and Srinath-STBC using MIMO configuration $(4, 4, 4)$ are compared at spectral efficiency of 10 bpcu. The correlation coefficient r is investigated in two scenarios 0 and 0.5. We can see in Fig. 3.7 that when there is no correlation, i.e., $r = 0$ and correlation, $r = 0.5$, the DT-SM scheme outperforms other schemes. Among the 4 schemes, the $C(4, 4, 4)$ scheme appears to be the least robust to the correlation phenomenon. In order to achieve the spectral efficiency of 10 bpcu, both the DSTTD and the Srinath-STBC schemes utilize the 32-QAM modulation, and the SM-OSTBC uses 256-QAM one while the DT-SM scheme only uses 16-QAM modulation. Because of high-order modulation utilization, the DSTTD, Srinath-STBC và SM-OSTBC $C(4, 4, 4)$ performance is less than that of the DT-SM.

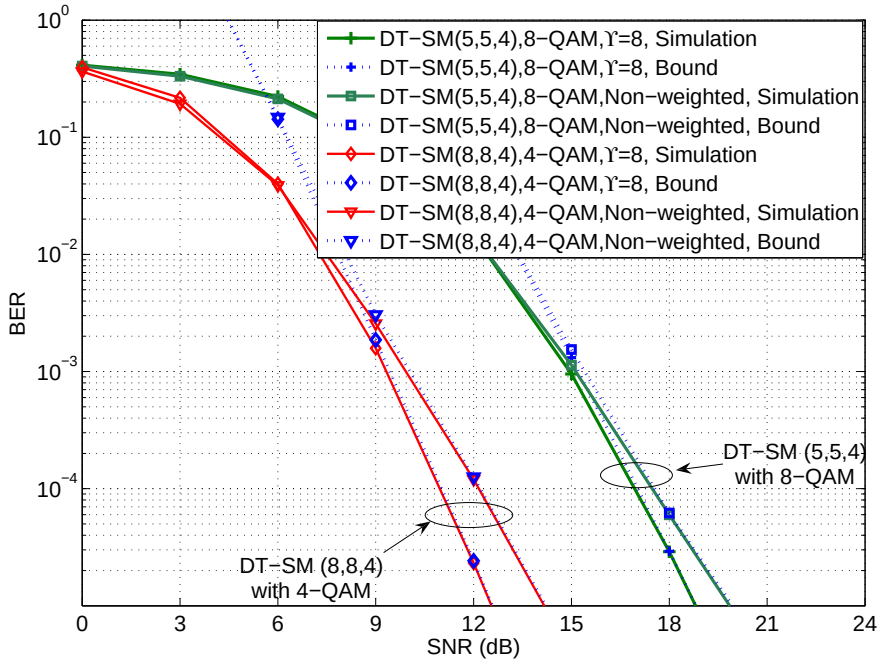

Figure 3.8: Theoretical and simulation results for the BERs of the DT-SM scheme with 4-QAM and 8-QAM modulations in different exponentially correlated MIMO channels when the SC codewords are non-weighted and weighted ($\Upsilon = 8$); correlation coefficient $r = 0.6$ for all scenarios.

By investigating the BER performances of the DT-SM scheme with the

range values $\Upsilon \in [1, 14]$, we found that $\Upsilon = 8$ is a value that allows the DT-SM scheme to perform robustly in correlated channels. Note, however, that this value is not necessarily the optimal one for all antenna configurations, all modulation schemes and correlated values. Illustrated in Fig. 3.8 are the theoretical and simulation results for the BERs of the DT-SM scheme with 4-QAM and 8-QAM modulations in exponentially correlated MIMO channels having correlation coefficient of $r = 0.6$. It can be observed from Fig. 3.8 that in all cases, as the SNR gets large enough, the BER performance of the DT-SM is noticeably degraded if the proposed weighting approach is not applied. Clearly, using the proposed approach is a simple, yet effective, means of combating the effect of spatial correlation, regardless of antenna configurations and modulation techniques.

The results from Fig. 3.6 and Fig 3.8 also show that the derived upper bound becomes very tight as the SNR grows towards sufficiently large values for all cases. Therefore, the upper bound can be adopted as a useful tool to estimate the error performance of the DT-SM scheme in different correlated and non-correlated scenarios.

3.8. Conclusion

A new MIMO-SM scheme, denoted DT-SM, having good performance and high spectral efficiency, for MIMO systems equipped with the number of transmit antennas greater than 4 is proposed by combining the conventional Double Space Time Transmit Diversity with the Spatial Modulation. The DT-SM scheme obtains the second order transmit diversity and its spectral efficiency is $\frac{1}{2}\log_2(16n_C) + 2\log_2 M$ (bpcu). In addition, a modified

low-complexity Schnorr-Euchner SD algorithm is proposed to reduce detection complexity at the DT-SM receiver. Furthermore, a BEP upper bound of the DT-SM system under the correlated quasi-static Rayleigh MIMO channel is derived to verify the DT-SM performance. Simulation and theoretical results show that the DT-SM system outperforms the existing MIMO and MIMO-SM ones such as Perfect Codes, SM-OSTBC, HR-SM, SM-DC, DSTTD, STBC-SM and Srinath-STBC ones in almost simulation scenarios. Besides, a generalize SC codeword design procedure combining with a weight factor is proposed to ensure the DT-SM performance under spatial correlation effecct. Therefore, the DT-SM scheme is suitable for MIMO transmission systems that requires high spectral efficiency and operates in uncorrelated or correlated channel. This study is published in the 4-th work.

Chapter 4
A NEW MIMO-SM SCHEME ACHIEVING HIGH ORDER TRANSMIT DIVERSITY.

Based on a combination the SM technique and the Diagonal Space Time Block Code, a Diagonal Space Time Block Coded Spatial Modulation scheme, called DS-SM, is proposed. The DS-SM scheme still achieves the main benefits of the SM scheme such as eliminating the ICI at the receiver and no IAS requirement at the transmitter by activating one transmit antenna at a time period. Based on the rank and determinant criteria, this model is designed to attain full diversity. Furthermore, a general design procedure for the DS-SM scheme equipped with an even number of transmit antennas larger than four is given by cyclically shifting two rows of the SC codewords. In addition, simulation results show that the DS-SM surpasses several SM schemes at the same spectral efficiency and antenna configuration with a reasonable complexity. This study is published in the 3-th and 6-th work.

4.1. The DS-SM system model

Fig. 4.1 illustrates the block diagram of the proposed SM scheme with n_T transmit antennas and n_R receive antennas. It is assumed that data bits arrive at the transmitter in blocks each of which consists of $(l + 4m)$ bits. Each block is split into two parts l bits and $4m$ bits. The part, l bits, are mapped into a $n_T \times 4$ SC matrix in the spatial constellation Ω_S including

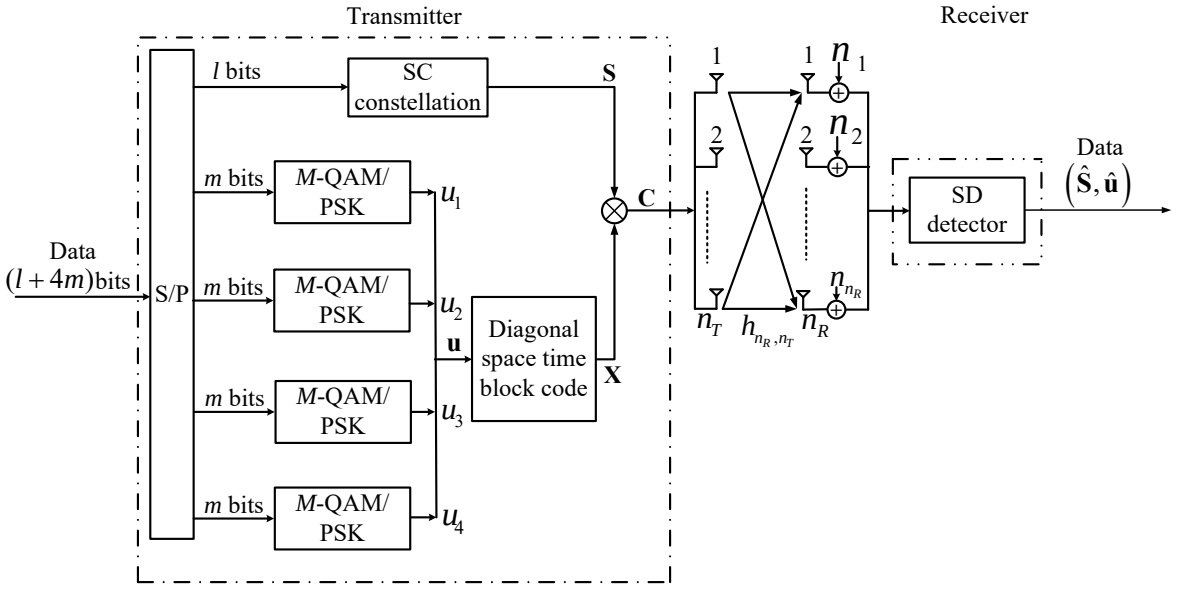

Figure 4.1: Block diagram of the DS-SM scheme.

K SC matrices ($l = \log_2 K$). The last part, $4m$ bits, are modulated by M-QAM/PSK modulators, ($M = 2^m$), to make a 4×1 modulated symbol vector $\mathbf{u} = \begin{bmatrix} u_1 & u_2 & u_3 & u_4 \end{bmatrix}^T$. Differently with the DT-SM scheme, in order to increase transmit diversity and ensure the main benefits of the SM technique, the modulated symbol vector $\mathbf{u}$ is multiplied by a rotation matrix $\mathbf{W}$ for maximizing the minimum product distance between any two points of the signal constellation [6]. Particularly, at the DSTBC block, using the multidimensional rotation matrix $\mathbf{W}$ [6], a rotated signal vector is created as given

$$\tilde{\mathbf{u}} = \mathbf{W}\left[\Re\left(\mathbf{u}\right), \Im\left(\mathbf{u}\right)\right]^T, \tag{4.1}$$

where $\Re\left(.\right)$ and $\Im\left(.\right)$ respectively denotes the real part and imagine part of a complex number.

The rotation matrix $\mathbf{W}$ [6] is presented as follows

$$\mathbf{W} = \sqrt{\frac{2}{n}} \begin{bmatrix} w_{11} & w_{12} & \cdots & w_{1n} \\ w_{21} & w_{22} & \cdots & w_{2n} \\ \vdots & \vdots & \ddots & \vdots \\ w_{n1} & w_{n2} & \cdots & w_{nn} \end{bmatrix}, \tag{4.2}$$

where $w_{tk} = \cos\left(\frac{\pi}{4n}(4t-1)(2k-1)\right)$ with $1 \leq t, k \leq n$ and $n = 8$.

After that, the elements of the rotated signal vector $\tilde{\mathbf{u}}$ are arranged to obtain the following vector as given

$$\tilde{\mathbf{x}} = [\ \tilde{u}_1 + j\tilde{u}_5 \quad \tilde{u}_2 + j\tilde{u}_6 \quad \tilde{u}_3 + j\tilde{u}_7 \quad \tilde{u}_4 + j\tilde{u}_8\ ]^T. \tag{4.3}$$

The 4×4 diagonal STBC matrix $\mathbf{X}$ is then obtained by arranging the vector $\tilde{\mathbf{x}}$ as $\mathbf{X} = \text{diag}(\tilde{\mathbf{x}})$ where $\text{diag}(\mathbf{x})$ is a way to create a diagonal matrix whose diagonal components are the entries of the vector $\mathbf{x}$. Finally, the $n_T \times 4$ transmitted codeword $\mathbf{C}$ is created simply by multiplying the SC matrix $\mathbf{S}$ by the diagonal matrix $\mathbf{X}$, i.e., $\mathbf{C} = \mathbf{SX}$. This resulted codeword $\mathbf{C}$ will be transmitted from 4 transmit antennas within 4 symbol periods.

Under the assumption that the channel is quasi-static and flat Rayleigh fading the $n_R \times 4$ received signal matrix $\mathbf{Y}$ is given by

$$\mathbf{Y} = \sqrt{\frac{\gamma}{E_s}}\mathbf{HC} + \mathbf{N} = \sqrt{\frac{\gamma}{E_s}}\mathbf{HSX} + \mathbf{N} \tag{4.4}$$

where γ is the average SNR at each receiver. E_s is the average energy of the M-QAM/PSK modulated symbols. $\mathbf{H}$ and $\mathbf{N}$ respectively denotes a $n_R \times n_T$ channel matrix and a $n_R \times 4$ noise matrix. The entries of $\mathbf{H}$ và $\mathbf{N}$ are are assumed to be i.i.d. random variables with zero mean and unit variance, i.e., $\mathcal{CN}(0, 1)$.

4.2. SC codeword design

As seen in 4.1, a part of data bits are conveyed by SC codewords, so these codewords should be carefully designed. First, a set of basic SC codewords is designed and then a generalized SC codeword design procedure for MIMO systems equipped with the even number of transmit antennas greater than 4 is presented in the later section.

4.2.1. Basic SC codewords for 4 transmit antennas

In the DS-SM system equipped with 4 transmit antennas, a spatial constellation Ω_S of 4 basic SC codewords is proposed as given

$$\mathbf{S}_1 = \begin{bmatrix} 1 & 0 & 0 & 0 \\ 0 & 1 & 0 & 0 \\ 0 & 0 & 1 & 0 \\ 0 & 0 & 0 & 1 \end{bmatrix}; \mathbf{S}_2 = \begin{bmatrix} 0 & e^{j\theta} & 0 & 0 \\ 0 & 0 & e^{j\theta} & 0 \\ 0 & 0 & 0 & e^{j\theta} \\ j & 0 & 0 & 0 \end{bmatrix}; \tag{4.5}$$
$$\mathbf{S}_3 = \mathbf{S}_2^2; \mathbf{S}_4 = \mathbf{S}_2^3.$$

Based on the rank and determinant criteria [61], the rotation angle θ is optimized to attain the full diversity and maximum coding gain. Particularly, the angle θ in the SC codewords is searched on computer in a range $[0, \pi/2]$ to find the optimal value of the angle, θ_o that maximizes the CDG, $\delta_{\min}(\theta)$ for a pair of DS-SM codewords $\mathbf{C} \neq \mathbf{C}'$ as follows

$$\delta_{\min} = \min_{\mathbf{C} \neq \mathbf{C}'} \det \left[(\mathbf{C} - \mathbf{C}')^H (\mathbf{C} - \mathbf{C}') \right], \tag{4.6}$$

$$\theta_o = \arg\max_{\theta \in [0, \pi/2]} \delta_{\min}(\theta). \tag{4.7}$$

Finally, the angle and CDG results for different modulation techniques are summarized in Table 4.1.

Table 4.1: Optimal values of θ and correspoding CDGs for basic SC codewords

Modulation	BPSK	4QAM	8QAM	16QAM
θ_o(rad)	0.52	1.36	0.2	0.4
$d_{\min}$	0.11	0.037	$3.6\,10^{-3}$	$7\,10^{-4}$

Then, the spectral efficiency of the DS-SM equipped with 4 transmit antennas is given as

$$C_{\text{DS-SM}} = \frac{1}{4}\left(\log_2 4 + \log_2 M^4\right) = \frac{1}{2} + \log_2 M\,(\text{bpcu})\,. \tag{4.8}$$

Compared with the existing MIMO-SM schemes such as the STBC-SM and STBC-CSM ones whose spectral efficiencies are $1+\log_2 M$ (bpcu) where these schemes are equipped with 4 transmit antennas. Although the DS-SM scheme is less 0.5 bit in spectral efficiency than the STBC-SM and STBC-CSM ones, this scheme obtains higher order transmit diversity than those ones.

4.2.2. SC codeword design for even transmit antennas

Based on basic set of SC codewords for 4 antennas in the equation (4.5), an extended set of SC codewords are constructed for the DS-SM equipped with even number of transmit antennas. Before going into the SC codeword design principle, a DS-SM with 6 transmit antennas is used for an illustrated purpose. From the first SC codeword $\mathbf{S}^1$ in Section 4.2.1, we insert a 2×4 zero matrix $\mathbf{0}$ below the columns of the $\mathbf{S}^1$ matrix, three SC codewords are generated by cyclically shifting two rows of the new matrix as given

$$\mathbf{S}_1^1 = \begin{bmatrix} \mathbf{s}_{1,1} \\ \mathbf{s}_{1,2} \\ \mathbf{0} \end{bmatrix}; \mathbf{S}_2^1 = \begin{bmatrix} \mathbf{0} \\ \mathbf{s}_{1,1} \\ \mathbf{s}_{1,2} \end{bmatrix}; \mathbf{S}_3^1 = \begin{bmatrix} \mathbf{s}_{1,2} \\ \mathbf{0} \\ \mathbf{s}_{1,1} \end{bmatrix}. \tag{4.9}$$

When the number of transmit antennas is even and greater than 4, i.e.,

$n_T = 2n > 4$, the number of SC matrices rise to $2n_T$. For example, a MIMO system equipped with 6 or 8 transmit antennas respectively has 12 or 16 SC codewords. As a result, the number of data bits conveyed by the SC matrices are $\lfloor \log_2 (2n_T) \rfloor$ bits while the number of data bits carried by modulated signals are $4m$ bits, $(M = 2^m)$. Therefore, the spectral efficiency of the DS-SM is presented as given

$$C_{\text{DS-SM}} = \frac{4m + \lfloor \log_2 (2n_T) \rfloor}{T} = m + \frac{\lfloor \log_2 (2n_T) \rfloor}{4} \text{ (bpcu)}. \tag{4.10}$$

Compared with the DT-SM spectral efficiency in the equation (3.14), it can be seen that the DS-SM spectral efficiency is low. However, the DS-SM scheme obtain higher order transmit diversity than the DT-SM one.

In general, the SC codeword design in a systematic procedure for an even number of transmit antennas, $n_T = 2n > 4$, is summarized as follows

1. For given even n_T transmit antennas, arbitrary M modulation level. using Table 4.1 to choose the suitable value of θ and generate the basic set of 4 SC codewords.

2. Adding a $(n_T - 4) \times 4$ zeros matrix $\mathbf{0}$ under the columns of the basic SC codewords from the equation (4.3). Then, these matrices are cycled in two rows to create $2n_T$ new SC codewords.

3. Depending on the information bits to choose the suitable number of SC codewords $\mathbf{S}_k, \forall k = 1, 2, ..., \lfloor \log_2 (2n_T) \rfloor$.

4.3. The DS-SM signal detection

4.3.1. Signal detection

For a given matrix $\mathbf{S}_k, k = 1, 2, ..., K$, we are able to construct the $n_R \times 4$ equivalent matrix $\tilde{\mathbf{H}}_k = \sqrt{\frac{\gamma}{E_s}}\mathbf{H}\mathbf{S}_k$. Therefore, the system equation in (4.4) can be re-written as

$$\mathbf{Y} = \tilde{\mathbf{H}}_k\mathbf{X} + \mathbf{N}. \tag{4.11}$$

Based on the diagonal structure of $\mathbf{X}$, the formula (4.11) can be re-expressed as follows

$$\mathbf{y} = \mathbf{H}_{e,k}\tilde{\mathbf{x}} + \mathbf{n}, \tag{4.12}$$

where $\mathbf{H}_{e,k} = [\ \mathrm{diag}(\tilde{\mathbf{h}}_1)\ \ \mathrm{diag}(\tilde{\mathbf{h}}_2)\ \ \cdots\ \ \mathrm{diag}(\tilde{\mathbf{h}}_{n_R})\ ]^T$. $\tilde{\mathbf{h}}_k, k = 1, ..., n_R$, is k-th row of $\tilde{\mathbf{H}}_k$. $\mathbf{y} = \mathrm{vec}\,(\mathbf{Y}^T)$, $\mathbf{n} = \mathrm{vec}\,(\mathbf{N}^T)$. $\mathrm{vec}\,(\mathbf{A})$ denotes vectorial stacking operation of the matrix $\mathbf{A}$.

Converting the formula (4.12) into the equivalent real system-equation and using the formula (4.1) and (4.4), we obtain

$$\mathbf{v} = \mathbf{M}_k\mathbf{s} + \mathbf{w}, \tag{4.13}$$

where

$$\mathbf{M}_k = \begin{bmatrix} \Re\,(\mathbf{H}_{e,q}) & -\Im\,(\mathbf{H}_{e,q}) \\ \Im\,(\mathbf{H}_{e,q}) & \Re\,(\mathbf{H}_{e,q}) \end{bmatrix} \mathbf{W},$$

$$\mathbf{s} = [\Re\,(\mathbf{u})\,, \Im\,(\mathbf{u})]^T, \mathbf{w} = [\Re\,(\mathbf{n})\,, \Im\,(\mathbf{n})]^T, \mathbf{v} = [\Re\,(\mathbf{y})\,, \Im\,(\mathbf{y})]^T.$$

The system equation in (4.13) is now similar to that of a conventional spatial multiplexing scheme. Therefore, the Sphere Decoders (SD) in [7], [11],

[13], [33], [35] can be used to detect $\mathbf{s}$ for a given $\mathbf{S}_k$ as follows

$$(\hat{\mathbf{s}})_k = \arg\min_{\mathbf{s}} \|\mathbf{t}_k - \mathbf{R}_k\mathbf{s}\|^2, \tag{4.14}$$

where $\mathbf{t}_k = \mathbf{Q}_k^H\mathbf{v}$ and $\mathbf{Q}_k\mathbf{R}_k$ is the QR decomposition of $\mathbf{M}_k$,i.e., $\mathbf{M}_k = \mathbf{Q}_k\mathbf{R}_k$. After that, the index k of the transmitted SC codeword is determined [35] as given

$$\hat{k} = \arg\min_{k} \|\mathbf{t}_k - \mathbf{R}_k(\hat{\mathbf{s}})_k\|^2 + \mathbf{v}^H\mathbf{v} - \mathbf{t}_k^H\mathbf{t}_k. \tag{4.15}$$

Finally, information bits are recovered from a pair of the detected SC codeword and the detected signal vector $\left(\hat{\mathbf{S}}_k, \hat{\mathbf{u}}_k\right)$ at the receiver.

4.3.2. Complexity analysis

In this section, the detection complexity of the DS-SM receiver is anlyzed and compared with several existing MIMO-SM schemes where all schemes implement the SD algorithm. The flop regulations is presented in Section 2.2, Chapter 2.

In the pre-processing state, the complexity of computing $\tilde{\mathbf{H}}_k$ (4.11), QR decomposition of $\mathbf{M}_k$ and an equivalent signal vector $\mathbf{t}_k, k = 1, 2, ..., K$, in (4.14) is calculated as given

$$\begin{aligned}\rho_{\text{pre}} = \tfrac{4}{T}\left(32n_Tn_R + 2040n_R - 36\right)K \\ + \left(143n_R + 7\right)K.\end{aligned} \tag{4.16}$$

Therefore, the DS-SM complexity is generalized as follows

$$\rho = \frac{\rho_{\text{pre}} + \rho_s}{4m + \lfloor \log_2\left(2n_T\right) \rfloor}, \tag{4.17}$$

where ρ_s is the number of average operations within SD searching stage. The DS-SM complexity is detailed in Appendix **F**.

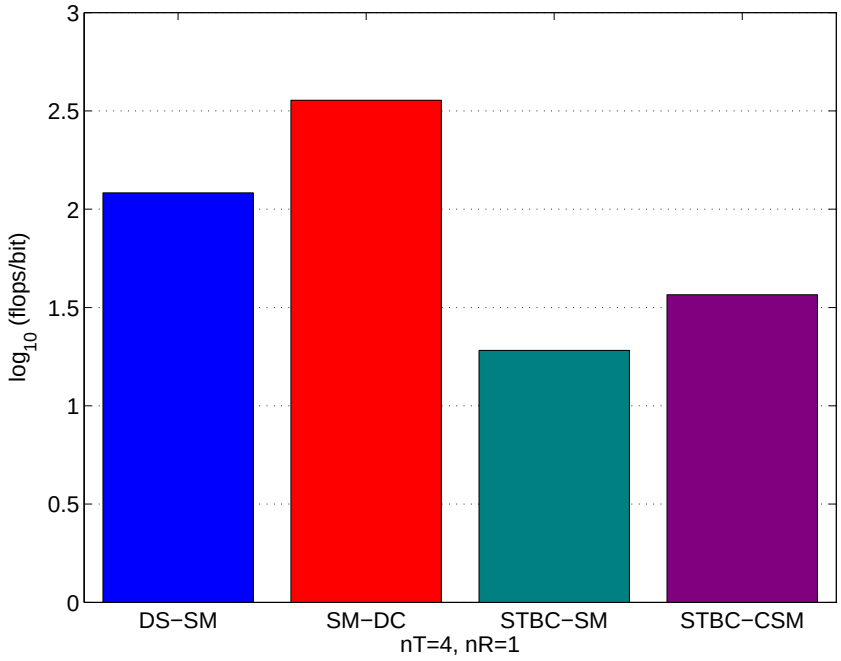

Figure 4.2: Complexity comparison of the DS-SM, SM-DC, STBC-SM, and STBC-CSM at the spectral efficiency 3 bpcu, SNR 9dB, 4 transmit and 1 receive antenna, $T = 80$ symbol periods.

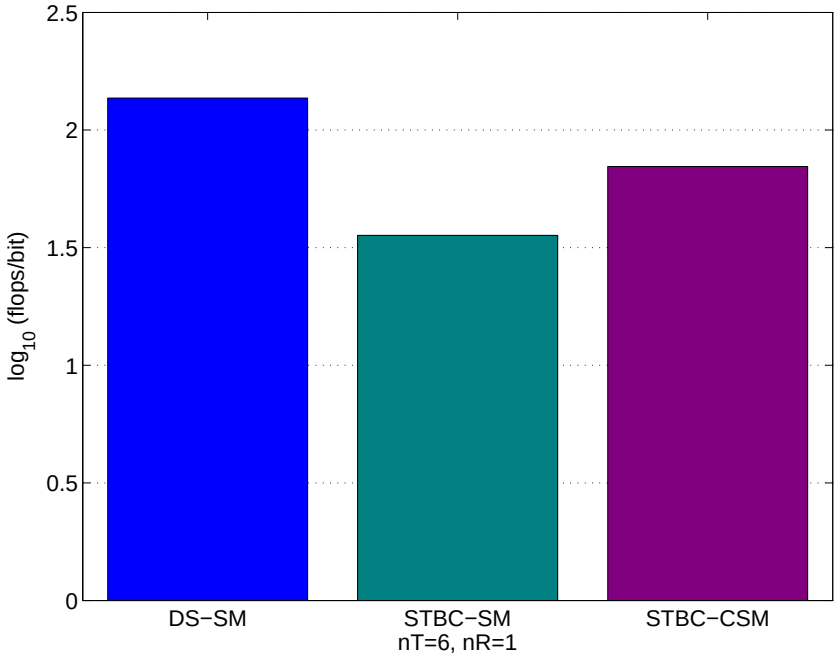

Figure 4.3: Complexity comparison of the DS-SM, SM-DC, STBC-SM, and STBC-CSM at the spectral efficiency 4 bpcu, SNR 9dB, 6 transmit and 1 receive antenna, $T = 80$ symbol periods.

Fig. 4.2 compares the detection complexity of the DS-SM with the existing MIMO-SM schemes such as SM-DC [70], STBC-SM [5], and STBC-CSM [36] in a MIMO configuration with 4 transmit and a receive antennas at spectral efficiency 3 bpcu. It can see that the DS-SM complexity is lower than the SM-DC one. However, the DS-SM scheme offers higher detection complexity than the STBC-SM và STBC-CSM ones. In return for this disadvantage, the DS-SM spectral efficiency is higher 0.5 bpcu than that of the STBC-SM and STBC-CSM ones. In Fig. 4.3, when the number of transmit antennas increases to 6, the DS-SM complexity gradually increases. Although the DS-SM system has higher detection complexity than the STBC-CSM and STBC-SM ones, the DS-SM performance is better than those ones by simulation results.

4.3.3. Theoretical BEP upper bound for the DS-SM system

Based on PEP $P(\mathbf{C}_i \to \mathbf{C}_q)$, upper bound of the DS-SM scheme can be derived [63] as given

$$P_b \leq \frac{1}{N} \sum_{i=1}^{N} \sum_{q=1}^{N} \frac{P(\mathbf{C}_i \to \mathbf{C}_q) w_{i,q}}{\log_2 N}, \tag{4.18}$$

where $N = KM^4$ và $w_{i,q}$ is the number of bits in error between the matrices $\mathbf{C}_i$ and $\mathbf{C}_q$.

The conditional PEP of the DS-SM system is calculated as

$$P\left(\mathbf{C}_i \to \mathbf{C}_q | \mathbf{H}\right) = Q\left(\sqrt{\frac{\gamma}{2}} d^2\left(\mathbf{C}_i, \mathbf{C}_q\right)\right), \tag{4.19}$$

where $Q(x) = (1/2\pi)\int_x^\infty e^{-y^2/2}dy$. From [3], the PEP is given as

$$P(\mathbf{C}_i \to \mathbf{C}_q) = \frac{1}{\pi}\int_0^{\frac{\pi}{2}} \left(\frac{1}{1+\frac{\gamma\lambda_{i,q,1}}{4\sin^2\phi}}\right)^{n_R}\left(\frac{1}{1+\frac{\gamma\lambda_{i,q,2}}{4\sin^2\phi}}\right)^{n_R}\cdots\left(\frac{1}{1+\frac{\gamma\lambda_{i,q,4}}{4\sin^2\phi}}\right)^{n_R} d\phi, \tag{4.20}$$

where $\lambda_{i,q,1}, \lambda_{i,q,2}, \lambda_{i,q,3}, \lambda_{i,q,4}$ is the eigenvalues of the codeword distance $(\mathbf{C}_i - \mathbf{C}_q)(\mathbf{C}_i - \mathbf{C}_q)^H$.

4.4. Simulation results

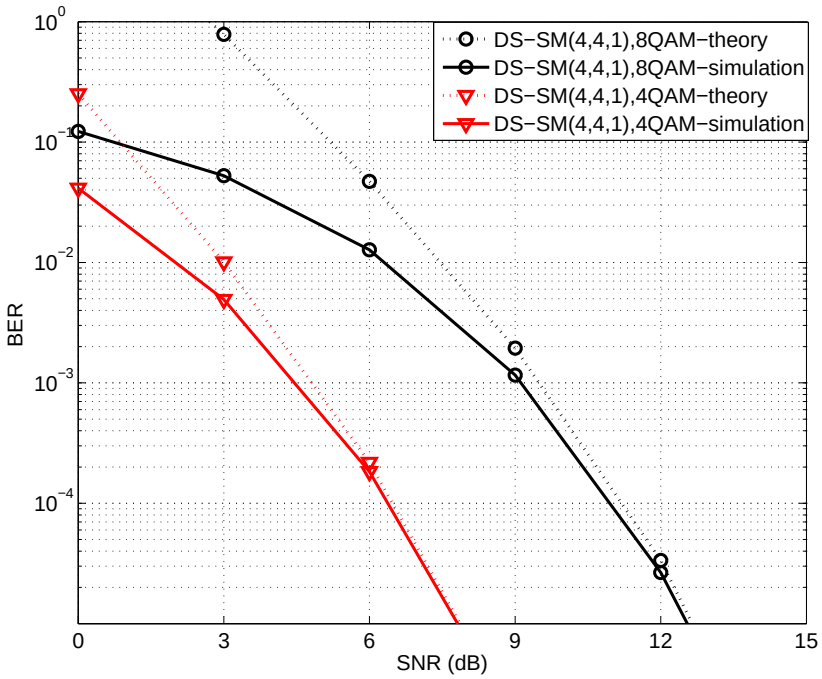

Figure 4.4: Simulation and theoretical results of the (4,4) DS-SM scheme using 4-QAM and 8-QAM.

The performance of the proposed SM is evaluated and compared with several existing MIMO-SM systems such as SM [42], SM-DC [70], STBC-SM [5], và STBC-CSM [36] for different modulation techniques to achieve the same spectral efficiency. The number of transmit antennas, receive antennas, and

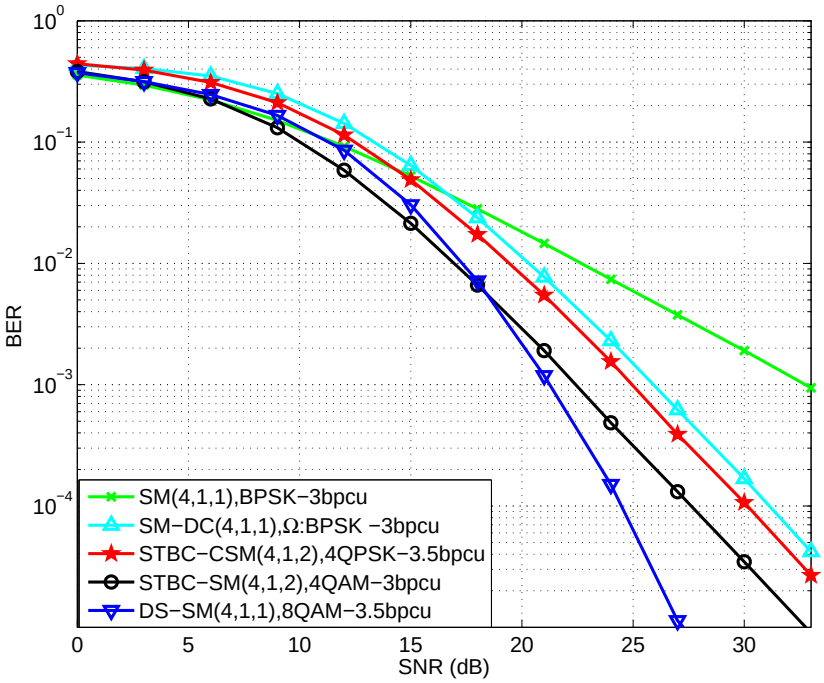

Figure 4.5: Performance comparison of the DS-SM with the SM, STC-SM, SM-DC, and STBC-CSM when $n_R = 1$ at spectral efficiency 3 bpcu.

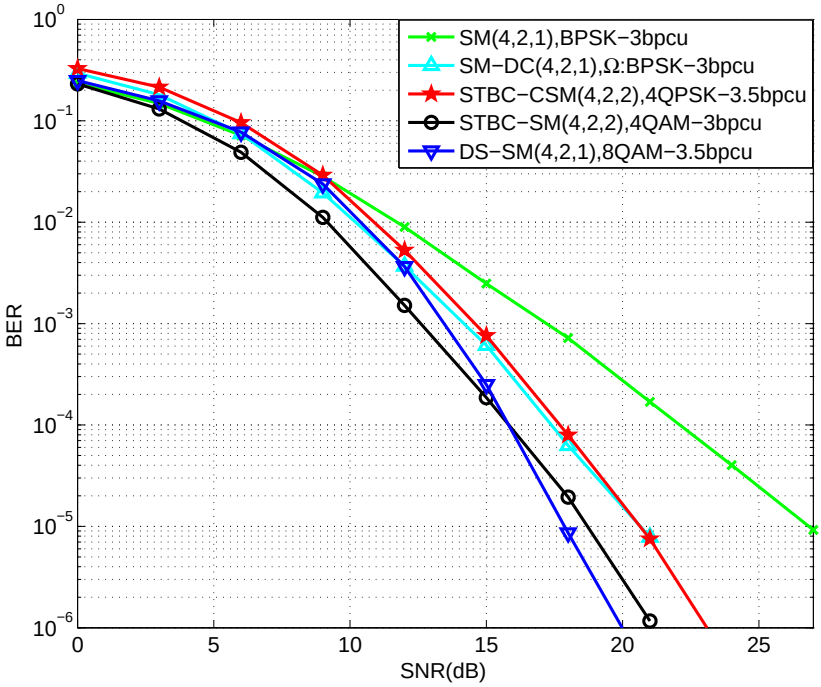

Figure 4.6: Performance comparison of the DS-SM with the SM, STC-SM, SM-DC, and STBC-CSM when $n_R = 2$ at spectral efficiency 3 bpcu.

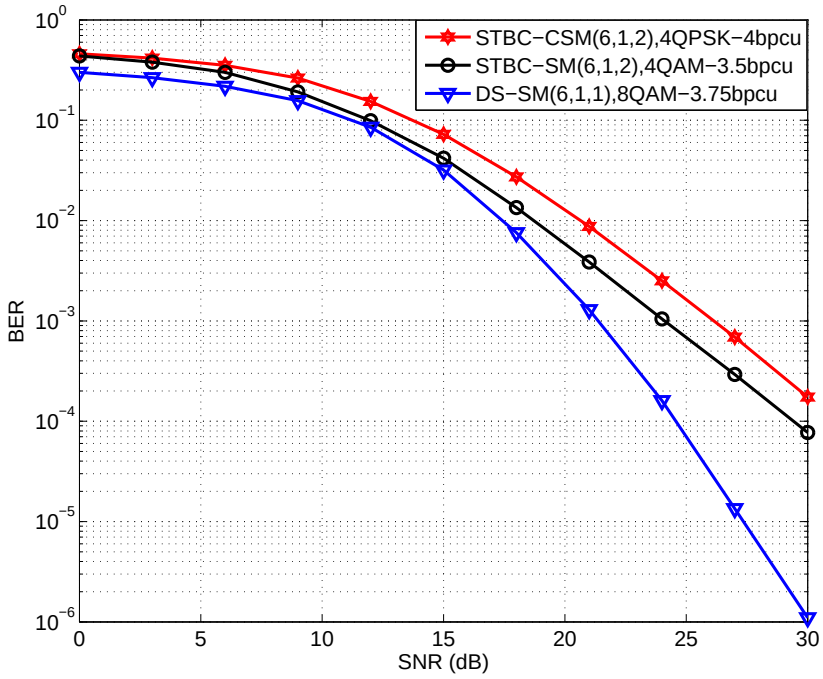

Figure 4.7: Performance comparison of the DS-SM, STBC-SM, and STBC-CSM when using 6 transmit and 1 receive antennas at spectral efficiency 4 bpcu.

active antennas in each scheme is denoted as (n_T, n_R, n_A). For fair comparison, it is assumed that all schemes employ the SD algorithm at the receiver.

Fig. 4.4 illustrates the theoretical and simulation results for the BER performance of the DS-SM scheme in two spectral efficiencies such as 2.5 and 3.5 bpcu. It can be seen from Fig. 4.4 that both curves are coincident at the high SNR region. This result comfirms the accuracy of the DS-SM performance. Fig. 4.5 and 4.6 illustrate the DS-SM $(4, n_R, 1)$, SM $(4, n_R, 1)$, STBC-SM $(4, n_R, 2)$, and STBC-CSM $(4, n_R, 2)$ with the receive antennas $n_R = 1$ or $n_R = 2$ at spectral efficiency 3 bpcu. It can be seen from two figures that the DS-SM scheme outperforms the existing ones at sufficiently high SNR region. Particularly, in Fig. 4.5 at BER $= 10^{-3}$, the DS-SM scheme achieves SNR gains about 1.1 dB, 2.7 dB, 4.7 dB, and 11.5 dB over the STBC-SM, STBC-CSM, SM-DC, and SM ones, respectively. In addition, when increas-

ing the number of receive antennas to 2, in Fig. 4.6 at BER $= 10^{-3}$, the DS-SM scheme obtains about 0.7 dB, 1.1 dB, and 3.8 dB SNR gains over the SM-DC, STBC-CSM, and SM ones. Although the DS-SM scheme has lower performance than the STBC-SM one at low SNR region, especially its value about 0.9 dB at BER $= 10^{-3}$, this scheme achieves higher spectral efficiency about 0.5 bpcu than the STBC-SM one and uses less than one RF chain. That means the DS-SM consumes less energy than the STBC-SM one.

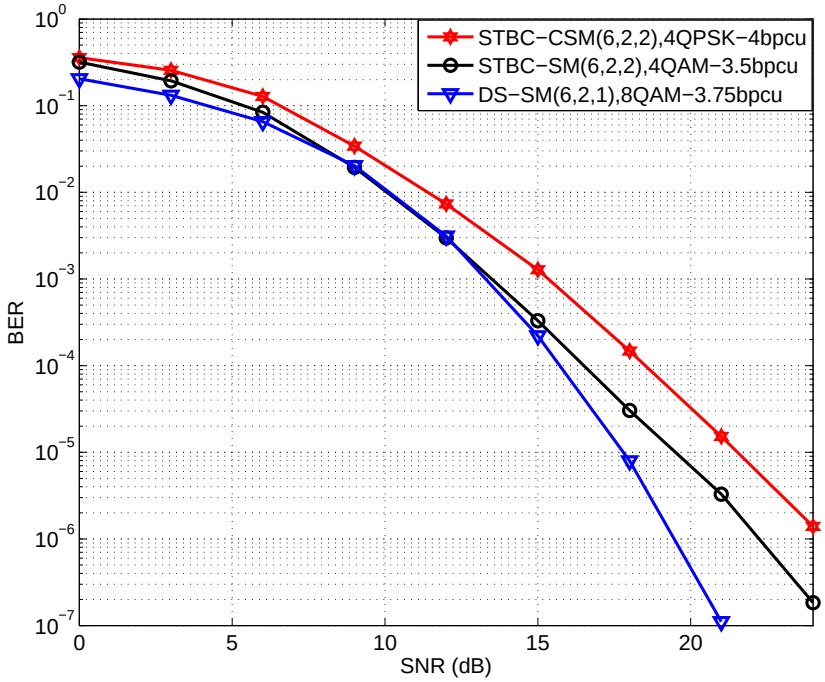

Figure 4.8: Performance comparison of the DS-SM, STBC-SM, and STBC-CSM when using 6 transmit and 2 receive antennas at spectral efficiency 4 bpcu.

Similarly, Fig. 4.7 and Fig. 4.8 compare the performance of the DS-SM $(6, n_R, 1)$ with STBC-SM $(6, n_R, 2)$, and STBC-CSM $(6, n_R, 2)$ with the receive antennas $n_R = 1$ and $n_R = 2$. From two figures, we can see that the DS-SM scheme outperforms the STBC-SM and STBC-CSM ones. In Fig. 4.7 at BER $= 10^{-3}$, the DS-SM scheme achieves about 2.8 dB and 5.5 dB SNR

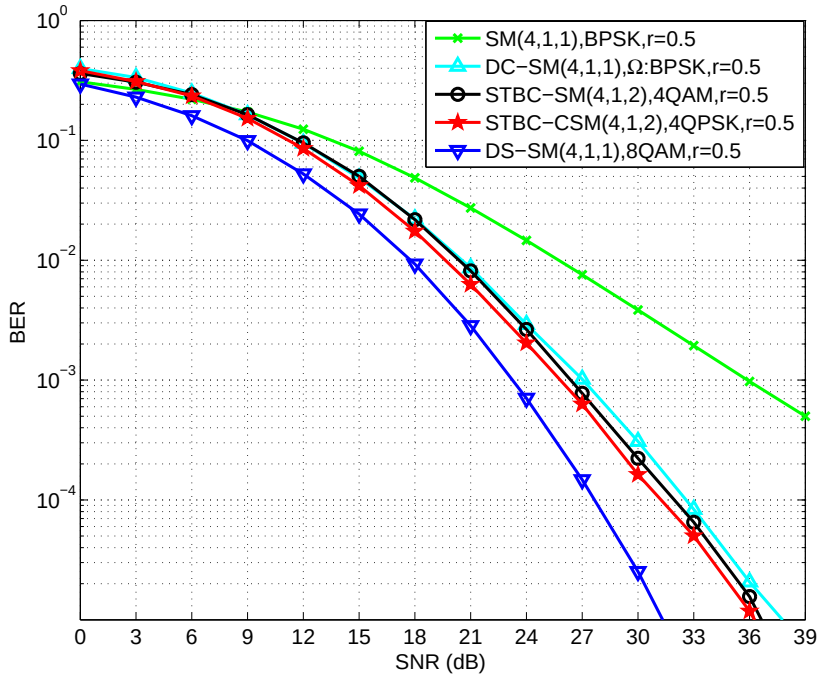

Figure 4.9: Performance comparison of the DS-SM, SM, SM-DC, STBC-SM, and STBC-CSM (4,1) at spectral efficiency 3 bpcu, the correlation coefficient $r = 0{,}5$.

gains over the STBC-SM and STBC-CSM ones, respectively. Meanwhile, in Fig. 4.8, this SNR gain gap is smaller. Particularly, at BER $= 10^{-3}$, the DS-SM scheme obtains 0.2 dB and 2 dB SNR gains over the STBC-SM and STBC-CSM ones, respectively. It can be explained that when increasing the number of receive antennas, the DS-SM diveristy order is lower than that of those schemes.

The correlation channel model is utilized as in Section 2.2.5, Chapter 2. The DS-SM, SM, SM-DC, STBC-SM, and STBC-CSM schemes are equipped with 4 transmit and 1 receive antennas at the spectral efficiency 3 bpcu. These schemes' performances are investigated with an intermediate correlation coefficient among transmit antennas or receive antennas, $r = 0.5$. Fig. 4.9 shows that the DS-SM scheme robustly performs under spatial correla-

tion effect. Particularly, at $\mathrm{BER} = 10^{-3}$, the DS-SM scheme obtains about 2.5 dB, 3 dB, 3.7 dB, and 12 dB SNR gains over the STBC-SM, SM-DC, and SM ones.

4.5. Conclusion

In this chapter, a new MIMO-SM system, called DS-SM, is proposed to keep the main advantages of the SM technique because this scheme only activates one of n_T transmit antennas at each symbol period. Based on the rank and determinant criteria of the STBCs, the DS-SM scheme obtains fouth order transmit diversity. Furthermore, a generalized SC codeword design procedure for the DS-SM system, equipped with the even number of transmit antennas greater than 4, is proposed. Simulation results show that the DS-SM scheme outperforms the existing MIMO-SM ones at high SNR region with a reasonable detection complexity and robustly operates under the correlation effect. besides, the DS-SM performance is verified by the BEP upper bound of the DS-SM scheme. As a result, the DS-SM scheme is suitable for MIMO systems having high communication reliability requirements.

CONCLUSION AND FUTURE WORKS

In this dissertation on MIMO-SM schemes, the Ph.D student has studied the basic knowledge of the SM technique, the STCs, as well as research works related to the SM techniques. From these works, the thesis proposed three low complexity detection algorithms and a new BEP upper bound for the HRSM system. In addition, two MIMO-SM schemes also were proposed to focus on improving the MIMO-SM spectral efficiency or increasing the transmit diversity order of the MIMO-SM one. Furthermore, the thesis contributions and future works are briefly presented as below.

A. The thesis contributions

1. Based on several sub-optimal detection algorithms for SDM systems, three modified detection algorithms such as the modified MMSE-VBLAST, the modified MMSE-SQRD, and the improved SQRD ones offering low complexity is proposed for the HRSM system. These detectors have potential applications for HRSM systems when deploying these systems in practise. Besides, a tighter BEP upper bound is derived to accurately estimate this system performance using M-QAM modulation at high SNR region;

2. A new MIMO-SM scheme, called Spatially Modulated Space Time Block Coding (DT-SM), for MIMO systems equipped with the number of transmit antennas greater than 4 is proposed by combining the SM technique

with the convetional Double Space Time Transmit Diversity (DSTTD). This system offers higher spatial spectral efficiency than several MIMO-SM ones. Simulation and theoretical results show that the DT-SM scheme outperforms the existing MIMO and MIMO-SM ones. In the DT-SM receiver, a modified SE-SD algorithm is proposed for the DT-SM system to reduce detection complexity. In addition, the DT-SM scheme has been demonstrated to robustly perform under correlated MIMO channel. As a result, the DT-SM scheme has potential applications for MIMO systems requiring high spectral efficiency and is suitable for utilization in spatial conditions that are not large enough to deploy transceiver antennas;

3. Proposing a Diagonal Space Time Coded Spatial Modulation for MIMO systems equipped with the even number of transmit antennas, called DS-SM, by embedding the Diagonal Sapce Time Code in the SM. The DS-SM scheme obtains fourth order transmit diversity. Simulation results and complexity analysis show that the DS-SM scheme surpasses several MIMO-SM ones with a reasonable detection complexity. As a result, this scheme is suitable for MIMO systems that require high communication quality.

B. Future works

The dissertation has studied the basic knowledge and also proposed new MIMO-SM schemes. However, according to my opinion, there are still some issues that should be further researched and implemented in the future as given

- Extending the reasearch of other low complexity detectors such as lattice reduction algorithm, soft detectors as well as PIC ones for the HRSM scheme;

- Evaluating the HRSM performance under correlated MIMO channel and imperfect CSI at the receiver as well as deriving a tighter BEP upper bound for the HRSM scheme at low SNR region;
- Studying optimal estimation algorithms for MIMO-SM schemess;
- Studing the SM applications in massive MIMO systems as well as investigating the index modulation technique.

APPENDICES

Appendix A

Deriving the equation (2.9)

In a SDM system, if using a MMSE detector, we will have

$$\tilde{\mathbf{c}} = \mathbf{G}_{\text{MMSE}}\mathbf{y}. \tag{A.1}$$

Then, quantizing this vector $\tilde{\mathbf{c}}$, we recovered the transmitted signal vector $\hat{\mathbf{c}}$. Based on the orthogonal principle, we can see that the error vector $(\tilde{\mathbf{c}} - \mathbf{c})$ is orthogonal with the received vector $\mathbf{y}$, i.e.,

$$E\left\{(\tilde{\mathbf{c}} - \mathbf{c})\,\mathbf{y}^H\right\} = E\left\{(\mathbf{G}_{\text{MMSE}}\mathbf{y} - \mathbf{c})\,\mathbf{y}^H\right\} = \mathbf{0}. \tag{A.2}$$

Changing the menber of the equation, we have

$$\mathbf{G}_{\text{MMSE}} E\left\{\mathbf{y}\mathbf{y}^H\right\} = E\left\{\mathbf{c}\mathbf{y}^H\right\}. \tag{A.3}$$

Putting $\tilde{\mathbf{H}} = \sqrt{\frac{\gamma}{n_T E_s}}\mathbf{H}$ and then subtituting each component of the equation (A.3), we obtain

$$\begin{aligned} E\left\{\mathbf{y}\mathbf{y}^H\right\} &= E\left\{\left(\tilde{\mathbf{H}}\mathbf{c} + \mathbf{n}\right)\left(\tilde{\mathbf{H}}\mathbf{c} + \mathbf{n}\right)^H\right\} \\ &= \tilde{\mathbf{H}} E\left\{\mathbf{c}\mathbf{c}^H\right\}\tilde{\mathbf{H}}^H + E\left\{\mathbf{n}\mathbf{n}^H\right\} \\ &= E_s\tilde{\mathbf{H}}\tilde{\mathbf{H}}^H + \mathbf{I} \end{aligned} \quad \cdot \tag{A.4}$$

Similarly

$$E\left\{\mathbf{c}\mathbf{y}^H\right\} = E\left\{\mathbf{c}\left(\tilde{\mathbf{H}}\mathbf{c} + \mathbf{n}\right)^H\right\} = E\left\{\mathbf{c}\mathbf{c}^H\right\}\tilde{\mathbf{H}}^H = E_s\tilde{\mathbf{H}}^H. \tag{A.5}$$

where because the HRSM scheme is considered as a SDM system, the entries of the HRSM transmitted vector $\mathbf{c}$ are assumed to be independent. Therefore,

$E\{\mathbf{c}\mathbf{c}^H\} = E_s\mathbf{I}$.

From (A.4) and (A.5), we have

$$\mathbf{G}_{\text{MMSE}}\left(E_s\tilde{\mathbf{H}}\tilde{\mathbf{H}}^H + \mathbf{I}\right) = E_s\tilde{\mathbf{H}}^H. \tag{A.6}$$

Finally

$$\mathbf{G}_{\text{MMSE}} = E_s\tilde{\mathbf{H}}^H\left(E_s\tilde{\mathbf{H}}\tilde{\mathbf{H}}^H + \mathbf{I}\right)^{-1} = \tilde{\mathbf{H}}^H\left(\tilde{\mathbf{H}}\tilde{\mathbf{H}}^H + \tfrac{1}{E_s}\mathbf{I}\right)^{-1}. \tag{A.7}$$

Appendix B

The ML, MSQRD, MBLAST, and ISQRD complexities

Complexity regulations

- Each real arithmetic calculation, i.e., real addition, multiplication, division, or square root, is considered a floating point operation (flop).
- A complex multiplication requires 4 real multiplications and 2 additions, i.e., 6 flops. A complex summation requires 2 flops.
- Denoting $x \in \mathbb{C}$ is a complex scalar, the vectors $\mathbf{a} \in \mathbb{C}^n, \mathbf{b} \in \mathbb{C}^n$, and $\mathbf{c} \in \mathbb{C}^m$ have dimension n, n, and m, respectively. The matrices $\mathbf{A} \in \mathbb{C}^{m\times n}, \mathbf{B} \in \mathbb{C}^{n\times l}$ have dimension $m \times n$ and $n \times l$, respectively.
- Scalar-vector multiplication $x\mathbf{a}$ requires $4n$ real multiplications and $2n$ additions, or $6n$ flops.
- Scalar-matrix multiplication $x\mathbf{A}$ requires $4nm$ real multiplications and $2nm$ additions, or $6nm$ flops.
- Inner product $\mathbf{a^H b}$ requires $4n$ real multiplications and $4n-2$ additions, or $8n - 2$ flops.

- Matrix-vector product $\mathbf{Ab}$ requires $4mn$ real multiplications and $4mn-2m$ additions, or $8mn-2m$ flops.
- Matrix-matrix product $\mathbf{AB}$ requires $4mnl$ real multiplications and $4mnl-2ml$ additions, or $8mnl-2ml$ flops.
- For a real matrix $\mathbf{M} \in \mathbb{R}^{m\times n}$ its QR decomposition based on the Modi ed Gram-Schmidt algorithm [50] requires $2mn^2+mn-\frac{n^2+n}{2}$ flops.

The ML complexity

- Step 2: Computing the equivalent channel $\tilde{\mathbf{h}}_k = \mathbf{H}\mathbf{s}_k, k = 1, ..., K$, with $\mathbf{H} \in \mathbb{C}^{n_R\times n_T}, \mathbf{s}_k \in \mathbb{C}^{n_T\times 1}$ requires $4n_Tn_R-2n_R$ real additions and $4n_Rn_T$ multiplications.
- Step 3: Computing $d_k(x) = \left\|\tilde{h}_k\right\|_F^2 |x|^2-2\sqrt{\Re}\left\{y^H\tilde{h}_kx\right\}$ requires $8n_RM+2M$ real additions and $(8n_R+4)M$ multiplications.
  - Computing $\left\|\tilde{h}_k\right\|_F^2 |x|^2$ requires $4n_RM$ real additions and $(4n_R+2)M$ multiplications.
  - Computing $2\Re\left\{y^H\tilde{h}_kx\right\}$ requires $(4n_R+2)M$ real additions and $(4n_R+2)M$ multiplications.

Then, the ML complexity is presented as follows

$$\rho_{\mathrm{ML}} = MK\left(16n_R+6\right)+\left(8n_Rn_T-2n_R\right)K \ \ (\mathrm{flop})\,.$$

The MBLAST complexity

- Step 2: Computing $\mathbf{G}_{\mathrm{MMSE}}$ [22] requires $\frac{15}{4}n_T^4+2n_T^3n_R+n_T^2n_R^2$ flops.
- Step 4: Computing $\tilde{c}_k = \mathbf{g}_{\mathrm{MMSE},k}\mathbf{y}$ requires $(8n_R-2)$ flops.

- Step 5: Quantizing requires 0 flop.
- Step 6: Eliminating the effect of $\hat{c}_1$ in $\mathbf{y}$ requires $4n_R + 2n_R + 2n_R = 8n_R$ flops.
- Step 7: Repeating from step 2 to step 7 requires $n_T\left(16n_R - 2\right)$ flops.

The MBLAST complexity is presented as given

$$\rho_{\text{MBLAST}} = 15n_T^4 + 2n_T^3 n_R + n_T^2 n_R^2 + n_T\left(16n_R - 2\right) \text{ (flop)}.$$

The MSQRD complexity

- Bước 2: Decomposing QR decomposition of the extended channel matrix requires $8n_T^3 + \left(8n_R - 15\right)n_T^2 - \left(18n_R + 1\right)n_T$ flops.
- Bước 3: Computing $\mathbf{v} = \mathbf{Q}^H\mathbf{y}$ requires $8\left(n_R + n_T\right)n_T - 2n_T$ flops.
- Step 4:
  - Quantizating $\hat{c}_{n_T} = Q\left(\frac{v_{n_T}}{r_{n_T,n_T}}\right)$ requires 2 flops.
  - Computes $v_k = v_k - \sum\limits_{n=k+1}^{n_T} r_{k,n}\hat{c}_n$ requires $8\left(n_T - 1\right) - 8k$ flops. Quantizing $\hat{c}_k = Q\left(\frac{v_k}{r_{k,k}}\right)$ requires 2 flops. This process is repeated untill $\hat{\mathbf{c}}$ is recovered. It requires $\sum\limits_{k=1}^{n_T-1} 8\left(n_T - 1\right) - 8k + 2 = 4n_T^2 - 10n_T + 6$ flops.

Then, the MSQRD complexity is presented as given

$$\rho_{\text{MSQRD}} = 8n_T^3 + n_T^2\left(8n_R - 3\right) - n_T\left(10n_R + 13\right) + 8 \text{ (flop)}.$$

The ISQRD complexity

- Step 2: Decomposing QR decomposition of the extended channel matrix requires $8(n_T - 1)^3 + \left(8n_R - 11\right)\left(n_T - 1\right)^2 - \left(14n_R + 2\right)\left(n_T - 1\right)$ flops.

- Step 3:
  - With each $x \in \Omega_x$, Computing $\mathbf{v} = \mathbf{Q}^H (\mathbf{y} - \mathbf{h}_1 x)$ requires $8(n_T - 1)^2 + (8n_R - 2)(n_T - 1) + 8n_R$ flops.
  - Quantizing $\hat{\bar{c}}_{n_T-1} = Q\left(\frac{v_{n_T-1}}{r_{n_T-1,n_T-1}}\right)$ requires 2 flops.
  - computing $v_k = v_k - \sum_{n=k+1}^{n_T-1} r_{k,n}\hat{c}_n$ requires $8(n_T - 2) - 8k$ flops. Quantizing $\hat{\bar{c}}_k = Q\left(\frac{v_k}{r_{k,k}}\right)$ requires 2 flops. This process is repeated untill $\hat{\bar{\mathbf{c}}}$ is recovered. It requires $4(n_T - 1)^2 - 10(n_T - 1) + 6$ flops.
  - Computing $d_x = \left\|\mathbf{t} - \bar{\mathbf{H}}\hat{\bar{\mathbf{c}}}_\mathbf{p}\right\|^2$ requires $8n_R(n_T - 1) + 2n_R - 1$ flops.

  This process calculates for entire signal constellation, then the complexity requires $M\left(12(n_T - 1)^2 + (16n_R - 12)(n_T - 1) + 10n_R + 7\right)$ flop.
- Step: Recovering $\hat{x} = \arg\min_x d_x$ requires 0 flop.
- Step 5: $\hat{\mathbf{s}} = \frac{1}{\hat{x}}\begin{bmatrix} \hat{x} & \hat{\bar{\mathbf{c}}}_\mathbf{p} \end{bmatrix}^T$ require $6(n_T - 1) + 5$ flops.

Then, the ISQRD complexity is presented as given

$$\begin{aligned}\rho_{\text{ISQRD}} &= 8(n_T - 1)^3 + (8n_R - 11 + 12M)(n_T - 1)^2 \\ &+ (M(16n_R - 12) - 14n_R + 4)(n_T - 1) + M(10n_R + 7) + 5.\end{aligned} \quad \text{(flop)}.$$

Appendix C

An example illustrates the overlap of the PEP calculation area in the union bound with QPSK constellation

The union bound presented in the equation (2.29) is calculated by summing all PEPs. However, in fact, some PEPs are counted several times, therefore, the union bound is not close to the simulation curve. It is demonstrated by an example where a wireless system using QPSK modulation presented in

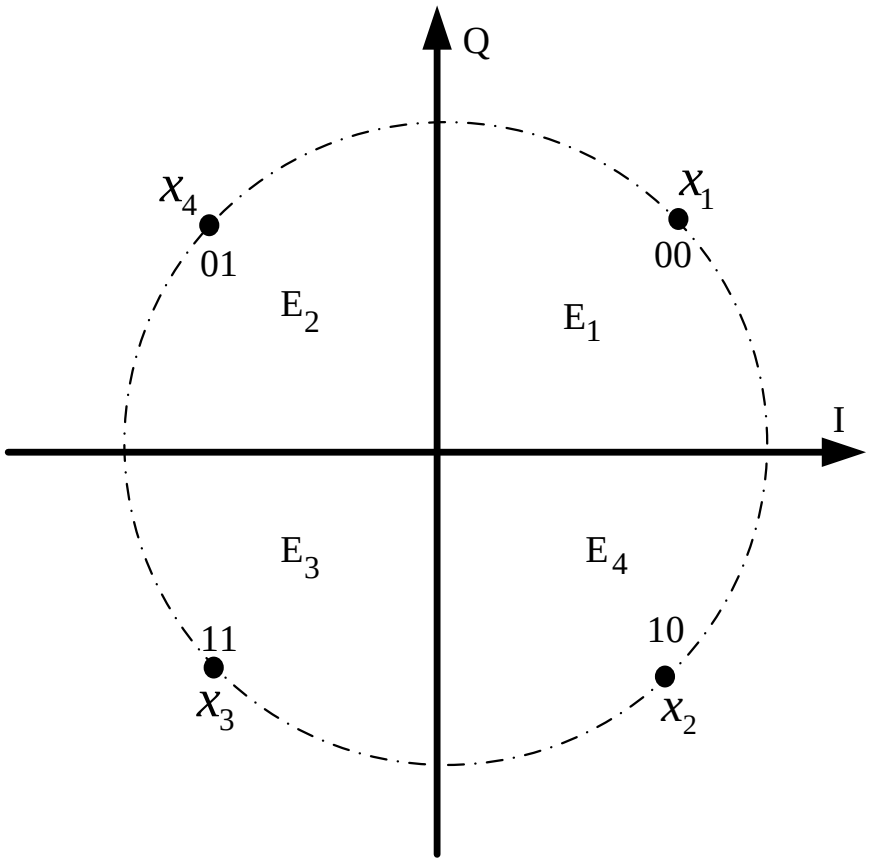

Figure C.1: A Voronoi diagram of the QPSK.

Fig. C.1 is considered. In this figure, the complex plane is split into 4 areas E_1, E_2, E_3, and E_4 respectively corresponding to 4 Voronoi areas of x_1, x_2, x_3, and x_4.

Assuming that x_1 is the transmitted symbol and the receiver could wrongly decide 1 of 3 three remaining symbols x_2, x_3, and x_4. The receiver exactly decides x_1 if the received signal is belong to the area E_1 and makes wrong decision if this signal is out of this area. At that time, the union bound is calculated as given

$$P_e \leq \sum_{i=2}^{4} P\left(x_1 \rightarrow x_i\right). \tag{C.1}$$

Fig. C.2 decribes PEPs $P\left(x_1 \rightarrow x_2\right)$, $P\left(x_1 \rightarrow x_3\right)$, and $P\left(x_1 \rightarrow x_4\right)$ where the gray area is wrong decision area. Fig. C.3 shows that the union bound

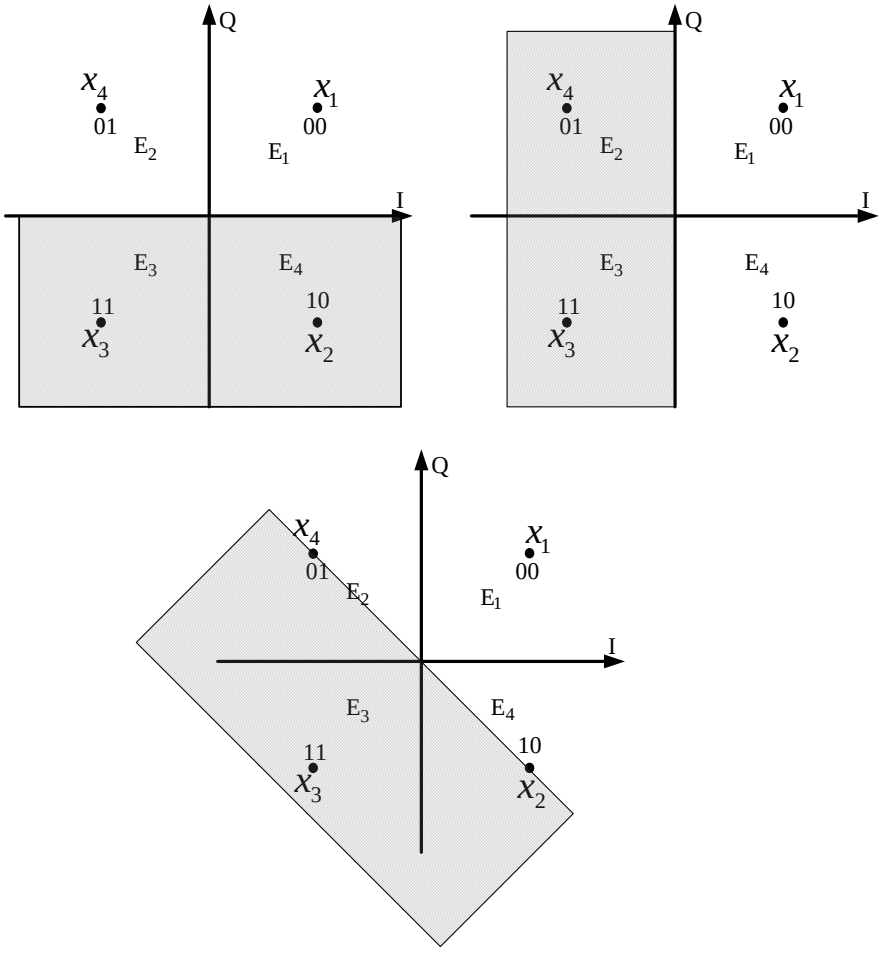

Figure C.2: PEP calculation areas in QPSK constellation.

calculates the E_3 area three times, a part of the E_2 area and E_4 area. Therefore, two PEPs $P(x_1 \to x_2)$ and $P(x_1 \to x_4)$ cover whole Voronoi diagram of QPSK constellation. As a result, a tighter new bound is presented as given

$$P_e \leq P(x_1 \to x_2) + P(x_1 \to x_4). \tag{C.2}$$

it can be seen that because of the PEP calculation overlap, a PEP $P(x_1 \to x_3)$ is eliminated. However, the $\mathbf{E}_3$ area is still calculated two times, so we can find a tigher bound. When signal constellation is larger, the problem eliminating redundant PEPs becomes difficult. Therefore, Verdu *et. al* [65] demonstrated a tighter new bound that suitably removes redundant PEPs. Verdu theorem

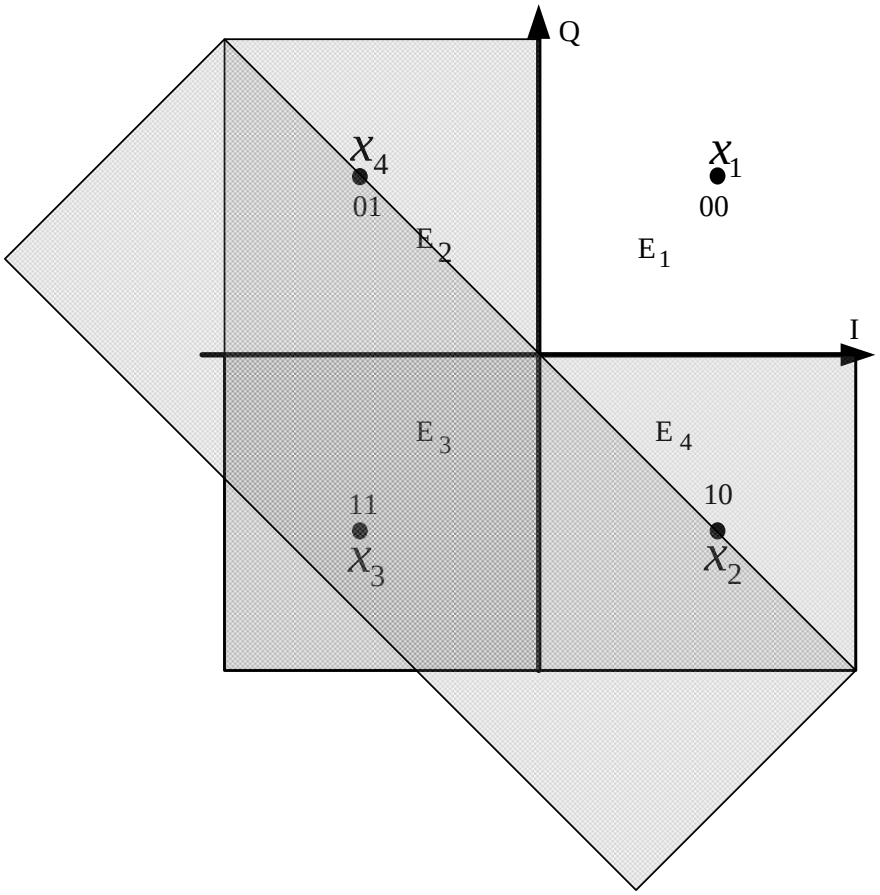

Figure C.3: The overlap of PEP calculation areas in the union bound.

is presented by Blahut *et. al* in [8]. Applying Verdu theorem in the HRSM union bound problem, a theorem is derived to eliminate redundant PEPs in this bound.

Appendix D

Constructions of CDGs of the DT-SM scheme with basic SC codewords

Let us consider two different DT-SM codewords $\mathbf{C} \neq \hat{\mathbf{C}}$, where

$$\mathbf{C} = \mathbf{S}\mathbf{X}, \tag{D.1}$$

$$\hat{\mathbf{C}} = \hat{\mathbf{S}}\hat{\mathbf{X}}. \tag{D.2}$$

The codeword distance matrix is defined as given

$$\mathbf{G} = (\mathbf{C} - \hat{\mathbf{C}})^H(\mathbf{C} - \hat{\mathbf{C}}) = (\mathbf{SX} - \hat{\mathbf{S}}\hat{\mathbf{X}})^H(\mathbf{SX} - \hat{\mathbf{S}}\hat{\mathbf{X}}). \tag{D.3}$$

In order for $\mathbf{C} \neq \hat{\mathbf{C}}$, we consider the two following cases

- $\mathbf{S} = \hat{\mathbf{S}}$, $\mathbf{X} \neq \hat{\mathbf{X}}$;
- $\mathbf{S} \neq \hat{\mathbf{S}}$, $\forall \mathbf{X}, \hat{\mathbf{X}}$.

Case 1: $\mathbf{S} = \hat{\mathbf{S}}$, $\mathbf{X} \neq \hat{\mathbf{X}}$

We can re-write D.3 as given

$$\mathbf{G} = (\mathbf{X} - \hat{\mathbf{X}})^H\mathbf{S}^H\mathbf{S}(\mathbf{X} - \hat{\mathbf{X}}). \tag{D.4}$$

It is straightforward to verify that for each of $\mathbf{S}_i, i = 1, 2, 3, 4$ in (3.3), we have $\mathbf{S}_i^H\mathbf{S}_i = \mathbf{I}_4$, where $\mathbf{I}_4$ is a 4×4 identity matrix. Therefore, equation (D.4) becomes

$$\begin{aligned}
\mathbf{G} &= (\mathbf{X} - \hat{\mathbf{X}})^H(\mathbf{X} - \hat{\mathbf{X}}) \\
&= \begin{bmatrix} x_1 - \hat{x}_1 & -x_2^* + \hat{x}_2^* \\ x_2 - \hat{x}_2 & x_1^* - \hat{x}_1^* \\ x_3 - \hat{x}_3 & -x_4^* + \hat{x}_4^* \\ x_4 - \hat{x}_4 & x_3^* - \hat{x}_3^* \end{bmatrix}^H \begin{bmatrix} x_1 - \hat{x}_1 & -x_2^* + \hat{x}_2^* \\ x_2 - \hat{x}_2 & x_1^* - \hat{x}_1^* \\ x_3 - \hat{x}_3 & -x_4^* + \hat{x}_4^* \\ x_4 - \hat{x}_4 & x_3^* - \hat{x}_3^* \end{bmatrix} \\
&= \begin{bmatrix} \sum_{i=1}^{4} |x_i - \hat{x}_i|^2 & 0 \\ 0 & \sum_{i=1}^{4} |x_i^* - \hat{x}_i^*|^2 \end{bmatrix}.
\end{aligned} \tag{D.5}$$

It follows that

$$f(\theta) = \det(\mathbf{G}) = \left(\sum_{i=1}^{4} |x_i - \hat{x}_i|^2 \right)^2 \quad \forall \theta. \tag{D.6}$$

Without loss of generality we assume that $\mathbf{X} \neq \hat{\mathbf{X}}$ amouts to $x_1 \neq \hat{x}_1$. Thus, for QAM modulations, we obtain

$$f(\theta) \geq \left(\left|x_1 - \hat{x}_1\right|^2\right)^2 \geq 16 \quad \forall\theta. \tag{D.7}$$

Case 2: $\mathbf{S} \neq \hat{\mathbf{S}}$ *for* $\forall \mathbf{X}, \hat{\mathbf{X}}$

- *When* $\mathbf{S} = \mathbf{S}_1$ *and* $\hat{\mathbf{S}} = \mathbf{S}_2$

  The SC codewords $\mathbf{C}$ and $\hat{\mathbf{C}}$ is respectively calculated as given

$$\mathbf{C} = \mathbf{S}_1.\mathbf{X} = \begin{bmatrix} 1 & 0 & 0 & 0 \\ 0 & 1 & 0 & 0 \\ 0 & 0 & e^{j\theta} & 0 \\ 0 & 0 & 0 & e^{-j\theta} \end{bmatrix} \begin{bmatrix} x_1 & -x_2^* \\ x_2 & x_1^* \\ x_3 & -x_4^* \\ x_4 & x_3^* \end{bmatrix},$$

$$\hat{\mathbf{C}} = \mathbf{S}_2.\hat{\mathbf{X}} = \begin{bmatrix} 0 & 0 & e^{j\theta} & 0 \\ 0 & 0 & 0 & e^{-j\theta} \\ 1 & 0 & 0 & 0 \\ 0 & 1 & 0 & 0 \end{bmatrix} \begin{bmatrix} \hat{x}_1 & -\hat{x}_2^* \\ \hat{x}_2 & \hat{x}_1^* \\ \hat{x}_3 & -\hat{x}_4^* \\ \hat{x}_4 & \hat{x}_3^* \end{bmatrix}.$$

The codeword distance matrix is now given by

$$\begin{aligned}\mathbf{G} &= (\mathbf{C}-\hat{\mathbf{C}})^H(\mathbf{C}-\hat{\mathbf{C}}) \\ &= \begin{bmatrix} x_1 - e^{j\theta}\hat{x}_3 & -x_2^* + e^{j\theta}\hat{x}_4^* \\ x_2 - e^{-j\theta}\hat{x}_4 & x_1^* - e^{-j\theta}\hat{x}_3^* \\ e^{j\theta}x_3 - \hat{x}_1 & -e^{j\theta}x_4^* + \hat{x}_2^* \\ e^{-j\theta}x_4 - \hat{x}_2 & e^{-j\theta}x_3^* - \hat{x}_1^* \end{bmatrix}^H \\ &\times \begin{bmatrix} x_1 - e^{j\theta}\hat{x}_3 & -x_2^* + e^{j\theta}\hat{x}_4^* \\ x_2 - e^{-j\theta}\hat{x}_4 & x_1^* - e^{-j\theta}\hat{x}_3^* \\ e^{j\theta}x_3 - \hat{x}_1 & -e^{j\theta}x_4^* + \hat{x}_2^* \\ e^{-j\theta}x_4 - \hat{x}_2 & e^{-j\theta}x_3^* - \hat{x}_1^* \end{bmatrix}. \end{aligned} \tag{D.8}$$

After some mathematical manipulations, we obtain the CDG as follows

$$\begin{aligned} f_{\mathbf{S}_1\mathbf{S}_2}(\theta) = \det(\mathbf{G}) = \Big(&\left|e^{j\theta}x_3 - \hat{x}_1\right|^2 + \left|x_2 - e^{-j\theta}\hat{x}_4\right|^2 \\ &+ \left|x_1 - e^{j\theta}\hat{x}_3\right|^2 + \left|e^{-j\theta}x_4 - \hat{x}_2\right|^2 \Big)^2. \end{aligned} \tag{D.9}$$

Sinilarly, we are able to compute the remaining cases as below.

- *When* $\mathbf{S} = \mathbf{S}_1$ *and* $\hat{\mathbf{S}} = \mathbf{S}_3$

$$\begin{aligned} f_{\mathbf{S}_1\mathbf{S}_3}(\theta) = &\Big(\left|x_1 - e^{j2\theta}\hat{x}_3\right|^2 + \left|x_2 - e^{-j\theta}\hat{x}_2\right|^2 \\ &+ \left|x_3 - \hat{x}_1\right|^2 + \left|x_4 - e^{-j\theta}\hat{x}_4\right|^2 \Big) \\ &\times \Big(\left|-x_2^* + e^{j2\theta}\hat{x}_4^*\right|^2 + \left|x_1^* - e^{-j\theta}\hat{x}_1^*\right|^2 \\ &+ \left|-x_4^* + \hat{x}_2^*\right|^2 + \left|x_3^* - e^{-j\theta}\hat{x}_3^*\right|^2 \Big) \\ &- \left|\left(x_3 - e^{-j\theta}x_1\right)\left(\hat{x}_2 - e^{-j\theta}\hat{x}_4\right)\right. \\ &+ \left.\left(x_4 - e^{j\theta}x_2\right)\left(\hat{x}_1 - e^{j\theta}\hat{x}_3\right)\right|^2. \end{aligned} \tag{D.10}$$

- *When* $\mathbf{S} = \mathbf{S}_1$ *and* $\hat{\mathbf{S}} = \mathbf{S}_4$

$$\begin{aligned} f_{\mathbf{S}_1\mathbf{S}_4}(\theta) = &\Big(\left|x_1 - e^{j\theta}\hat{x}_1\right|^2 + \left|x_2 - e^{-j2\theta}\hat{x}_4\right|^2 \\ &+ \left|x_3 - e^{j\theta}\hat{x}_3\right|^2 + \left|x_4 - \hat{x}_2\right|^2\Big) \\ &\times \Big(\left|-x_2^* + e^{j\theta}\hat{x}_2^*\right|^2 + \left|x_1^* - e^{-j2\theta}\hat{x}_3^*\right|^2 \\ &+ \left|-x_4^* + e^{j\theta}\hat{x}_4^*\right|^2 + \left|x_3^* - \hat{x}_1^*\right|^2\Big) \\ &- \left|\left(x_3 - e^{-j\theta}x_1\right)\left(\hat{x}_2 - e^{-j\theta}\hat{x}_4\right)\right. \\ &\left. + \left(x_4 - e^{j\theta}x_2\right)\left(\hat{x}_1 - e^{j\theta}\hat{x}_3\right)\right|^2. \end{aligned} \tag{D.11}$$

- *When* $\mathbf{S} = \mathbf{S}_2$ *and* $\hat{\mathbf{S}} = \mathbf{S}_3$

$$\begin{aligned} f_{\mathbf{S}_2\mathbf{S}_3}(\theta) = &\Big(\left|x_1 - e^{j\theta}\hat{x}_1\right|^2 + \left|x_2 - e^{-j2\theta}\hat{x}_4\right|^2 \\ &+ \left|x_3 - e^{j\theta}\hat{x}_3\right|^2 + \left|x_4 - \hat{x}_2\right|^2\Big) \\ &\times \Big(\left|-x_2^* + e^{j\theta}\hat{x}_2^*\right|^2 + \left|x_1^* - e^{-j2\theta}\hat{x}_3^*\right|^2 \\ &+ \left|-x_4^* + e^{j\theta}\hat{x}_4^*\right|^2 + \left|x_3^* - \hat{x}_1^*\right|^2\Big) \\ &- \left|\left(x_3 - e^{-j\theta}x_1\right)\left(\hat{x}_2 - e^{-j\theta}\hat{x}_4\right)\right. \\ &\left. + \left(x_4 - e^{j\theta}x_2\right)\left(\hat{x}_1 - e^{j\theta}\hat{x}_3\right)\right|^2. \end{aligned} \tag{D.12}$$

- *When* $\mathbf{S} = \mathbf{S}_2$ *and* $\hat{\mathbf{S}} = \mathbf{S}_4$

$$\begin{aligned} f_{\mathbf{S}_2\mathbf{S}_4}(\theta) = &\Big(\left|x_1 - e^{j2\theta}\hat{x}_3\right|^2 + \left|x_2 - e^{-j\theta}\hat{x}_2\right|^2 \\ &+ \left|x_3 - \hat{x}_1\right|^2 + \left|x_4 - e^{-j\theta}\hat{x}_4\right|^2\Big) \\ &\times \Big(\left|-x_2^* + e^{j2\theta}\hat{x}_4^*\right|^2 + \left|x_1^* - e^{-j\theta}\hat{x}_1^*\right|^2 \\ &+ \left|-x_4^* + \hat{x}_2^*\right|^2 + \left|x_3^* - e^{-j\theta}\hat{x}_3^*\right|^2\Big) \\ &- \left|\left(x_3 - e^{-j\theta}x_1\right)\left(\hat{x}_2 - e^{-j\theta}\hat{x}_4\right)\right. \\ &\left. + \left(x_4 - e^{j\theta}x_2\right)\left(\hat{x}_1 - e^{j\theta}\hat{x}_3\right)\right|^2. \end{aligned} \tag{D.13}$$

- *When* $\mathbf{S} = \mathbf{S}_3$ *and* $\hat{\mathbf{S}} = \mathbf{S}_4$

$$f_{\mathbf{S}_3\mathbf{S}_4}(\theta) = \Big(\left|e^{j\theta}x_3 - \hat{x}_1\right|^2 + \left|x_2 - e^{-j\theta}\hat{x}_4\right|^2 + \left|x_1 - e^{j\theta}\hat{x}_3\right|^2 + \left|e^{-j\theta}x_4 - \hat{x}_2\right|^2\Big)^2. \quad \text{(D.14)}$$

From equations (D.9)-(D.14), we can see that $f_{\mathbf{S}_1\mathbf{S}_2}(\theta) = f_{\mathbf{S}_3\mathbf{S}_4}(\theta)$ and $f_{\mathbf{S}_1\mathbf{S}_3}(\theta) = f_{\mathbf{S}_1\mathbf{S}_4}(\theta) = f_{\mathbf{S}_2\mathbf{S}_3}(\theta) = f_{\mathbf{S}_2\mathbf{S}_4}(\theta)$. Therefore, we actually have to evaluate the two following cases

$$f_{\mathrm{I}}(\theta) = f_{\mathbf{S}_1\mathbf{S}_2}(\theta),$$
$$f_{\mathrm{II}}(\theta) = f_{\mathbf{S}_1\mathbf{S}_3}(\theta). \quad \text{(D.15)}$$

Furthermore, since we have ở trên $\delta_{\min,1}(\theta) < 16$ and $\delta_{\min,2}(\theta) < 16$ for all θ. It follows that θ_o is determined based on equations 3.6-3.9.

Appendix E

The DT-SM complexity

Preprocessing stage

In this stage, the proposed decoder needs to

- Calculating the equivalent channel matrix $\tilde{\mathbf{H}}_k = \mathbf{H}\mathbf{S}_k, k = 1, ..., K$, with $\mathbf{H} \in \mathbb{C}^{n_R \times n_T}, \mathbf{S}_k \in \mathbb{C}^{n_T \times 4}$ requires $32n_Rn_T - 8n_R$ flops.
- Calculating the QR Decomposition the channel matrix $\mathbf{M}_k \in \mathbb{R}^{4n_R \times 8}$ [50] requires $2mn^2 - mn - \frac{n^2+n}{2} = 2 \times 4n_R \times 8^2 + 4n_R \times 8 - \frac{8^2+8}{2} = 544n_R - 36$ flops.
- Calculating $\mathbf{t} = \mathbf{Q}^H\mathbf{v}$ with $\mathbf{Q} \in \mathbb{R}^{4n_R \times 8}$, $\mathbf{v} \in \mathbb{R}^{4n_R \times 1}$ requires $2 \times 8 \times 4n_R - 8 = 64n_R - 8$ flops. $|\mathbf{t}|^2$ and $|\mathbf{v}|^2$ accumulates in the Step 3 of the proposed SD algorithm.

Under the assumption that the channel matrix remains unchanged within a code block of T symbol periods, the preprocessing stage needs to be carried out every T symbol periods, or equivalently, every block of $\frac{T}{2}$ DT-SM codewords. Therefore, the total complexity of the preprocessing stage for a block of $\frac{T}{2}$ codewords is equal to

$$\rho_{T,\text{Pre}} = \left(32n_R n_T - 8n_R + 544n_R - 36\right) K + \frac{T}{2}\left(64n_R - 8\right) K,$$

Thus, the average complexity per DT-SM codeword in this stage is given by

$$\rho_{\text{Pre}} = \frac{\rho_{T,\text{Pre}}}{\frac{T}{2}} = \frac{2}{T}\left(32n_R n_T + 536n_R - 36\right) K + \left(64n_R - 8\right) K,$$

Searching stage

- In the searching stage, the average complexity ρ_s per DT-SM codeword is obtained by counting the number of flops required to obtain the recovered signals (i.e., the flops required to carry out Step 3 to Step 11 of the proposed sphere decoder) and averaged over a sufficiently large number of DT-SM code matrices.

The number of information bits conveyed by a DT-SM codeword is denoted as $\eta = l + 4m$ bits. Detection complexity of the proposed SD, in terms of flops per bit, is given by

$$\rho = \frac{\rho_{\text{Pre}} + \rho_s}{\eta} \left(\text{flop/bit}\right).$$

Appendix F

The DS-SM complexity

Preprocessing stage

In this stage, the SD decoder needs to

- Calculating the equivalent channel matrix $\tilde{\mathbf{H}}_k = \mathbf{H}\mathbf{S}_k, k = 1, ..., K$, with $\mathbf{H} \in \mathbb{C}^{n_R \times n_T}, \mathbf{S}_k \in \mathbb{C}^{n_T \times 4}$ reequires $32n_R n_T - 8n_R$ flops.

- Calculating the extended channel matrix $\mathbf{M}_k = \mathbf{F}\mathbf{W}$ with $\mathbf{F} = \begin{bmatrix} \Re(\mathbf{H}_{eq}) & -\Im(\mathbf{H}_{eq}) \\ \Im(\mathbf{H}_{eq}) & \Re(\mathbf{H}_{eq}) \end{bmatrix}$, $\mathbf{F} \in \mathbb{R}^{8n_R \times 8}, \mathbf{W} \in \mathbb{R}^{8 \times 8}$ requires $15 \times 8 \times n_R \times 8 = 960n_R$ flops.

- Calculating the QR Decomposition the channel matrix $\mathbf{M}_k \in \mathbb{R}^{8n_R \times 8}$ [50] requires $2mn^2 + mn - \frac{n^2+n}{2} = 2 \times 8n_R \times 8^2 + 8n_R \times 8 - \frac{8^2+8}{2} = 1088n_R - 36$ flops.

- Computing $\mathbf{t} = \mathbf{Q}^H\mathbf{v}$ with $\mathbf{Q} \in \mathbb{R}^{8n_R \times 8}$, $\mathbf{v} \in \mathbb{R}^{8n_R \times 1}$ requires $2 \times 8 \times 8n_R - 8 = 128n_R - 8$ flops.

- Calculating $|\mathbf{t}|^2$ requires 15 flop and $|\mathbf{v}|^2$ requires $15n_R$ flops.

Under the assumption that the channel matrix remains unchanged within a code block of T symbol periods. This is equivalent to every block of $\frac{T}{4}$ DS-SM codewords. Therefore, the total complexity of the preprocessing stage for a block of $\frac{T}{4}$ DS-SM codewords is equal to

$$\rho_{T,\text{Pre}} = (32n_R n_T - 8n_R + 2048n_R - 36)\, K + \frac{T}{4}(143n_R + 7)\, K,$$

Thus, the average complexity per DS-SM codeword in this stage is given by

$$\rho_{\text{Pre}} = \frac{\rho_{T,\text{Pre}}}{\frac{T}{4}} = \frac{4}{T}(32n_R n_T + 2040n_R - 36)\, K + (143n_R + 7)\, K,$$

Searching stage

- In the searching stage, the average complexity ρ_s per DS-SM codeword is obtained by counting the number of flops required to obtain the recovered

signals in the steps of the SD algorithm and averaged over a sufficiently large number of DS-SM code matrices.

The number of information bits conveyed by a DT-SM codeword is denoted as $\eta = l + 4m$ bits, Detection complexity of the SD algorithm, in terms of flops per bit, is given by

$$\rho = \frac{\rho_{\text{Pre}} + \rho_s}{\eta} \,(\text{flop/bit})\,.$$

LIST OF PUBLISHED WORKS

A. The published works are used in the thesis

1. **T. D. Nguyen**, X. N. Tran, T. M. Do, V. D. Ngo, and M. T. Le, "Low-complexity detectors for High-rate Spatial Modulation," in *Proceeding of International Conference on Advanced Technologies for Communications (ATC),* 2014, pp. 652-656.
2. V. T. Luong, M. T. Le, **T. D. Nguyen**, X. N. Tran, and V. D. Ngo, "New upper bound for high-rate spatial modulation systems using QAM modulation," in *Proceeding of International Conference on Advanced Technologies for Communications (ATC),* 2015, pp. 657-661.
3. **T. D. Nguyen**, X. N. Tran, T. M. Do, V. D. Ngo, and M. T. Le, "A spatial modulation scheme with full diversity for four transmit antennas," in *Proceeding of International Conference on Advanced Technologies for Communications (ATC),* 2015, pp. 16-19.
4. M. T. Le, **T. D. Nguyen**, X. N. Tran, and V. D. Ngo, "On the Combination of Double Space Time Transmit Diversity with Spatial Modulation," *IEEE Transactions on Wireless Commmunications*, vol. 17, no. 1, pp. 170-181, Jan 2018. (available online)
5. **Nguyen Tien Dong**, Le Thi Thanh Huyen, Tran Xuan Nam, "Effect of imperfect channel estimation on high-rate spatial modulation detectors," *Journal of Military Science and Technology*, no. 48A, pp. 31-39, 5-2017.

6. **T. D. Nguyen**, M. T. Le, V. D. Ngo, and X. N. Tran, "Diagonal Space Time Block Code in Spatial Modulation," *Mobile Networks and Applications*, vol. , pp. , 2018. (submitted)

B. The published works is related to the thesis

7. **T. D. Nguyen**, M. T. Le, V. D. Ngo, and X. N. Tran, "A New Spatial Modulation Scheme with Transmit Diversity for Four Transmit Antennas," *REV Journal on Electronics and Communications*, vol. , pp. , 2018. (submitted)

Bibliography

Vietnamese

[1] Tran Xuan Nam va Le Minh Tuan, *Xu ly tin hieu khong gian thoi gian-ly thuyet va mo phong*, Nha xuat ban Khoa hoc va Ky thuat, Ha Noi, 2013.

English

[2] S. Alamouti, "A simple transmit diversity technique for wireless communications," *IEEE Journal on Selected Areas in Communication,* vol. 16, no. 8, pp. 1451-1458, 1998.

[3] M. S. Alouini and M. K. Simon, *Digital communications over fading channels,* vol. 2, John & Wiley, 2005.

[4] E. Basar and U. Aygolu, "High-rate full-diversity space-time block codes for three and four transmit antennas," *IET Communications,* vol. 3, no. 8, pp. 1371-1378, 2009.

[5] E. Basar, U. Aygolu, E. Panayirci, and H. V. Poor, "Space-time block coding for spatial modulation," in *Proceeding of International Symposium on Personal Indoor and Mobile Radio Communications (PIMRC),* 2010, pp. 803-808.

[6] J. C. Belfiore, X. Giraud, and J. Rodriguez-Guisantes, "Optimal linear labelling for the minimization of both source and channel distortion," in *Proceeding of IEEE International Symposium on Information Theory,* 2000, p. 404.

[7] E. Biglieri and E. Viterbo, "A universal decoding algorithm for lattice codes," in *Proceeding of GRETSI,* France, September 1993, pp. 611- 614.

[8] R. E. Blahut, *Digital transmission of information,* Addison-Wesley, 1990.

[9] R. Bohnke, D. Wubben, V. Kuhn, and K. D. Kammeyer, "Reduced complexity MMSE detection for BLAST architectures," in *Proceeding of IEEE Global Telecommunications Conference,* 2003, vol. 4, pp. 2258-2262.

[10] H. Bölcskei and A. J. Paulraj, "Performance of space-time codes in the presence of spatial fading correlation," in *Proceeding of Asilomar Conference on Signals, Systems and Computers,* Pacific Grove, CA, Oct. 2000, pp. 687-693.

[11] A. M. Chan and L. Inkyu, "A new reduced-complexity sphere decoder for multiple antenna systems," in *Proceeding of IEEE International Conference on Communications*, 2002, pp. 460-464.

[12] Y. A. Chau and Y. Shi-Hong, "Space modulation on wireless fading channels," in *Proceeding of 54th IEEE Vehicular Technology Conference*, 2001, vol. 3, pp. 1668-1671.

[13] O. Damen, H. El Gamal, and G. Caire, "On maximum-likelihood detection and the search for the closest lattice point," *IEEE Transactions on Information Theory,* vol. 49, no. 10, pp. 2389-2402, 2003.

[14] M. Di Renzo, and H. Haas, "Performance comparison of different spatial modulation schemes in correlated fading channels," in *Proceeding of IEEE International Communications Conference*, 2010, pp. 1-6.

[15] M. Di Renzo and H. Haas, "Space shift keying (SSK) MIMO over correlated Rician fading channels: performance analysis and a new method for transmit-diversity," *IEEE Transactions on Communications,* vol. 59, no. 1, pp. 116-129, 2011.

[16] M. Di Renzo and H. Haas, "Space shift keying (SSK) modulation: on the transmit-diversity / multiplexing trade-off," in *Proceeding of IEEE International Conference on Communication,* 2011, pp. 1-6.

[17] M. Di Renzo and H. Haas, "On transmit diversity for spatial modulation MIMO: impact of spatial constellation diagram and shaping filters at the transmitter," *IEEE Transactions on Vehicular Technology*, vol. 62, no. 6, pp. 2507-2531, 2013.

[18] M. Di Renzo, H. Haas, A. Ghrayeb, S. Sugiura, and L. Hanzo, "Spatial modulation for generalized MIMO: challenges, opportunities, and implementation," in *Proceedings of the IEEE,* vol. 102, no. 1, pp. 56-103, 2014.

[19] M. Di Renzo, H. Haas, and P. M. Grant, "Spatial modulation for multiple-antenna wireless systems: a survey," *IEEE Communications Magazine,* vol. 49, no. 12, pp. 182-191, 2011.

[20] G. Ganesan and P. Stoica, "Space-time block codes: a maximum SNR approach," *IEEE Transactions on Information Theory*, vol. 47, no. 4, pp. 1650-1656, 2001.

[21] H. Haas, E. Costa, and E. Schulz, "Increasing spectral efficiency by data multiplexing using antenna arrays," in *Proceeding of 13th IEEE International Symposium on Personal, Indoor and Mobile Radio Communications*, 2002, vol. 2, pp. 610-613.

[22] B. Hassibi, "A fast square-root implementation for BLAST," in *Proceeding of IEEE International Conference on Ascoustics, Speech, and signal processing,* 2000, vol. 2, pp. 1255 - 1259.

[23] T. Handte, J. Speidel and A. Muller, "BER analysis and optimization of generalized spatial modulation in correlated fading channels," in *Proceeding of 70th IEEE Vehicular Technology Conference Fall,* 20-23 Sept. 2009, pp. 1 - 5.

[24] A. Hedayat, H. Shah and A. Nosratinia, "Analysis of space-time coding in correlated fading channels," *IEEE Transactions on Communications,* vol. 4, no. 6, pp. 2882-2891, Nov. 2005.

[25] F. Heliot, M. A. Imran, and O. Tafazolli, "On the energy efficiency-spectral efficiency trade-off over the MIMO Rayleigh fading channel," *IEEE Transactions on Communications,* vol. 60, no. 5, pp. 1345-1356, 2012.

[26] J. Hoydis, S. ten Brink, and M. Debbah, "Massive MIMO: how many antennas do we need," in *Proceeding of 49th Annual Allerton Conference on Communication, Control, and Computing,* 2011, pp. 545-550.

[27] Texas Instruments, "Double-STTD scheme for HSDPA systems with four transmit antennas: link level simulation results" *TSG-R WG1 document, TSGR1#20(01)0458*, 21st-24th May, 2001, Busan, Korea.

[28] H. Jafarkhani, "A quasi-orthogonal space-time block code," *IEEE Transactions on Communications*, vol. 49, no. 1, pp. 1-4, 2001.

[29] J. Jeganathan, A. Ghrayeb, and L. Szczecinski, "Spatial modulation: optimal detection and performance analysis," *IEEE Communications Letters,* vol. 12, no. 8, pp. 545-547, 2008.

[30] J. Jeganathan, A. Ghrayeb, L. Szczecinski, and A. Ceron, "Space shift keying modulation for MIMO channels," *IEEE Transactions on Wireless Communications,* vol. 8, no. 7, pp. 3692-3703, 2009.

[31] W. Jingxian, Y. R. Zheng, A. Gumaste, and X. Chengshan, "Error performance of double space time transmit diversity system," *IEEE Transactions on Wireless Communications,* vol. 6, no. 9, pp. 3191-3196, 2007.

[32] G. Larsson and P. Stoica, *Space-time block coding for wireless communications,* Cambrige University Press, 2008.

[33] M. T. Le, V. S. Pham, L. Mai, and G. Yoon, "Very-low-complexity maximum likelihood decoders for four transmit antenna quasi-orthogonal space-time code," *IEICE Transactions on Communications,* E88-B, no. 9, pp. 3802-3805, 2005.

[34] M. T. Le, N. V. Duc, H. A. Mai, and X. N. Tran, "High-rate space-time block coded spatial modulation," in *Proceeding of International Conference on Advanced Technologies for Communications,* 2012, pp. 278-282.

[35] M. T. Le, V. D. Ngo, H. A. Mai, X. N. Tran, and M. Di Renzo, "Spatially modulated orthogonal space-time block codes with non-vanishing determinants," *IEEE Transactions on Communications,* vol. 62, no. 1, pp. 85-99, 2014.

[36] X. F. Li and L. Wang, "High rate space-time block coded spatial modulation with cyclic structure," *IEEE Communication Letters,* vol. 18, no. 4, pp. 532-535, 2014.

[37] Y. Li, B. Vucetic, Y. Tang and Q. Zhang, "Space-time trellis codes with linear transformation for fast fading channels," *IEEE Signal Processing Letters,* vol. 11, no. 11, pp. 895-898, 2004.

[38] Z. Liu, Y. Xin and G. B. Giannakis, "Space-time-frequency coded OFDM over frequency-selective fading channels," *IEEE Transactions on Signal Processing,* vol. 50, no. 10, pp. 2465-2476, 2002.

[39] S. L. Loyka, "Channel capacity of MIMO architecture using the exponential correlation matrix," *IEEE Communication Letters,* vol. 5, no. 9, pp. 369-371, 2001.

[40] H. A. Mai, T. C. Dinh, X. N. Tran, M. T. Le, and V. D. Ngo, "A novel spatially-modulated orthogonal space-time block code for 4 transmit antennas," in *Proceeding of IEEE International Symposium on Signal Processing and Information Technology* , 2012, pp. 000119-000123.

[41] R. Mesleh, H. Haas, A. Chang Wook, and Y. Sangboh, "Spatial modulation - a new low complexity spectral efficiency enhancing technique," in *Proceeding of First International Conference on Communication and Networking,* China, 2006, pp. 1-5.

[42] R. Y. Mesleh, H. Haas, S. Sinanovic, A. Chang Wook, and Y. Sangboh, "Spatial modulation," *IEEE Transactions on Vehicular Technology,* vol. 57, no. 4, pp. 2228-2241, 2008.

[43] J. Mietzner, R. Schober, L. Lampe, H. Gerstacker, and A. Hoeher, "Multiple-antenna techniques for wireless communications - a comprehensive literature survey," *IEEE Communications Surveys & Tutorials,* vol. 11, no. 2, pp. 87-105, 2009.

[44] A. Mohammadi and F. M. Ghannouchi, "Single RF front-end MIMO transceivers," *IEEE Communications Magazine,* vol. 49, no. 12, pp. 104-109, 2011.

[45] B. Myung-kwang and L. Byeong Gi, "New bounds of pairwise error probability for space-time codes in Rayleigh fading channels," in *Proceeding of IEEE Wireless Communications and Networking Conference,* 2002, vol. 1, pp. 89-93.

[46] T. P. Nguyen, M. T. Le, V. D. Ngo, X. N. Tran, and H. W. Choi, "Spatial modulation for high-rate transmission systems," in *Proceeding of 79th IEEE Vehicular Technology Conference,* 2014, pp. 1-5.

[47] F. Oggier, G. Rekaya, J. C. Belfiore, and E. Viterbo, "Perfect space-time block codes," *IEEE Transaction on Information Theory,* vol. 52, no. 9, pp. 3885-3902, 2006.

[48] M. C. Park, B. G. Jo, and D. S. Han, "Double space-time transmit diversity with spatial modulation," *Electronics Letters,* vol. 51, no. 25, pp. 2155-2156, 2015.

[49] A. Paulraj, R. Nabar, and D. Gore, *Introduction to space-time wireless communications,* New York: Cambridge University Press, 2003.

[50] P. Persson, *Gram-Schmidt Orthogonalization,* MIT 18.335J/ 6.337J, Introduction to Numerical Methods, September, 2006.

[51] M. Pohst, "On the computation of lattice vectors of minimal length, successive minima and reduced bases with applications," *SIGSAM Bull,* vol. 15, no. 1, pp. 37-44, 1981.

[52] U. Fincke and M. Pohst, "Improved methods for calculating vectors of short length in a lattice, including a complexity analysis," *Mathematics of Computation,* vol. 44, no. 170, pp. 463-471, 1985.

[53] C. Qian, J. Wu, Y. R. Zheng, and Z. Wang, "Simplified parallel interference cancelation for underdetermined MIMO systems," *IEEE Transactions on Vehicular Technology,* vol. 63, no. 7, pp. 3196-3208, 2014.

[54] N. Serafimovski, S. Sinanovic, M. Di Renzo, and H. Haas, "Multiple access spatial modulation," *EURASIP Journal on Wireless Communications and Networking,* vol. 2012, no. 1, pp. 299, 2012.

[55] S. Song, Y. Yang, Q. Xionq, K. Xie, B. J. Jeong, and B. Jiao, "A channel hopping technique I: theoretical studies on band efficiency and capacity," in *Proceeding of International Conference on Communications, Circuits and Systems,* 2004, vol. 1, pp. 229-233.

[56] E. Soujeri and G. Kaddoum, "Performance comparison of spatial modulation detectors under channel impairments," in *IEEE International Conference on Ubiquitous Wireless Broadband (ICUWB),* 2015, pp. 1-5.

[57] K. P. Srinath and B. S. Rajan, "Low ML-decoding complexity, large coding gain, full-rate, full-diversity STBCs for 2 x 2 and 4 x 2 MIMO systems," *IEEE Journal of Selected Topics in Signal Processing,* vol. 3, no. 6, pp. 916-927, 2009.

[58] S. Sugiura, C. Sheng, and L. Hanzo, "Coherent and differential space-time shift keying: a dispersion matrix approach," *IEEE Transactions on Communications,* vol. 58, no. 11, pp. 3219-3230, 2010.

[59] S. Sugiura, C. Sheng, and L. Hanzo, "Generalized space-time shift keying designed for flexible diversity-, multiplexing- and complexity-tradeoffs," *IEEE Transactions on Communications,* vol. 10, no. 4, pp. 1144-1153, 2011.

[60] V. Tarokh, N. Seshadri, A. Naguib and A. R. Calderbank, "Space-time codes for high data rate wireless communication: performance criteria in the presence of channel estimation errors, mobility, and multiple paths," *IEEE Transactions on Communications,* vol. 47, no. 2, pp. 199-207, 1999.

[61] V. Tarokh, H. Jafarkhani, and A. R. Calderbank, "Space-time block codes from orthogonal designs," *IEEE Transactions on Information Theory,* vol. 45, no. 1, pp. 1456-1467, 1999.

[62] V. Tarokh, H. Jafarkhani, and A. R. Calderbank, "Space-time block coding for wireless communications: performance results," *IEEE Journal on Selected Areas in Communications,* vol. 17, no. 3, pp. 451-460, 1999.

[63] V. Tarokh, N. Seshadri, and A. R. Calderbank, "Space-time codes for high data rate wireless communication: performance criterion and code construction," *IEEE Transactions on Information Theory*, vol. 44, no. 2, pp. 744-765, 1998.

[64] T. P. Ren, Y. L. Guan, C. Yuan, and E. Y. Zhang, "Block-orthogonal space time code structure and its impact on QRDM decoding complexity

reduction," *IEEE Journal of Selected Topics in Signal Processing,* vol. 5, no. 8, pp. 1438-1450, 2011.

[65] S. Verdu, "Maximum likelihood sequence detection for intersymbol interference channels: a new upper bound on error probability," *IEEE Transactions on Information Theory*, vol. 33, no. 1, pp. 62-68, 1987.

[66] H. Vikalo, *Sphere decoding algorithms for digital communications,* Doctoral, Stanford University, 2003.

[67] E. Viterbo, and J. Boutros, "A universal lattice code decoder for fading channels," *IEEE Transactions on Information Theory*, vol. 45, no. 5, pp. 1639-1642, 1999.

[68] B. Vucetic and J. Yuan, *Space-time coding,* Wiley, 2003.

[69] J. Wang, S. Jia, and J. Song, "Generalised spatial modulation system with multiple active transmit antennas and low complexity detection scheme," *IEEE Transactions on Wireless Communications,* vol. 11, no. 4, pp. 1605-1615, 2012.

[70] L. Wang and Z. Chen, "Spatially modulated diagonal space time codes," *IEEE Communication Letters,* vol. 19, no. 7, pp. 1245-1248, 2015.

[71] W. Wolniansky, J. Foschini, D. Golden, and R. Valenzuela, "V-BLAST: an architecture for realizing very high data rates over the rich-scattering wireless channel," in *Proceeding of International Symposium on Signals, Systems, and Electronics,* 1998, pp. 295-300.

[72] D. Wubben, R. Bohnke, V. Kuhn, and K. D. Kammeyer, "MMSE extension of V-BLAST based on sorted QR decomposition," in *Proceeding of 58th IEEE Vehicular Technology Conference,* 2003, vol. 1, pp. 508-512.

[73] D. Wubben, R. Bohnke, V. Kuhn, and K. D. Kammeyer, "Near-maximum-likelihood detection of MIMO systems using MMSE-based lattice reduction," in *Proceeding of IEEE International Conference on Communications,* 2004, vol. 2, pp. 798-802.

[74] Y. Yang and B. Jiao, "Information-guided channel-hopping for high data rate wireless communication," *IEEE Communication Letters,* vol. 12, no. 4, pp. 225-227, 2008.

[75] W. Zhu, J. Jin, and Y. Park, "Detection algorithm improving parallel interference cancellation for V-BLAST system over error propagation," in *Proceeding of 8th International Conference Advanced Communication Technology,* 2006, pp. 5-15.